MECHANISMS CONTROLLING THE EXPANSION OF CD11B^{+} DCS IN ATHEROSCLEROSIS

WONG HUI SIAN FIONA

(B.Sc (Hons), NUS)

A THESIS SUBMITTED FOR THE DEGREE OF MASTER OF SCIENCE

DEPARTMENT OF MICROBIOLOGY

NATIONAL UNIVERSITY OF SINGAPORE

2013

DECLARATION

I hereby declare that the thesis is my original work and it has been written by me in its entirety. I have duly acknowledged all the sources of information which have been used in the thesis.

This thesis has also not been submitted for any degree in any university previously.

_____

WONG HUI SIAN FIONA

20 AUGUST 2013

Acknowledgements

I want to thank my supervisor, Dr Veronique Angeli for her invaluable guidance and opportunity for obtaining my Master degree. You have always kept your doors open to us and squeeze out time no matter how hectic your schedule is. I deeply appreciate your efforts in molding me into a better scientist and would not forget the lessons and values you have imparted.

I wish to give thanks to my collaborator, Dr Florent Ginhoux. Without your advice and expertise especially in multicolor flow cytometry and DC subsets, I would not have advanced as far as on my own. Your passion for science is inspiring. I would also like to thank Dr Pearline Teo for her advice on progenitors and Peter See for helping me when I was over at the Ginhoux lab.

To my honours supervisor, Dr Lim Yaw Chyn, you have given me a great foundation to start with and learning that negative results still count for something is one lesson I always hold to my heart and keep me from feeling down when experiments fail. Thank you for this valuable lesson.

To Dr Paul Edward Hutchinson, thank you for choosing IP and sharing your experience in flow cytometry with the rest of us.

I would also like to express my gratitude to various friends whom I have met over the years, whose camaraderie make this a smoother journey. Thank you Kar Wai, for being my sounding board, scientific advisor and foodie friend and for knocking me on the head whenever I needed it. To Jocelyn, I give thanks that we enter the lab on the same day and became fast friends. Thank you for giving me support, experimental advice and inspiration to persevere.

Thank you Shuzhen for your joy in my creations and emotional support. Thank you Fei Chuin for being the great friend you are, helping me to sort cells till late and teaching me that frankness has its advantages. Thank you Hazel and Victoria for the company and barrel of laughs.

I wish to thank my colleagues in the VA lab, Angeline, Kim, Lawrence, Michael, Serena, Junxiang, who have one way or another help me along the way. I also wish to thank my colleagues in SA lab for wonderful time spent together. Thank you Wenwei and Regina for sharing the anxiety in submitting our theses on time and Michelle for being as crazy as I am in baking. I am glad to have known all of you in the last few months.

To my ex-colleagues in the Department of Pathology, thank you Aw Yibing and Sharon Pek for your support and patience while waiting for me to wrap up my thesis before going for holidays. Thank you to my ex-supervisor, Dr Eng Chon Boon for the reference in starting my Master degree and for giving me many opportunities to shine.

I want to thank my friends who are not in the field but who have touched my life in many ways and given their unwavering support.

Last but not least, I want to thank my family especially my parents for letting me pursue my dreams.

Table of Contents

Abstract

Atherosclerosis is the leading cause of mortality in many countries. It is an inflammatory disease of large and medium sized arteries characterized by hyperlipidemia. Dendritic cells (DCs) are one of the key players of the inflammatory brigade in atherosclerotic plaques and are known to accumulate in atherosclerosis. Past studies in atherosclerosis rely on classical markers such as CD11c and MHC class II to characterize DCs. However, recent identification of non-lymphoid tissue DC subsets based on additional markers such as CD11b and CD103 was introduced. Consequently, the need to distinguish DC populations in the atherosclerotic plaques arises. Based on the new classification, we managed to identify two different DC subsets, $CD11b^+$ and $CD103^+$ in the aorta at steady state, which localized at sites of predilection for atherosclerosis. Using the $apoE^{-/-}$ mouse model of atherosclerosis, we showed that both $CD11b^+$ and $CD103^+$ DCs expanded during disease, with $CD11b^+$ DCs being the dominant population. Expansion of $CD11b^+$ DCs was abrogated when we treated $apoE^{-/-}$ mice with a cholesterol-lowering drug, Ezetimibe. Since monocytosis is prominent in $apoE^{-/-}$ mice and was also abolished in Ezetimibe-treated $apoE^{-/-}$ mice, we hypothesized that monocytes may be the precursors of $CD11b^+$ DCs. Supporting this hypothesis, adoptively transferred monocytes differentiated into $CD11b^+$ DCs in the aortas of $apoE^{-/-}$ mice. Moreover, employing the use of a monocyte-derived cell marker CD64, we showed that the proportion of $CD11b^+$ DCs expressing CD64 in $apoE^{-/-}$ mice was increased as compared to wild-type (WT) controls. For DC

differentiation to occur, growth factors are essential to the process. When we investigated which growth factors were present in atherosclerotic plaques, we discovered that only granulocyte-macrophage colony-stimulating factor (GM-CSF) was highly expressed in atherosclerotic aorta compared to normal aorta. Interestingly, this over-expression of GM-CSF was only detected in atherosclerotic plaques and not found in the circulation and aorta-associated draining lymph node. Subsequently, we showed that neutralizing GM-CSF partially diminished monocytosis and $CD11b^+$ DC accumulation, demonstrating that GM-CSF is required for the expansion of $CD11b^+$ DCs. We have also explored other possible mechanisms such as proliferation, expansion of bone marrow progenitors and extramedullary hematopoiesis and discounted their role in $CD11b^+$ DC accumulation.

Next, we initiated a study to examine the function of $CD11b^+$ DCs. $CD11b^+$ DCs produce pro-inflammatory factors, tumor necrosis factor alpha (TNF-α) and inducible nitric oxide synthase (iNOS) which are known to be pathogenic in atherosclerosis. As one of the by-products of iNOS activity is peroxynitrite which results in protein nitration and alteration of protein function, we found that $CD11b^+$ DCs localized with sites of nitration in atherosclerotic plaques. Likely, $CD11b^+$ DCs have a pro-inflammatory role in atherosclerosis. According to our findings, we suggest that by targeting monocytosis and GM-CSF, we could devise therapeutic strategies for atherosclerosis treatment.

Publications

1) Tan KW, Yeo KP, Wong FH, Lim HY, Khoo KL, Abastado JP, Angeli V. (2012). Expansion of cortical and medullary sinuses restrains lymph node hypertrophy during prolonged inflammation. *J Immunol* 188, 4065-80
2) Chong SZ, Wai Tan K, Wong FH, Leong Chua Y, Tang Y, Guan Ng L, Angeli V, Kemeny DM (2013). CD8 T-cells regulate allergic contact dermatitis by modulating CCR2-dependent TNF/iNOS-expressing $Ly6C^+$ $CD11b^+$ monocytic cells. *J Invest Dermatol* (*in press*)
3) Wong FH, See P, Ginhoux F, Angeli V. Mechanisms underlying $CD11b^+$ DC subset accumulation in atherosclerotic aorta. (*manuscript in preparation*)

List of Figures

List of Abbreviations

ApoE	Apolipoprotein E
APC	Antigen-presenting cell
BSA	Bovine serum albumin
cDC	Conventional dendritic cell
CDP	Common DC precursor
Csf1r	Colony-stimulating factor 1 receptor
DAPI	4’,6-Diamidino-2-phenylindole dihydrochloride
DC	Dendritic cells
EdU	5-ethynyl-2’-deoxyuridine
EGFP	Enhanced green fluorescent protein
FCS	Fetal calf serum
G418	Geniticin®
GM-CSF	Granulocyte-macrophage colony-stimulating factor
GMFI	Geometric mean fluorescence intensity
HBSS	Hank’s buffered salt solution
HSPC	Hematopoietic stem and multipotential progenitors
HSP	Heat shock protein
IMDM	Iscove’s modified Dulbecco’s media

iNOS	Inducible nitric oxide synthase
IFN-α	Interferon-α
LAG-3	Lymphocyte activation marker-3
Ldlr	Low density lipoprotein receptor
LRP	Low density lipoprotein receptor-related protein
LC	Langerhans cell
LPS	Lipopolysaccharide
Mafia	Macrophage fas-induced apoptosis
MALT	Mucosa-associated lymphoid tissue
M-CSF	Macrophage colony-stimulating factor
MCP-1	Monocyte-chemoattractant protein 1
MDP	Macrophage/DC precursor
MoDC	Monocyte-derived dendritic cell
mDC	Myeloid dendritic cell
NO	Nitric oxide
oxLDL	Oxidized low-density lipoprotein
pDC	Plasmacytoid DC
RA	Rheumatoid arthritis
RPMI	Roswell Park Memorial Institute

SIRP-α	Signal regulatory protein α
SLE	Systemic lupus erythematosus
TipDC	TNFα and inducible nitric oxide synthase producing DCs
TNF-α	Tumor necrosis factor α
VALT	Vascular-associated lymphoid tissue
WT	Wild-type

Chapter 1

Introduction

Chapter 1 – Introduction

1.1 Function and composition of aorta

Aorta is the largest artery in the body and functions to distribute oxygenated blood throughout the body. The most important role of the aorta is its non-linear elasticity in response to pulsatile flow (Grotenhuis and de Roos, 2011). It is composed of three layers: intima, media and adventitia (Figure 1.1). The intima layer is lined with endothelial cells responsive to blood flow whereas the media layer consists of smooth muscle cells interspersed between elastic fibers. The outermost layer which is the adventitia provides further support to aorta with its connective tissue network.

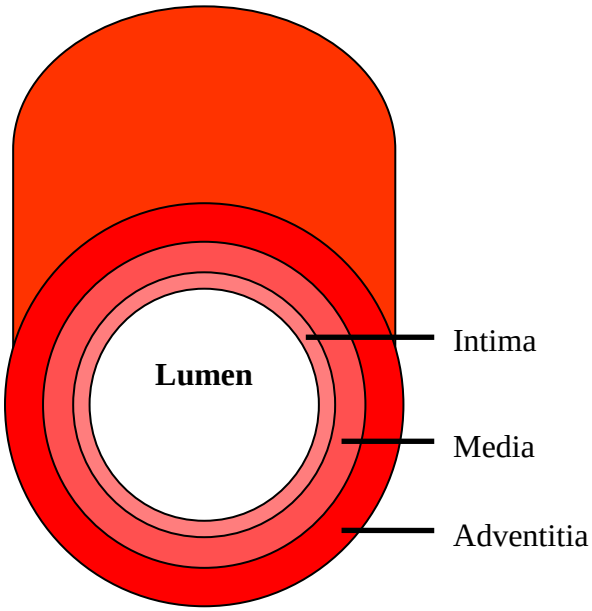

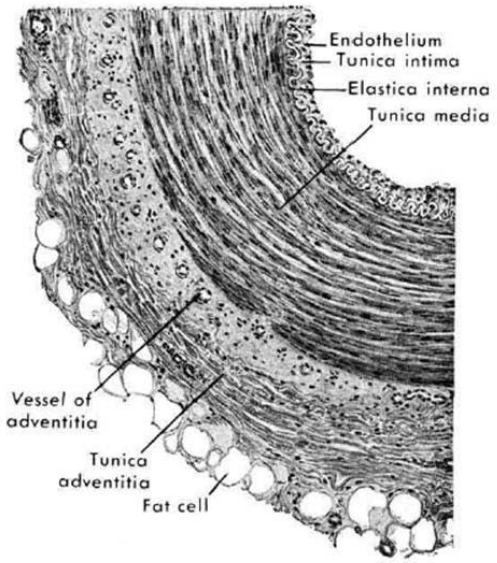

Figure 1.1 Diagram of an arterial wall.

Artery wall of aorta is made up of 3 layers: intima, media and adventitia. The innermost layer which is the intima is lined with endothelial cells. Media lies between the intima and adventitia and is composed of smooth muscle cells and elastic fibers, providing elasticity to the aorta. The adventitia made up of connective tissue and collagen extends additional support and structure to the aorta. Image on the right adapted from *(Fawcett, 1986).*

1.2 Anatomy of the aorta and its role in the development of atherosclerosis – the "response to injury" hypothesis

The aorta is a highly-branched and curved tubular structure with bifurcations (Berillis, 2013) (Figure 1.2). As a result, the pulsatile flow of blood through the aorta generates hemodynamic forces – biomechanical forces such as wall shear stress that can alter vessel biology. Notably, disturbed flow patterns are found at branching points, curvature and bifurcations of the aorta and seem to correlate well with sites of atherosclerosis (Figure 1.3) (VanderLaan et al., 2004).

Atherosclerosis is a complex disease of the aorta associated with hyperlipidemia and is characterized by intimal thickening. There are numerous hypotheses behind the development of atherosclerosis. Regardless, it is universally agreed that atherosclerosis is initiated by the activation and dysfunction of endothelial cells (Weber et al., 2008). As endothelial cells are the one in close contact with blood flow, they are predictably most affected by hemodynamic forces. Indeed, their ellipsoidal shape and parallel alignment in laminar flow regions (atherosclerosis-resistant regions) were disrupted in disturbed flow areas (atherosclerosis-prone regions) (Figure 1.4) (Gimbrone and Garcia-Cardena, 2013). This change allows increased permeability of the endothelium to lipoproteins. Thus, "the response to injury" model was born (Ross, 1999).

1.3 The “response to modified lipoprotein” theory in the development of atherosclerosis

Another theory behind the development of atherosclerosis is “the response to modified lipoprotein” (Steinberg and Witztum, 1990). Hyperlipidemia, a condition whereby abnormally high levels of lipids circulate in the blood, is a well-known risk factor for atherosclerosis. It has been shown that hyperlipidemia can cause a focal loss of endothelial cells with alterations in their morphology (Ross and Harker, 1976). In addition, circulating lipids and lipoproteins can be modified by an oxidation process in atherosclerotic lesions. These modified lipids and lipoproteins in turn induced the expression of cell adhesion molecules and monocyte-chemoattractant protein 1 (MCP-1) in endothelial cells, resulting in increased migration and adhesion of monocytes, encouraging foam cell formation (Stancu et al., 2012).

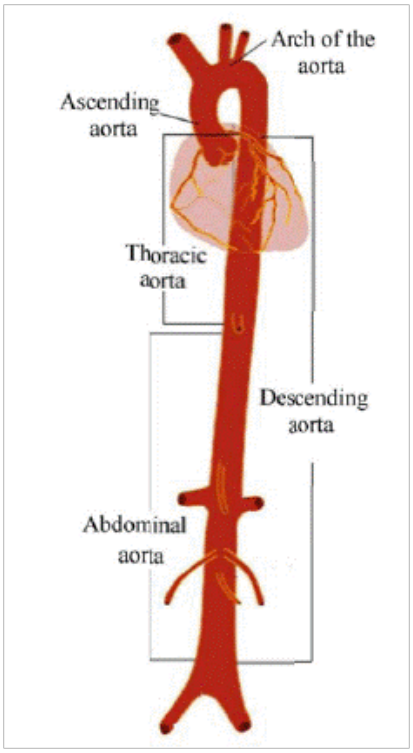

Figure 1.2. Anatomy of aorta.

The aorta can be divided into five sections: ascending aorta, aortic arch, thoracic aorta, descending aorta and abdominal aorta. The ascending aorta is the area between the heart and aortic arch. The aortic arch as its name suggests is the area of curvature after the ascending aorta. The descending aorta which is the region after the arch and all the way to the iliac bifurcation is further separated into thoracic and abdominal regions. Thoracic aorta is above the diaphragm while abdominal aorta is below the diaphragm. Adapted from (Berillis, 2013).

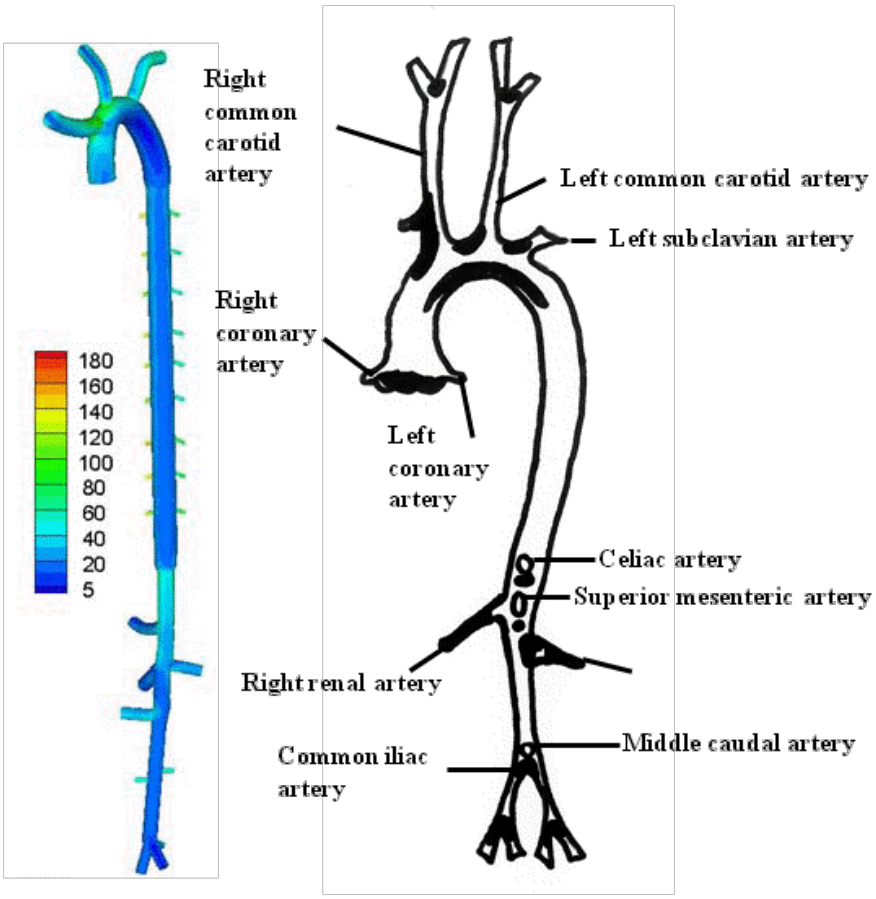

Figure 1.3. Wall shear stress correlates with sites of atherosclerotic lesions.

Left: time-averaged wall shear stress in a C57BL/6 mouse adapted from (Huo et al., 2008). *Right*: Predilection sites of atherosclerotic lesions in atherosclerotic apoE$^{-/-}$ mice adapted and modified from (Nakashima et al., 1994).

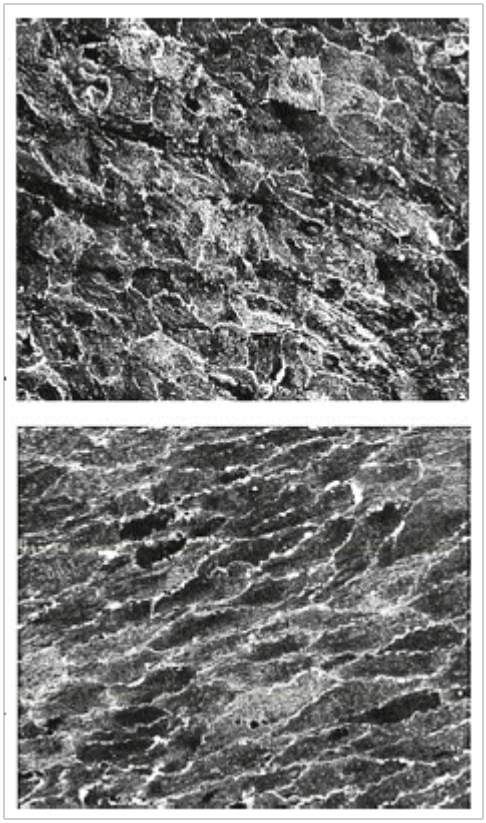

Figure 1.4. Morphology of endothelial cells in atherosclerosis-prone and atherosclerosis-resistant areas in aorta.

En face confocal microscopy of endothelium stained with CD31. Adapted from (Gimbrone and Garcia-Cardena, 2013).

1.4 The "immunological hypothesis" in development of atherosclerosis

Infiltration of immune cells into atherosclerotic lesions was observed as early as mid 19th century. While Carl *von Rokitansky* believed that the injury to the endothelium resulted in damaged endothelium and inflammation, Rudolf *Virchow* advocated their primary role in triggering atherosclerosis (Mayerl et al., 2006). In fact, activated T lymphocytes could be found in early and late atherosclerotic plaques (Hansson et al., 1988; Stratford et al., 1986; Xu et al., 1990). However, the nature of antigen involved was unknown until immunization with heat shock protein (hsp) 65 was found to induce atherosclerosis at predisposed sites in normocholesterolemic rabbits (Xu et al., 1992). Moreover, hsp65-reactive T cells were found in the circulation and atherosclerotic lesions of these animals (Xu et al., 1993).

Heat shock proteins are a group of stress proteins that are constitutively expressed or induced by bacterial infections, high temperature, mechanical stress, hypoxia etc. Remarkably, expression of hsp60 is up-regulated in endothelial cells when exposed to shear stress (Hochleitner et al., 2000) or when exposed to cytokines (Xu et al., 1994), reiterating the importance of endothelial cell dysfunction in atherogenesis.

Since hsp 65 and other members of the family have been implicated as possible autoantigens in autoimmune diseases such as systemic lupus erythematosus (SLE) (Minota et al., 1988) and rheumatoid arthritis (RA) (Tsoulfa et al., 1989), likewise it could function as an autoantigen in atherosclerosis (Blasi, 2008; Nilsson and Hansson, 2008). In fact, patients with

SLE and RA have a higher risk of atherosclerosis (Abou-Raya and Abou-Raya, 2006; Frostegard, 2002).

The discovery of mononuclear cell infiltration in normal healthy children at sites subjected to hemodynamic stress led to the postulation of a "vascular-associated lymphoid tissue" (VALT) (Waltner-Romen et al., 1998). Analogous to mucosa-associated lymphoid tissue (MALT), VALT is assumed to function as a local immune surveillance site for potentially harmful antigens (Millonig et al., 2001b; Wick et al., 1997). The consequence of destabilization of VALT by autoantigens such as hsp and oxidized low-density lipoprotein (oxLDL) is hypothesized to be the initiating event in the development of atherosclerosis (Lord and Bobryshev, 2002). At present, atherosclerosis is recognized as a chronic inflammatory disease with contributions from both the innate and adaptive immunity (Hansson and Libby, 2006).

1.5 The developmental stages of atherosclerotic lesions

The development of atherosclerosis is a continual process with contributions from various immune cells at different stages. Thus, to differentiate the type of atherosclerotic lesions and facilitate the identification of cells that contribute to the disease progression, atherosclerosis can be classified into Type I to VI lesions (Stary et al., 1995; Stary et al., 1994) (Figure 1.5).

Briefly, Type I lesions are composed of lipid deposits in the intima and minimal foam cell formation. Accumulation of lipid-laden foam cells and smooth muscle cells constitute Type II lesions. Foam cells are cholesterol loaded macrophages displaying a “foamy” appearance and are typically present in atherosclerotic lesions. Type III lesions, which are termed preatheromas, consist of scattered extracellular lipid pools lying below layers of foam cells that disrupt smooth muscle cell organization.

Formation of a lipid core that is postulated to form from the extracellular lipid pools in Type III lesions distinguished Type IV lesions from Type III and atherosclerotic lesions from this stage onwards are considered to be advanced. Type V lesions are classified as lesions in which prominent new fibrous connective tissue is formed and a fibrous cap is developed. When disruption of the plaque surface, hematoma or hemorrhage and thrombotic deposits occurs in Type IV or Type V lesions, the lesions then become Type VI lesions.

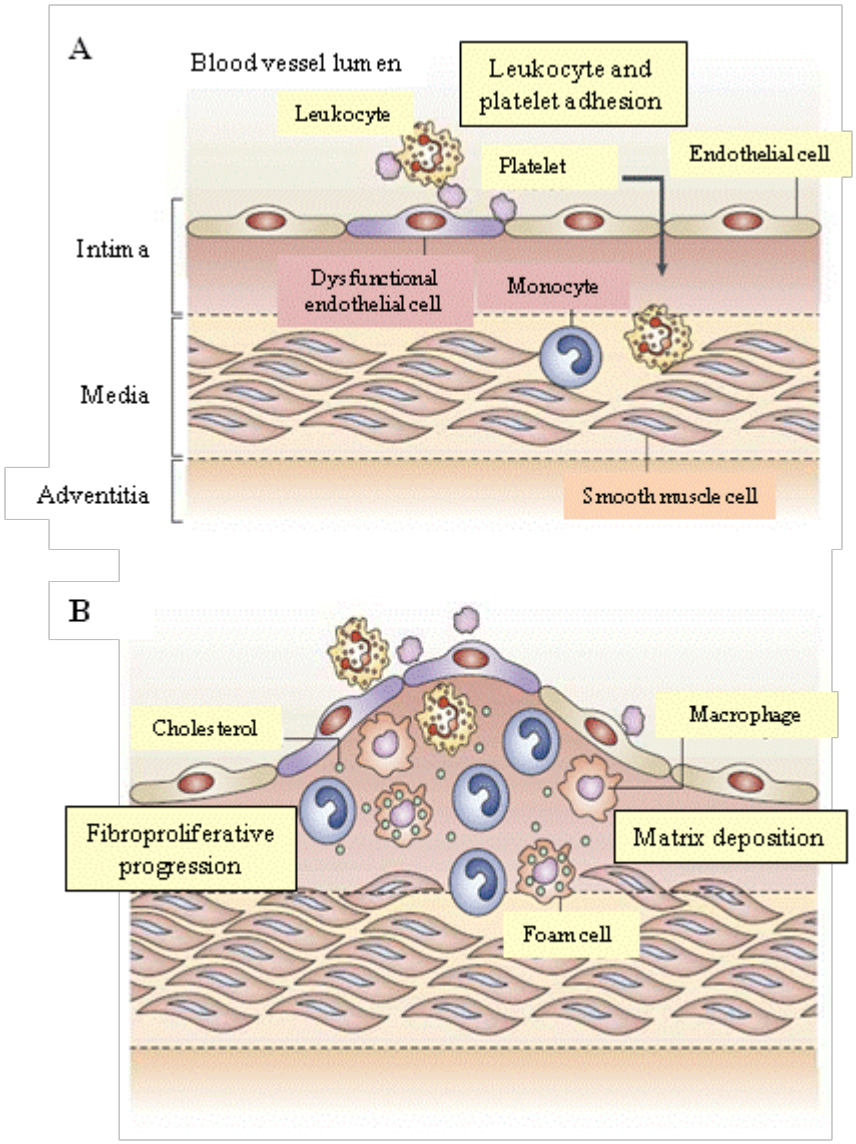

Figure 1.5. Stages in the development of atherosclerosis.

(A) Endothelial-cell dysfunction and activation under hyperlipidemia led to increased leukocyte adhesion and increased permeability of endothelium (Type I lesion). (B) Monocytes are recruited to the intima, accumulate lipids and transform into foam cells. Fibroproliferative plaques result from the continual mononuclear cell infiltration and smooth muscle cell recruitment (Type II and III lesion). (C) Apoptosis of foam cells leads to necrotic core formation and a fibrous cap of smooth muscle cells forms on top of the plaque at this stage (Type IV and V lesion). (D) Thinning of fibrous cap in unstable plaques lead to plaque rupture and activation of coagulation system and thrombosis (Type VI lesion). Adapted and modified from (Weber et al., 2008).

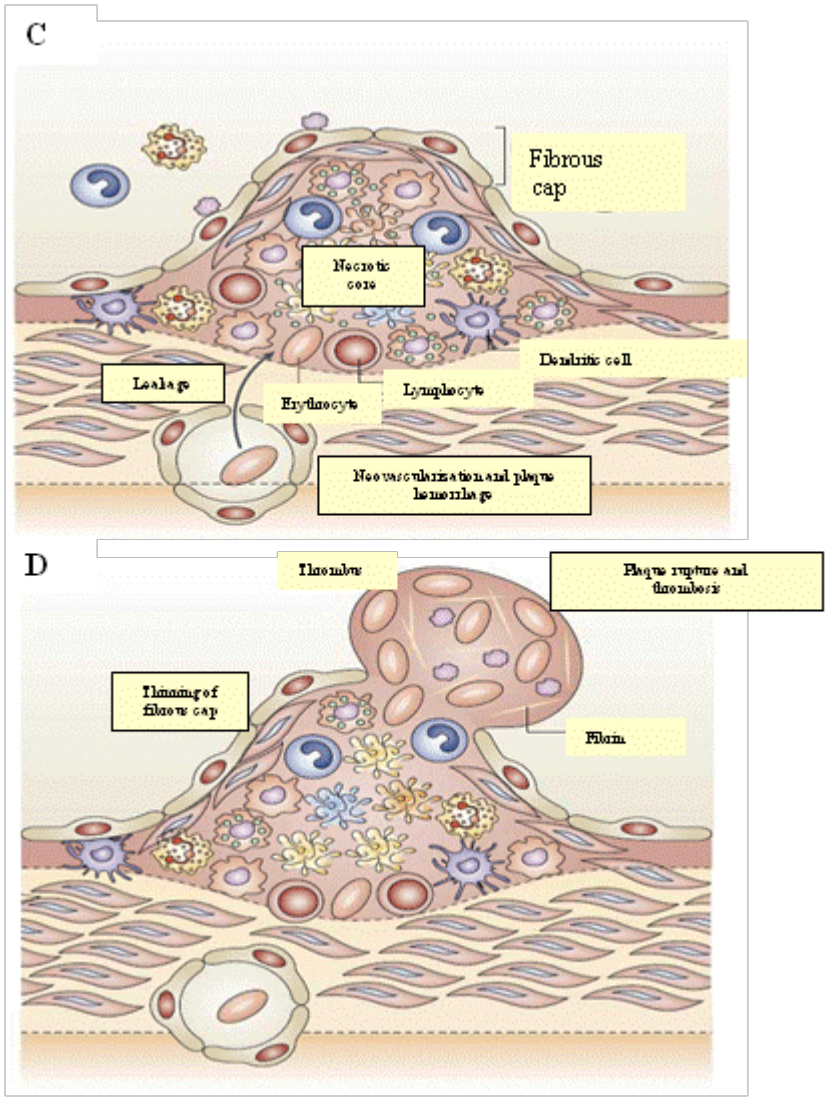
C
Fibrous cap
Necrotic core
Dendritic cell
Lumen
Lymphocyte
Erythrocyte
Neovascularization and plaque hemorrhage
D
Thrombus
Plaque rupture and thrombosis
Thinning of fibrous cap
Fibrin

1.6 Animal models of atherosclerosis

Much of what we know about atherosclerosis came about with animal models of atherosclerosis and there are many available in the field. However, mouse models are preferred over the larger animal models mainly due to the ease of genetic manipulation and a shorter period for disease development (Getz and Reardon, 2012). The two most commonly used mouse model of atherosclerosis are: apolipoprotein E-deficient ($apoE^{-/-}$) and low-density lipoprotein receptor-deficient ($Ldlr^{-/-}$) mice.

ApoE was first discovered as a lipoprotein constituent of very low density lipoprotein (VLDL) in 1973 (Shore and Shore, 1973). It is also part of a subclass of high density lipoproteins (HDL) and chylomicrons. Patients with type III hyperlipoproteinemia showed an accumulation of apoE-enriched β-VLDL (Havel and Kane, 1973). Coupled with the observations that apoE became a major constituent of cholesterol-enriched lipoproteins that accumulated in monkeys fed with cholesterol (Mahley et al., 1976), it was clear that apoE plays a major role in cholesterol metabolism. Since apoE functions as a ligand for lipoprotein recognition and clearance by lipoprotein receptors, $apoE^{-/-}$ mice have a delayed clearance of lipoproteins, resulting in severe hypercholesterolemia in these mice. $ApoE^{-/-}$ mice developed atherosclerotic lesions spontaneously on normal chow diet but the disease progression is accelerated when the mice are fed a high fat, rich cholesterol, diet (Nakashima et al., 1994).

Ldlr is a surface glycoprotein that regulates plasma cholesterol by mediating endocytosis of LDL and is the receptor for apoE. Mutations in this gene caused familial hypercholesterolemia in humans with cutaneous xanthomas (Hobbs et al., 1990). $Ldlr^{-/-}$ mice were created to recapitulate the characteristics of this disease. $Ldlr^{-/-}$ mice only develop atherosclerosis when placed on a high fat, rich cholesterol diet and display widespread xanthomatosis (Ishibashi et al., 1994).

Typically, Type I to Type V lesions can be observed in $apoE^{-/-}$and in $Ldlr^{-/-}$ mice, only lesions up to Type IV have been classified (Whitman, 2004). However, Type VI lesions have been only reported in the inominate arteries of $apoE^{-/-}$ mice (Rosenfeld et al., 2000) and is still a matter of contention (Getz, 2000). The severity of disease observed in $apoE^{-/-}$ mice compared to $Ldlr^{-/-}$ mice is due to a receptor known as LDLR-related protein (LRP). In mice, apolipoprotein B48 (apo-B48) in the liver uptake lipoproteins via apoE and is dependent on LRP for their clearance from plasma (Veniant et al., 1998).

The pattern of atherosclerosis development in both mouse models is remarkably similar to humans except that mice seldom develop atherosclerosis in coronary arteries and do not exhibit unstable atherosclerotic plaque with features of thrombosis (Getz and Reardon, 2012; Reddick et al., 1994).

1.7 Dendritic cells

Dendritic cells are one of the predominant immune cell types found in atherosclerotic plaques (Libby et al., 2013; Shimada, 2009; Weber et al., 2008; Woollard, 2013). The first account of dendritic cells (DCs) describing their stellate morphology was attributed to Steinman and Cohn (Steinman and Cohn, 1973). DCs are the most potent antigen-presenting cells (APCs) in the immune system and have an unparalleled ability in priming naïve T cells (Liu, 2001; Steinman, 1991). Their functions in the immune system can be summarized as follows: 1) as sentinels, they can sample the environment to uptake, process and present antigens; 2) migrate to lymph nodes where they can activate the adaptive immune response; 3) as cross-presenting APCs, they regulate $CD8^+$ T cell tolerance and initiate anti-viral and anti-tumor immunity (Brode and Macary, 2004; Hart, 1997; Joffre et al., 2012; Shortman and Liu, 2002).

1.7.1 Ontogeny of DCs

Since DCs have a limited lifespan, they are thought to be replenished by circulating precursors in the blood (Liu et al., 2007) or local tissue-derived precursors (Naik et al., 2006). Recent literature has revealed that progenitors for DCs exist in the bone marrow (Auffray et al., 2009a; del Rio et al., 2008; Fogg et al., 2006; Liu et al., 2009; Naik et al., 2007; Onai et al., 2007) (Figure 1.6).

In the bone marrow, macrophage and DC progenitor (MDP) is the first step towards commitment to DC lineage. MDP is identified by CX_3CR1, c-kit, Flt3, CD115 and does not express markers for lineage-committed cells. They are able to differentiate into monocytes, macrophages and steady state DCs in vivo, having lost the potential for giving rise to granuloctyes, erythrocytes and megakaryocytes (Fogg et al., 2006; Liu et al., 2009).

Common DC progenitor (CDP), defined similarly as MDP but expressing a lower expression of c-kit was discovered later as a descendent of MDP. CDP is only able to generate plasmacytoid DCs (pDCs) and DCs in vivo (Naik et al., 2007; Onai et al., 2007). An intermediate population known as pre-DC is produced from CDP. Pre-DCs do not possess lineage markers and start expressing CD11c, distinguishing them from MDP and CDP. They can be found in the bone marrow, blood, spleen and lymph nodes (Liu et al., 2009) and are able to give rise to non-lymphoid tissue DCs in the liver and kidney (Ginhoux et al., 2009).

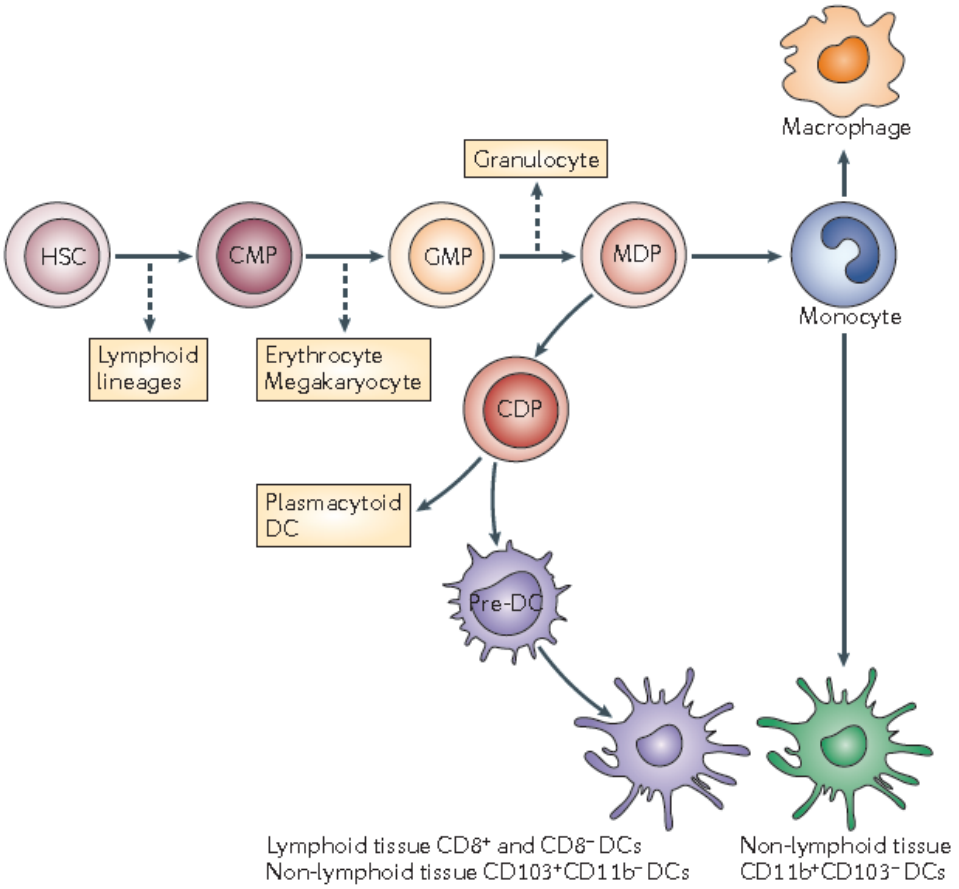

Figure 1.6. Dendritic cell lineage.

The two main DC precursors in the bone marrow are MDP and CDP. MDP gives rise to monocytes and CDP. Monocytes can become either macrophages or DCs. CDP subsequently becomes pre-DCs that exits from the bone marrow into circulating blood and into tissues to differentiate into lymphoid and non-lymphoid tissue DCs. HSC, hematopoietic stem cell; CMP, common myeloid progenitor; GMP, granulocyte and macrophage progenitor; CDP, common DC progenitor; MDP, macrophage and DC progenitor. Adapted from (Chow et al., 2011)

1.7.2 Heterogeneity of DCs in mice

With a multitude of functions to play, it is expected that DCs are made up of different subpopulations diverse in functions and origin and differ in their migratory abilities. They can be categorized into two groups: conventional and non-conventional DCs.

Conventional DCs (cDCs) are further subdivided into lymphoid-tissue-resident DCs and migratory DCs (Shortman and Naik, 2007). In mice, lymphoid-tissue-resident DCs can be separated into $CD8\alpha^+$ ($CD205^{hi}$ $CD11b^-$) and $CD8\alpha^-$ cDCs ($CD205^-$ $CD11b^+$) (Vremec et al., 2000). Both subtypes differ in cytokine production and immune functions (Shortman and Heath, 2010). $CD8\alpha^-$ DCs can be segregated into $CD4^+CD8\alpha^-$ and $CD4^-CD8\alpha^-$ subsets.

There are an additional two DC subsets in lymph nodes that are not found in the spleen because they are tissue-derived migratory DCs. They are distinguished by their expression of CD11b and CD103 ($CD4^-CD8\alpha^-$ $CD11b^+$ $CD103^-$ and $CD8\alpha^-$ $CD11b^-$ $CD11b^-$ $CD103^+$) (Henri et al., 2001). With the exception of mesenteric lymph node (Bogunovic et al., 2009) and pancreatic islet lymph node (Yin et al., 2012), $CD11b^+$ $CD103^+$ DCs do not exist in other draining lymph nodes. Another subset, Langerhans cells (LCs) ($CD8\alpha^-$ $CD11b^+$ $CD205^+$ $Langerin^+$) are present only in cutaneous draining lymph nodes (Bursch et al., 2007; Merad et al., 2008).

On the other hand, unique in their ability to produce high amounts of interferon-α (IFN-α), pDCs are classified as non-conventional DCs (Kushwah

and Hu, 2011; Shortman and Naik, 2007). pDCs are thus named for their plasma cell-like morphology and their expression of the B cell marker, B220. Not only distinct in function, pDCs are markedly different in their phenotype ($B220^{+}$ $Gr\text{-}1^{+}$ $CD11c^{low}$) (Martin et al., 2002; Nakano et al., 2001) and can be further characterized by expression of Siglec-H (Blasius et al., 2006a), CCR9 (Wendland et al., 2007), PDCA-1 (Bierly et al., 2008; Blasius et al., 2006b) and lymphocyte activation marker-3 (LAG-3) (Workman et al., 2009).

1.7.3 DCs in atherosclerosis

DCs are key players of VALT and form immunological synapses with T lymphocytes in inflammatory infiltrates of atherosclerotic lesions and aortic aneursyms (Bobryshev and Lord, 2001). During steady state, indigenous DC populations can be found at the media-adventitia junction (Han et al., 2008; Pryshchep et al., 2008). They are capable of sensing pathogens and respond to TLR ligands such as LPS in bioengineered arteries. They could induce autologous T cell activation and accumulation, leading to breakdown of self-tolerance (Han et al., 2008).

Most vascular DCs in human atherosclerotic lesions exhibit a mature phenotype (Kawahara et al., 2007). Activated DCs in the plaque in close contact with T cells often express markers such as CD40, CD83, CD86 and HLA-DR that is used for co-stimulation in T cell activation. Vascular DCs also produced chemokines such as CCL19 and CCL21 that can regulate T cell trafficking into the lesion (Erbel et al., 2007). These DC-T cell interactions

were shown to promote atherosclerosis by production of pro-inflammatory cytokines such as TNF-α and IFN-γ which sustained chronic inflammation (Koltsova et al., 2012).

Giant cell arteritis (GCA), a granulomatous vasculitis that affects medium- and large-sized arteries is remarkably similar to atherosclerosis. Vascular DCs can be found at the media-adventitia border and they are enriched and activated in arteries affected by GCA. Moreover, activated DCs in GCA produced CCL19 and CCL21, leading to their immobilization in GCA lesions (Krupa et al., 2002; Ma-Krupa et al., 2004).

Vascular DCs may also play a role in cholesterol homeostasis as short-term depletion of these cells has been shown to enhance hypercholesterolemia (Gautier et al., 2009).

1.7.4 Heterogeneity of DCs in atherosclerosis

Earlier studies on DCs in the aorta in atherosclerosis focused on generic $CD11c^+$ DCs (Choi et al., 2009; Galkina et al., 2006; Jongstra-Bilen et al., 2006). However, it is increasingly obvious that aortic DCs are also heterogeneous.

Resident aortic DCs ($CD11c^+$ $CD11b^-$ $CD68^+$ MHC-II^+ $33D1^+$) are capable of lipid uptake, which contributes to foam cell formation (Paulson et al., 2010). They accumulate in atherosclerotic lesions by proliferation in response to GM-CSF (Zhu et al., 2009).

In contrast, CCL17^{+} DCs (CD11c^{+} CD11b^{+} CD8α^{-} CD115^{-} F4/80^{-} PDCA-1^{-}) are not found in steady state but accumulates during atherosclerotic lesion development and are found to drive the disease by limiting regulatory T cell homeostasis (Weber et al., 2011).

pDCs have been observed in human and murine atherosclerotic lesions and the role of pDCs in experimental atherosclerosis is controversial (Grassia et al., 2013). Although they are rare in atherosclerotic plaques, specific depletion of pDCs in Ldlr$^{-/-}$ mice worsened atherosclerotic lesions due to loss of suppressive effect of pDCs on T cell proliferation in the periphery (Daissormont et al., 2011). On the contrary, in apoE$^{-/-}$ mice, depletion of pDCs reduced atherosclerosis by dampening T cell activation and induction of systemic reduction of pro-atherosclerotic mediators such as IL-12 (Macritchie et al., 2012). The contradicting data may be due to the use of different depleting antibodies and mouse models but it does not negate the fact that pDCs are one of the players in atherosclerosis.

Following the widely recognized characterization of non-lymphoid tissue DC subsets (Helft et al., 2010), two DC subsets, namely CD103^{+} (CD11b^{-} F4/80^{-}) and CD11b $^{+}$ (CD103^{-} F4/80^{+}) DC subsets have been described in normal murine aorta and both were expanded in atherosclerotic Ldlr$^{-/-}$ mice (Choi et al., 2011). In this latter study, lack of CD103^{+} DCs increased atherosclerotic lesions and was associated with a reduction in regulatory T cells, suggesting that CD103^{+} DCs are athero-protective.

Lastly, not to be confused with CCL17^{+} DCs, CD11b^{+} CD11c^{+} DCs that express F4/80 antigen are another DC subset that can be found accumulating

in atherosclerotic aorta. They are capable of prolonged interaction with $CD4^+$ T cells, leading to T cell activation, proliferation and production of pro-inflammatory cytokines. This in turn supported foam cell formation by increasing uptake of modified lipoproteins by macrophages (Koltsova et al., 2012).

1.8 Monocytes

Monocytes are circulating blood leukocytes derived from bone marrow progenitors that can further differentiate into macrophages and dendritic cells (DCs). They are also one of the key players in the initiation of atherosclerosis development.

1.8.1 Phenotype and function of murine monocyte subsets

Circulating monocytes in mice express CD115, F4/80 and CD11b. They are divided into two subsets: classical $Ly6C^{hi}$ and non-classical $Ly6C^{low}$ monocytes (Geissmann et al., 2003). The subsets are further distinguished by the chemokine receptors and adhesion molecule they express (Shi and Pamer, 2011). $Ly6C^{hi}$ monocytes express CCR2, CD62L and have low expression of CX_3CR1 whereas $Ly6C^{low}$ monocytes express high levels of CX_3CR1 but do not express CCR2 and CD62L (Auffray et al., 2009b).

Developmentally, $Ly6C^{hi}$ monocytes are precursors of $Ly6C^{low}$ monocytes. Based on depletion by clodronate liposomes, $Ly6C^{hi}$ monocytes were found to repopulate first in circulation and give rise to $Ly6C^{low}$ monocytes (Sunderkotter et al., 2004).

In terms of function, $Ly6C^{hi}$ monocytes are specifically recruited to inflammatory sites where they give rise to effector APCs (Auffray et al., 2009a; Geissmann et al., 2003; Palframan et al., 2001; Serbina and Pamer,

2006; Sunderkotter et al., 2004; Zigmond et al., 2012), thus earning their title as "inflammatory" monocytes. Ly6C^{hi} monocytes depend on CCR2 for mobilization from bone marrow into the circulation (Tsou et al., 2007).

On the other hand, Ly6C^{low} monocytes are termed as "resident" monocytes as they reside longer in peripheral tissues in the absence of inflammation (Geissmann et al., 2003; Sunderkotter et al., 2004). They depend on CX_3CR1 for homing to peripheral tissues (Geissmann et al., 2003). The function of Ly6C^{low} monocytes was only recently described. Due to observations that this monocyte subset exhibit "crawling" behavior and stay within blood vessels in steady state, they appear to function as patrollers of blood vessels (Auffray et al., 2007). Owing to their patrolling behavior, Ly6C^{hi} monocytes are able to extravasate rapidly in response to tissue damage, aseptic wounding and peritoneal infection with *Listeria monocytogenes* and are responsible for early inflammatory response against *Listeria monocytogenes*.

The dichotomy in function of the two monocyte subsets was also shown in the healing mycocardium whereby Ly6C^{hi} monocytes were first recruited with inflammatory functions to digest damaged tissue and Ly6C^{low} monocytes were mobilized later to attenuate inflammation and promote healing (Nahrendorf et al., 2007).

1.8.2 Monocyte subsets in atherosclerosis

Prior to lesion development, monocytes are the major immune cell component in the intima of lesion-prone areas and constitute the major source of foam cells in early lesion formation (Gerrity, 1981). Although neutrophils are known to be involved in atherosclerosis (Soehnlein, 2012), we focused on monocytes due to their developmental relationship with DCs. It has been shown that neutrophilia occurred as early as 4 weeks after high fat diet induction in the bone marrow and aorta under the influence of granulocyte colony-stimulating factor (G-CSF). However, neutrophil count in the aorta decreased over time during atherosclerosis progression (Drechsler et al., 2010) and almost returned to baseline count after 16 weeks of high fat diet. In addition, the study has shown that in comparison to mice with normal white blood count after 1 month of high fat diet, the reduction of $CD45^+$ leukocytes in the aorta of neutropenic mice reduced mainly neutrophils, inflammatory monocytes and macrophages. However, aortic DCs and $Ly6C^{low}$ monocytes were unaffected.

The importance of monocytes in atherosclerosis is highlighted when plaque burden is reduced in rabbits administered with clodronate liposomes to deplete circulating monocytes (Ylitalo et al., 1994). In addition, depletion of $CD11b^+$ cells resulted in a reduction of monocytes and plaque lesion size during initial phase of atherosclerosis (Stoneman et al., 2007). However, depletion by CD11b is not specific and may affect other populations that express it. In a disease regression model, plaque macrophage content was reduced and this

effect was attributed to suppression of monocyte recruitment (Potteaux et al., 2011).

Similar to *Listeria monocytogenes* infection, monocytosis developed in hypercholesterolemic apoE$^{-/-}$ mice (Ingersoll et al., 2011). Interestingly, hypercholesterolemia led to a skewing towards Ly6C^{hi} monocytosis, disrupting the 50:50 ratio of Ly6C^{hi}:Ly6C^{low} monocyte profile in the blood (Swirski et al., 2007; Tacke et al., 2007). Ly6C^{hi} monocytosis occurred as a result of increased survival, cell proliferation and impaired conversion of Ly6C^{hi} to Ly6C^{low} monocytes (Swirski et al., 2007). However, under moderate hypercholesterolemia conditions, both Ly6C^{hi} and Ly6C^{low} monocytes accumulated in circulating blood (Combadiere et al., 2008). In a recent study, ApoE complementation to apoE$^{-/-}$ mice reduced monocytosis, suggesting that ApoE itself regulates monocytosis (Murphy et al., 2011).

Since both monocyte subsets possess different chemokine receptor profile, studies were undertaken to investigate their dependence on chemokines in entry into atherosclerotic plaques. Despite expressing low levels of CX_3CR1, Ly6C^{hi} monocytes unexpectedly depend on CX_3CR1 to enter atherosclerotic lesions (Tacke et al., 2007). Ly6C^{hi} monocytes were also dependent on CCR2 for trafficking to atherosclerotic plaques at two levels: one at the level of egress from the bone marrow and the other is trafficking from blood into plaques. In the same study, Ly6C^{low} monoctyes were surprisingly independent of CX_3CR1 for their accumulation in atherosclerotic plaques. Neither were they dependent on CCR2 but their migration into the atherosclerotic plaques was partially dependent on another chemokine receptor, CCR5. Thus, to abolish both Ly6C^{hi} and Ly6C^{low} monocyte accumulation in atherosclerotic

plaques, combined inhibition of CCL2, CX_3CR1 and CCR5 is needed. Indeed, inhibition of all three signals abrogated monocytosis and reduced lesion size (Combadiere et al., 2008).

1.9 Monocyte-derived cells

Monocytes are plastic cells that can terminally differentiate into macrophages and dendritic cells (Gordon and Taylor, 2005; Leon and Ardavin, 2008). They were initially thought to only give rise to tissue macrophages at steady state (Dominguez and Ardavin, 2010).

However, evidence of monocyte-derived DCs (MoDCs) at steady state is becoming apparent. Adoptive transfer of monocytes into recipient mice that were first depleted of DCs showed efficient seeding and differentiation of donor monocytes into DCs in lamina propria (Bogunovic et al., 2009) and lung parenchyma but not into splenic cDCs (Varol et al., 2007). Furthermore, employing latex bead labeling for monocytes, $Ly6C^{hi}$ and $Ly6C^{low}$ monocytes were shown to differentiate into two different DC subsets, $CD103^{+}$ and $CD11b^{+}$ DCs respectively in the lung at steady state (Jakubzick et al., 2008). $Ly6C^{low}$ monocytes are also able to differentiate into lung macrophages at the same time (Landsman et al., 2007). Otherwise, recovery of adoptively transferred monocytes proved to be challenging at steady state in other non-lymphoid tissues (Ginhoux et al., 2009). Recently, MoDCs in skeletal muscles at steady state have been identified using the marker, CD64 (Langlet et al., 2012), which perhaps will pave the way in studying MoDCs at steady state.

Nonetheless, the discovery of this cell type *in vivo* was originally first made during inflammatory conditions because of the large numbers of MoDCs generated during inflammation. Of interest, a DC subset that arises during inflammation is the TNF-α/iNOS-producing DCs (TipDCs) and is important in the clearance of *Listeria monoctyogenes* infection in mice infected with the bacteria (Serbina et al., 2003). TipDCs arise from $Ly6C^{hi}$ monocytes and express CD11b and Mac-3. They have high expression of MHC class II and Ly6C and low expression of CD11c. As its name suggests, they produce high levels of TNF-α and iNOS. TipDCs are required for $CD8^+$ T cell response in influenza virus infection (Aldridge et al., 2009) and contribute to pathogenesis of psoriasis (Lowes et al., 2005). They can also be naturally occurring in MALT where they regulate IgA production important for gut homeostasis (Tezuka et al., 2007).

In atherosclerosis, $Ly6C^{hi}$ monocytes were shown to differentiate into macrophages (Swirski et al., 2007) whereas $Ly6C^{low}$ monocytes were associated with $CD11c^+$ DCs in atherosclerotic plaques (Tacke et al., 2007). Consequently, different monocyte subsets are able to differentiate into different cell types during steady state and inflammation.

1.10 Aims and rationale

Heterogeneity of DCs in atherosclerosis is a recent insight. The disparate characterization of DC subsets in atherosclerotic aorta and the use of different experimental mouse models of atherosclerosis make it challenging to identify and compare findings. However, the recent classification of DC subsets in non-lymphoid tissues provides a platform for a standardized classification of DC subsets in atherosclerotic aorta. Insofar, the focus of literature has been on $CD103^+$ DC subsets. Little is known about the $CD11b^+$ DC subset in the $apoE^{-/-}$ mouse model. In this study, we first examined and characterized $CD11b^+$ DCs at steady state, whether they accumulate in $apoE^{-/-}$ mouse model and their localization. Subsequently, once we had established their existence and accumulation in atherosclerotic $apoE^{-/-}$ aorta, we investigated the origin of these cells and the mechanisms by which they accumulate. Lastly, the function of this DC subset in atherosclerosis was explored.

Chapter 2

Materials and Methods

Chapter 2 – Materials and Methods

2.1 Mouse models

Heterozygous $CX_3CR1^{+/gfp}$ and transgenic Mafia [C57BL/6-Tg(Csf1r-EGFP-NGFR/FKBP1A/TNFSRSF6)2Bck/J] (Burnett et al., 2004) were kindly provided by Dr. Florent Ginhoux (Singapore Immunology Network, A*STAR). $ApoE^{-/-}$, $Ldlr^{-/-}$, CD45.1 and CD45.2 wild-type (WT) male mice on a C57/BL6 background were obtained from The Jackson Laboratory (Bar Harbor, ME, USA). $ApoE^{-/-}$, $Ldlr^{-/-}$ and CD45.2 wild type littermates were fed normal chow diet (18% protein and > 5% fat; Harlen Teklad, Madison, Wl, USA). At 6 weeks of age, mice were switched to a high-fat diet (21% milk fat and 0.15% cholesterol; Harlan Teklad) for 18 to 22 weeks, corresponding to 24 to 28 weeks of age unless otherwise stated. Mice were maintained under specific pathogen-free conditions with free access to food and water within National University of Singapore's animal housing unit. All studies were approved by National University of Singapore and Biological Resource Center Institutional Animal Care and Use Committee.

2.2 Treatment of Mice

2.2.1 Treatment of mice with Ezetimibe

Oral administration of cholesterol-lowering drug, Ezetimibe (5mg/kg/day) or vehicle (corn oil) to $apoE^{-/-}$ and matching WT mice started at 12 weeks of age when the disease is well advanced and was maintained for 12 weeks.

2.2.2 Treatment of mice with neutralizing anti-GM-CSF antibody

50μg of neutralizing anti-GM-CSF antibody (R&D Systems, MN, USA) was injected intraperitoneally per mouse at the age of 16-18 weeks for 4 days before sacrifice 24 hours later after last injection.

2.3 Isolation of Cells

2.3.1 Isolation of cells from murine aorta

Mice were sacrificed by CO_2 inhalation and aortas were perfused through the heart with 20ml of PBS and thereafter with 10ml of Ca^{2+}/Mg^{2+} Hank's Buffered Salt Solution (HBSS) medium (Sigma, MO, USA) containing 0.1% BSA. Adventitial fat and surrounding lymph nodes were removed and aortas were dissected under a stereomicroscope. Single cells were prepared by cutting aortas into small pieces and digesting in Ca^{2+}/Mg^{2+} HBSS containing 1mg/ml Collagenase Type IV (Gibco, CA, USA) at 37^{o}C for 2 hours. Digested aortas were further disaggregated by passing through a syringe with 19G needle (BD Biosciences, NJ, USA). Cell suspensions were then filtered through a nylon net filter (Millipore, MA, USA) and washed before proceeding to staining for flow cytometry. In most experiments, aortas from 2 mice were pooled and analyzed for flow cytometry unless otherwise stated.

2.3.2 Isolation of bone marrow cells

Femurs and tibiae of mice were cut and the marrow was flushed out with RPMI-1640 (Sigma) complete medium (Appendix 1). The bone marrow suspension was passed through a 30μm cell strainer and centrifuged at 1200 rpm for 5 minutes. The cell pellet was lysed with 0.9% ammonium chloride

solution (Appendix 1) to remove red blood cells, washed with PBS and resuspended in RPMI-1640 complete medium unless otherwise stated. Viable cells were counted with trypan blue (Sigma) viability assay.

2.3.3 Isolation of bone marrow monocytes

Bone marrow cells were isolated as described in Section 2.3.2 except lysis of red blood cells was not performed as advised by manufacturer. Cell pellet was resuspended in EasySep^{TM} buffer (Appendix 1). Monocytes were pre-enriched by EasySep^{TM} immunomagnetic negative selection using the mouse monocyte enrichment kit (STEMCELL, Vancouver, BC, Canada) following manufacturer's instructions. Briefly, the bone marrow cells were incubated with rat serum to block non-specific binding and EasySep^{TM} Mouse Monocyte Enrichment Cocktail was added to label unwanted cells (non-monocytes). This was followed by a washing step and incubating the cell suspension with EasySep^{TM} Biotin Selection Cocktail. EasySep^{TM} D Magnetic Particles were added to form tetrameric antibody complexes with unwanted cells. These magnetically labeled cells were then separated in the presence of a magnetic field, allowing unlabeled monocytes to pass through.

2.3.4 Isolation of cells from blood

Where mice were not sacrificed immediately, facial vein bleed was performed. Otherwise, cardiac puncture was employed to obtain blood. Blood collected was prevented from coagulating by adding 40µl of 0.5M EDTA. Thereafter, blood was lysed with Pharm Lyse^{TM} (BD), washed and resuspended in FACS buffer for staining.

2.3.5 Isolation of cells from spleen

Spleen was removed and digested with 1mg/ml Collagenase Type IV at 37^{o}C as before (Section 2.3.1) for 1 hour and 30 minutes. Tissue pieces were then passed through a 19G needle and 70µm cell strainer (BD Biosciences) to obtain a homogeneous cell suspension. Cell suspension was centrifuged at 1200 rpm for 5 minutes and erythrocytes were lysed with 0.9% ammonium chloride solution, washed and resuspended in FACS buffer.

2.4 Generation of bone marrow-derived dendritic cells

Generation of bone marrow-derived dendritic cells has been described previously (Inaba et al., 1992). Briefly, after isolation of bone marrow cells (Section 2.2.2), cells were counted and cell concentration was adjusted to 1 x 10^6/ml in RPMI-1640 complete medium. Conditioned medium from J558L cell line which contained granulocyte-macrophage colony-stimulating factor (GM-CSF) was added at 1:30 dilution. The cells were then plated at 1ml per well in a 24-well plate and fed every 2 days. On day 6 of culture, the cells were either left unstimulated or stimulated with 1µg/ml *Escherichia coli* LPS, serotype O111:B4 (Sigma).

2.5 Adoptive cell transfer - transfer of CD45.1 monocytes into congenic CD45.2 apoE$^{-/-}$ recipients

4 to 5 x 10^6/200µl of CD45.1^{+} bone marrow monocytes (Section 2.3.3) were intravenously injected into the lateral tail of CD45.2^{+} apoE$^{-/-}$ recipient mice.

2.6 Generation of chimeric mice

$CD45.2^+$ WT mice were lethally irradiated (2 times, 4.8 Gy, 3 hours apart) at 6 weeks of age and reconstituted with 5 x 10^6 cells of $CD45.1^+$ bone marrow cells.

2.7 Proliferation study

Mice were injected intraperitoneally with 1mg EdU (Invitrogen) and euthanized by CO_2 inhalation after 2 hours or 12 hours. Cells from aorta and blood were prepared as described in Section 2.3. Detection of EdU for flow cytometry is detailed in Section 2.9.4.

2.8 Culture of cell line

J558L cell line is a transfected cell line which secretes GM-CSF into its culture supernatant. When cells were first thawed out, they were cultured in IMDM complete medium with Geneticin (G418) (Life Technologies, CA, USA). Once cell line is established, cells were propagated in IMDM complete medium without G418. Culture supernatant from the cells was collected, sterile filtered and stored at -80^{o}C until needed for generation of BMDCs.

2.9 Flow cytometry

The panel of antibodies used for this study is listed under Appendix 2.

2.9.1 Viable cell staining for flow cytometry

Initially, DAPI was used to discriminate between the live and dead cells during flow cytometry. Cells were resuspended in DAPI solution just before flow cytometry acquisition. DAPI negative cells were gated as viable cells. Otherwise, a LIVE/DEAD® Fixable Aqua Dead Cell Stain Kit (Life Technologies) was used according to manufacturer's instructions. Briefly, cells were resuspended in 1ml of PBS and 1 µl of Aqua dye was added, mixed well and incubated for 30 minutes. Cells were then washed with PBS twice before proceeding to surface or intracellular staining for flow. Aqua negative cells were gated as viable cells.

2.9.2 Surface staining for flow cytometry

Cells were stained with fluorochrome-conjugated primary antibodies and matched isotype control antibodies as required in FACS buffer (Appendix 1). Where non-conjugated primary antibodies were used, suitable fluorochrome-conjugated secondary antibodies were applied.

2.9.3 Intracelluar staining for flow cytometry

Intracellular staining of cells for flow cytometry was performed with Intracellular Fixation and Permeabilization Buffer Set (eBioscience, CA, USA) according to manufacturer's instructions. Briefly, after surface antigen staining was performed (Section 2.9.2), cells were fixed by adding fixation buffer for 10 minutes. Fixed cells were then permeabilized by washing in 1x permeabilization buffer. Permeabilized cells were resuspended with antibody or matched isotype control in 1x permeabilization buffer. Cells were washed with 1x permeabilization buffer and resuspended in PBS prior to running flow.

2.9.4 Detection of EdU by flow cytometry

Detection of EdU was carried out with Click-iT® EdU Flow Cytometry Assay Kit (Life Technologies). Prior to staining for EdU, single cells obtained were stained with a Fixable Live/Dead cell stain as previously described. Surface antigens of cells were stained as per normal except staining with PE or PE-tandem conjugated antibodies were only performed after detection of EdU. Cells were fixed with fixative provided in the kit and permeablized with a reaction cocktail (containing a fluorescent azide dye to reveal EdU positive cells) as stated in manufacturer's data sheet and washed before proceeding on to staining with PE or PE-tandem dyes.

2.9.5 Cell counting by beads for flow cytometry

Prior to use, CountBright® Absolute Counting Beads (Life Technologies) were vortexed to ensure consistent concentration of beads. 10µl of beads was added to suspension and mixed well. The counting beads can be gated on an empty fluorescence channel and will appear at the upper right corner of a dot plot. To ensure an accurate determination of cell numbers, at least 1,000 bead events were acquired. The number of cells in each sample was calculated based on the following formula:

No of cells = No of cell events/No of bead events x No of beads

where the no of beads is obtained from a predetermined concentration stated on the product (can vary between lots) multiplied by volume of bead added to samples

2.9.6 Acquisition and analysis for flow cytometry

Stained cell suspensions were acquired on either LSR Fortessa, LSR II (BD Biosciences, CA, USA) with FACS Diva software or on Cyan flow cytometer (Dako, Denmark) with Summit software. Data was analyzed post-acquisition with Flowjo software (Treestar, OR, USA).

2.10 Immunofluorescence staining

2.10.1 Preparation of tissue sections

Aortas were perfused with PBS and fixed in 2% w/v paraformaldehyde with 30% w/v sucrose for at least 6 hours to overnight at 4^{o}C, washed in PBS on a rotator for 2 hours and embedded in tissue freezing compound (Sakura Finetek, CA, USA). 5µm thick tissue sections were cut on a cryostat machine (Leica, Wetzlar, Germany) and mounted on polysine-coated slides (Thermo Scientific, MA, USA) and stored at -20^{o}C.

2.10.2 Staining of tissue sections

Prior to staining, slides were air-dried for at least 2 hours. Sections were first blocked with PBS supplemented with 0.2% BSA for 10 minutes. Primary antibodies were diluted in PBS containing 1% normal mouse serum (Jackson ImmunoResearch Laboratories, PA, USA) and applied to tissue sections kept in humidified chambers for 1 hour at room temperature or overnight at 4^{o}C. Following this, slides were washed 3 times in PBS, 5 minutes each. Suitable fluorochrome-conjugated secondary antibodies raised in different species with minimal cross-reactivity were similarly diluted in PBS containing 1% normal mouse serum and added to tissue sections for 1 hour at room temperature in

the dark. The slides were washed 3 times in PBS, 5 minutes each and subsequently stained with DAPI (1:20,000) (KPL, Maryland, USA) for 5 minutes followed by a final wash in PBS for 5 minutes. Slides were then mounted with cover slips using Dako fluorescent mounting medium (Dako). A list of antibodies used for immunofluorescence staining can be found in Appendix 3.

2.10.3 Staining of tissue sections with tyramide amplification

When tyramide signal amplification (Perkin Elmer) was needed, an additional blocking with 3% hydrogen peroxide to quench endogenous peroxidase was performed for 10 minutes after blocking with BSA. Slides were then washed and primary antibodies applied in the same manner. After washing off the primary antibodies, tissue sections were incubated with peroxidase-conjugated secondary antibodies diluted in PBS with 1% normal mouse serum for 1 hour at room temperature in the dark. The slides were washed in PBS for 3 times, 5 minutes each. Where double signal amplification was required for 2 different antigens, an additional blocking with 3% hydrogen peroxide was performed before the second peroxidase-conjugated secondary antibody was added. Fluorochrome-conjugated tyramide solution (1:50) was prepared using tyramide amplification diluents according to manufacturer's instructions and applied to sections after incubation with peroxidase-conjugated secondary antibodies. Slides were then washed in PBS containing 0.05% v/v Tween-20 for 3 times, 5 minutes each before mounting with Dako fluorescent mounting medium as before.

2.10.4 Preparation of whole mounts

Aortas were perfused with PBS and followed by 2% w/v paraformaldehyde with 30% w/v sucrose. Surrounding adipose tissue was dissected and aorta samples were fixed in 2% w/v paraformaldehyde with 30% w/v sucrose overnight at 4^{o}C, washed in PBS twice and stored at 4^{o}C.

2.10.5 Staining of whole mounts

Endogenous peroxidase in whole aorta samples was quenched by 3% hydrogen peroxide for 2 hours in the dark at 4^{o}C and washed with PBS for 1 hour at room temperature. Samples were blocked with blocking buffer (PBS with 0.5% BSA and 0.3% v/v Triton X-100) at 4^{o}C overnight. Thereafter, samples were washed in washing buffer (PBS with 0.2% BSA, 0.1% v/v Triton X-100 and 0.1M glycine) for an hour on a rotator at room temperature. Staining with antibodies were then carried out as described in Section 2.9.2 and 2.9.3 with the exception that antibodies were diluted in blocking buffer and incubated overnight at 4^{o}C. When tyramide amplification was performed, samples were incubated with fluorochrome-conjugated tyramide solution for at least 3 hours before washing. The aorta samples were cut open and flattened segments were mounted on glass slides with Dako fluorescent mounting medium.

2.10.6 Acquisition of images

Images were captured with a fluorescence microscope (Axio imager.Z1, Axiocam HRM camera; Carl Zeiss Micro Imaging, Inc., Jena, Germany). Images were processed with Axiovision software.

2.11 Quantitative gene expression analysis

2.11.1 RNA extraction and Reverse-Transcriptase Polymerase Chain Reaction (RT-PCR)

Adventitial fat was removed from aorta samples and aortas were divided into thoracic and abdominal regions before placing them into RNAlater™ (Qiagen, CA, USA) for archival storage at -80°C until homogenization can be performed. Samples were transferred into Trizol® solution (Invitrogen) and homogenized with Omni Bead Ruptor Homogenizer (Omni International, GA, USA). Extraction of total RNA was performed with Nucleospin® RNA II kit (Macherey-Nagel, Dueren, Germany) according to the manufacturer's instructions. Messenger RNA (mRNA) concentrations and purity were measured with Nanodrop 1000 Spectrophotometer™ (Thermo Scientific). RT-PCR was carried out using TaqMan® Reverse Transcription Reagents (Applied Biosystems, CA, USA) and Thermal Cycler (Applied Biosystems) as follows:

1. A reaction mixture consisting of:
    a. 1000ng mRNA
    b. 1.25µM oligo-dT
    c. 1.25µM random hexamer
    d. 2.5mM dNTPS (500µM per dNTP)

    was prepared.

2. Tertiary structure of mRNA was first linearized by placing the reaction mixture under the following conditions:

Step	1	2	3
Time	5 minutes	2 minutes	Infinite
Temperature	65^{o}C	4^{o}C	4^{o}C

3. A master mix containing the following reagents:

	Working Concentration
10x RT buffer	1x
25mM $MgCl_2$	5.5mM
RNase Inhibitor (20U/L)	0.4U/µl
Multiscribe Reverse Transcriptase	1.25U/µl

was added to the previous reaction mixture.

4. The following thermal cycling parameters was used for the final mixture for cDNA synthesis:

Step	Incubation	Reverse Transcription	Reverse Transcription Inactivation	Hold
Time	10 minutes	30 minutes	5 minutes	Infinite
Temperature	25°C	48°C	95°C	4°C

2.11.2 Real – time polymerase chain reaction (qPCR)

A mixture containing: 1µl of template cDNA, 10µl of iTaq™ SYBR® Green supermix with ROX (Biorad, CA, USA), 250nM gene-specific primers and 7µl of RNase-free water was prepared and real-time PCR was performed in a 7500 Real-Time PCR System (Applied Biosystems) under the following thermal cycling conditions:

Step	Activation of enzyme	PCR		
		Cycle (40 cycles)		
		Denaturation	Annealing	Extension
Temperature	95°C	95°C	55°C	72°C
Time	10 minutes	30 seconds	1 minute	1 minute

Data was acquired at the extension phase. After 40 cycles of PCR, a dissociation curve analysis was also carried out by cooling to 55°C for 1 minute and increasing the temperature to 95°C. Measurement of the changes in

fluorescence was measured simultaneously and plotted against temperature, allowing the discrimination between specific and non-specific PCR products. Target gene expression was analyzed by normalizing to expression of the endogenous control GAPDH. List of genes and primer sequences can be found in Appendix 4.

2.12 Enzyme-Linked Immunoabsorbent Assay (ELISA)

Aortas removed of adventitial fat were harvested and placed in a lysis solution, RIPA buffer (Sigma) with protease inhibitor cocktail (Roche Diagnostics, IN, USA) and homogenized with Omni Bead Ruptor Homogenizer. Supernatants were collected after centrifugation for 10 minutes at 4^{o}C at 14000g and measured for GM-CSF using a commercial GM-CSF ELISA kit (R&D Systems, MN, USA) according to manufacturer's instructions.

2.13 Statistical analysis

Data were analyzed with Prism 5 (GraphPad Software, Inc., CA, USA). Mann-Whitney U test or unpaired Student's t test with two-tailed distributions was used to compare two groups. p-values of less than 0.05 were considered significant.

Chapter 3

Results

Dendritic cell subsets in murine aorta at steady state and atherosclerosis

Chapter 3 – Dendritic cell subsets in murine aorta at steady state and atherosclerosis

3.1 Introduction

Atherosclerosis is an inflammatory disease of the aorta characterized by lipid accumulation and infiltration of immune cells (Hansson and Hermansson, 2011). Among the heterogeneous population of immune cells present in the atherosclerotic plaque, dendritic cells are known to be the most potent antigen-presenting cell in the immune system. The discovery of vascular DCs in normal arteries of young children (Millonig et al., 2001a) and accumulation of these cells in human adult atherosclerotic lesions (Bobryshev and Lord, 1995b) suggest that DCs may have a role to play in the developing plaques.

Similar to human atherosclerosis, accumulation of DCs in a mouse model of atherosclerosis (Bobryshev et al., 2001) was observed. Vascular DCs were first detected by flow cytometry in the mouse using markers such as CD11c and MHC class II (Choi et al., 2009; Galkina et al., 2006). However, CD11c has been proven to be a non-specific marker for DCs as both macrophages and DCs can express high levels of CD11c in the murine lung (Jakubzick et al., 2008; Vermaelen et al., 2001). In addition, $CD11c^+$ vascular DCs in the intimal layer of murine aorta were shown to be $CD68^+$, a classical marker for macrophages (Jongstra-Bilen et al., 2006), showing that CD11c alone is insufficient to delineate DCs.

With the recent emergence of non-lymphoid tissue DC subsets (Helft et al., 2010), where $CD11b^+$ and $CD103^+$ DC subsets have been identified, the need to redefine DCs in the murine aorta arises. In a recent report, both $CD11b^+$ and $CD103^+$ DC subsets were described in the murine aorta (Choi et al., 2011). However, this study did not extensively characterize the DC subsets and their origin at steady state and focused on the function of $CD103^+$ DC subset in the $Ldlr^{-/-}$ mouse model of atherosclerosis. Furthermore, whether the same DC subsets exist in the $apoE^{-/-}$ mouse model of atherosclerosis and if a particular DC subset or both accumulate in this model remains largely unknown.

Hence, we were interested in establishing a comprehensive phenotypic characterization of the DC subsets and investigating the origin of these DCs in the murine aorta at steady state. Based on steady-state studies, we also investigated the DC subsets in the $apoE^{-/-}$ mouse model of atherosclerosis.

3.2 Results

3.2.1 Similar non-lymphoid tissue dendritic cell subsets are present in normal (or healthy) murine aorta

Akin to other non-lymphoid tissues (Helft et al., 2010) , we show that I-A$^+$ CD11c$^+$ DCs in the murine aorta at steady state can be divided into two populations, CD11b$^+$ and CD103$^+$ (Figure 3.1A). Moreover, CD11b$^+$ DC subset is the dominant DC subset in the murine aorta (approximately 70% of CD11b+ DCs: 10% of CD103+ DCs) as observed in the other non-lymphoid tissues. However, there is no evidence of a discrete population of CD11b$^+$ CD103$^+$ DC subset in the murine aorta as compared to murine intestine (Bogunovic et al., 2009). Consistent with previous report (Ginhoux et al., 2009), the CD11b$^+$ DC subset which lacks CD103 expression, expressed high levels of F4/80 and SIRP-α (Figure 3.1B). Using the heterozygous $CX_3CR1^{+/gfp}$ and Mafia mouse models, we were able to further characterize the two DC subsets. Expectedly, CD11b$^+$ DC subset expressed high levels of CX3CR1 and CD115 whereas CD103$^+$ DC subset did not express these receptors (Figure 3.1B). The DC subsets present in the aorta resembled most non-lymphoid tissues in that the CD11b$^+$ CD103$^+$ DC subset present in lamina propia remains unique to that tissue site possibly due to the existence of microbiota.

A

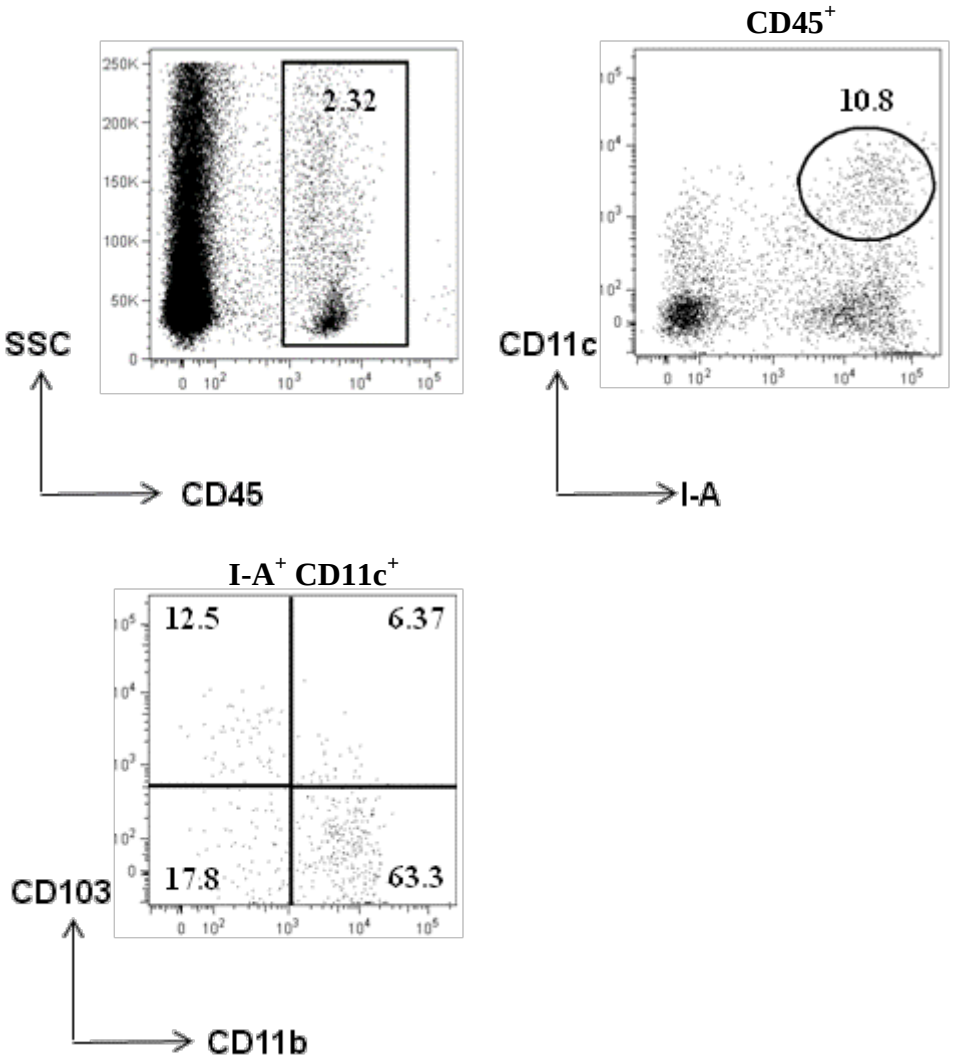
CD45+
2.32
SSC
CD45
10.8
CD11c
I-A
I-A+ CD11c+
12.5
6.37
17.8
63.3
CD103
CD11b

B

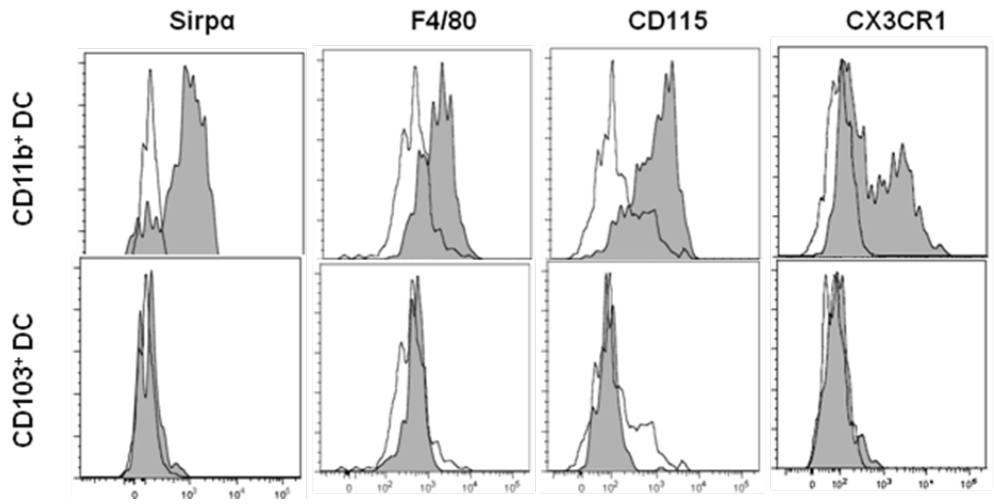

Figure 3.1. DC subsets present in murine aorta at steady state.

(A) After gating for live and singlet cells, aortic DCs were identified as $CD45^+$, $I\text{-}A^+$ and $CD11c^+$ cells and can be distinguished into $CD11b^+$ and $CD103^+$ DCs. (B) Histograms show expression levels (grey) of Sirp-α, F4/80, CD115 and CX_3CR1 with controls (open) on $CD11b^+$ (top panel) and $CD103^+$ DCs (bottom panel). Data shown are representative of 3 independent experiments of 2-3 mice in each experiment.

3.2.2 Aortic DCs are localized in atherosclerosis-prone regions of the murine aorta at steady state

Since the development of atherosclerotic lesions occurs at sites of disturbed blood flow, the aorta is known to be divided into atherosclerosis-prone and atherosclerosis-resistant regions (Jongstra-Bilen et al., 2006; Mullick et al., 2008). Vascular DCs are known to accumulate in atherosclerosis-prone regions. The localization of the DC subsets in murine aorta at steady state has so far been confined to the aortic sinus, cardiac valves and aortic ostium (Choi et al., 2009). Aorta whole mount was cut open longitudinally and laid flat onto microscopic slides for en face analysis. We observed DC subsets being situated at atherosclerosis-prone areas with this method. They were also mainly located in the intimal layer of the murine aorta. Consistent with the results from flow cytometry, the $CD11b^+$ DC subset was the dominant population in the murine aorta and most of them have a dendritic-like morphology (Figure 3.2).

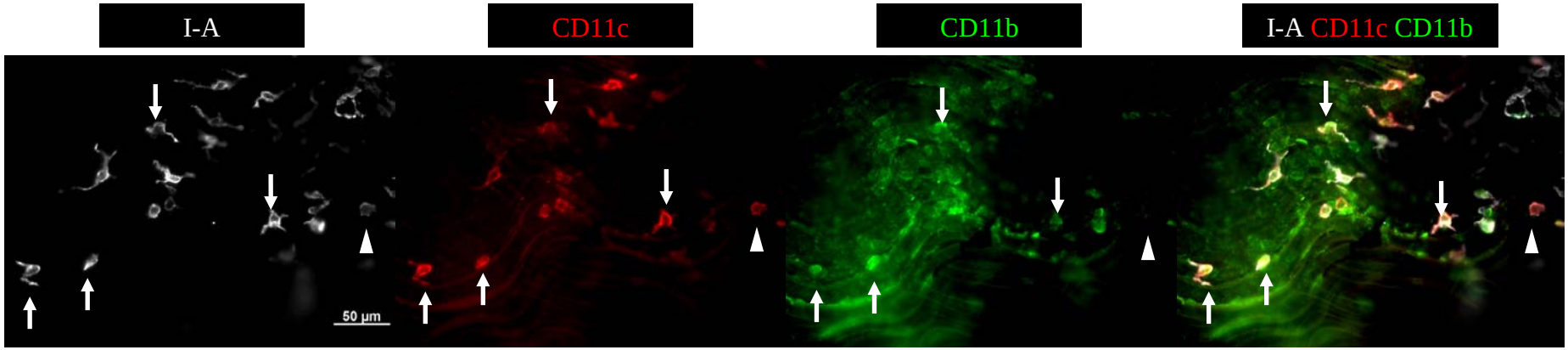

Figure 3.2. Aortic DCs are localized in atherosclerosis-susceptible regions in WT mouse.

Whole mount (adventitial layer removed) immunofluorescent staining revealed the presence of aortic DCs in the intimal layer of aortic arch. $CD11b^{+}$ (arrows) and $CD103^{+}$ (arrowheads) DCs can both be found in this region. Elastic fibers of the aorta are auto-fluorescent; magnification 200X. Scale bar 50µm.

3.2.3 Aortic DCs come from the bone marrow at steady state

During homeostasis, non-lymphoid tissue DCs are known to be generated by hematopoietic cells from the bone marrow with the exception of Langerhans cells (LC) which can self-renew (Helft et al., 2010; Merad et al., 2002). To determine the origin of aortic DCs at steady state, CD45.2 WT mice were irradiated and re-constituted with congenic CD45.1 bone marrow cells. 18 weeks after transplant, when the mice were 24 weeks old, both $CD11b^+$ and $CD103^+$ DC subsets in the aorta were mostly of donor CD45.1 origin (Figure 3.3A and 3.3B). Thus, aortic DCs originate from the bone marrow at steady state and do not have potential for self-renewal.

A

Live cells

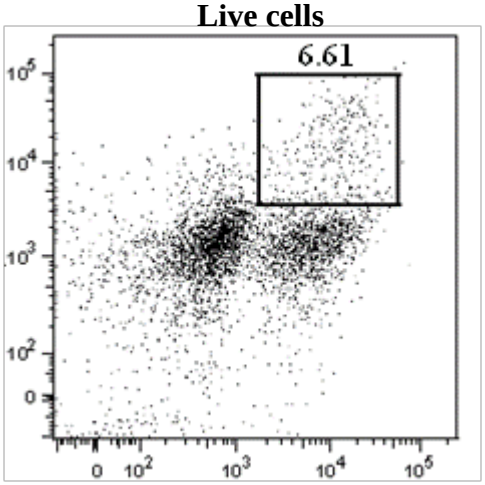

I-A$^+$ CD11c$^+$

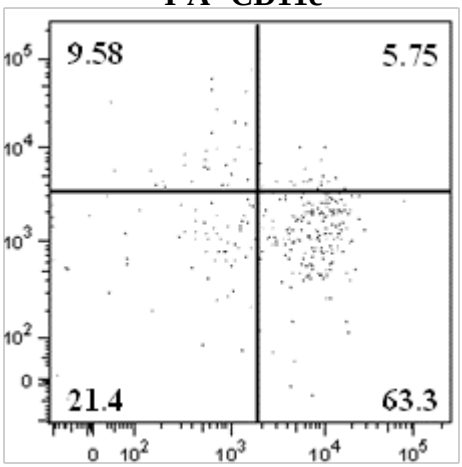

CD11b$^+$ DCs or CD103$^+$

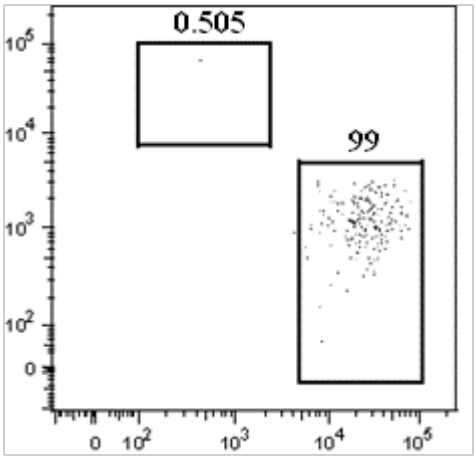

B

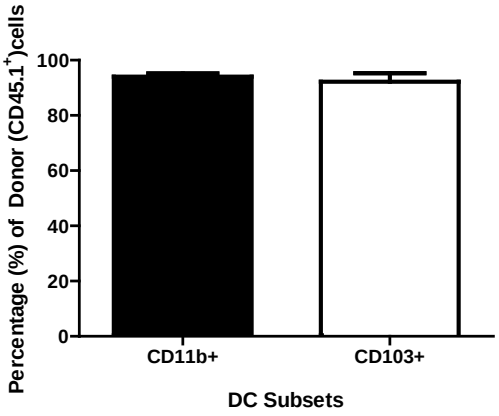

Figure 3.3 Aortic DCs originate from the bone marrow at steady state.

(A) CD45.1 donor WT total bone marrow cells were injected into irradiated congenic CD45.2 WT recipient mice at 6 weeks of age and aortic cell suspensions were analyzed by flow cytometry 18 weeks after the transplant. After gating for live singlet cells which are I-A$^+$ CD11c$^+$, CD11b$^+$ (black) and CD103$^+$ (white) DC subsets were further analyzed for their origin. (B) Bar graph showing percentage of CD11b$^+$ and CD103$^+$ DCs which comes from donor CD45.1$^+$ cells. Data shown are representative of two independent experiments with n = 2. Error bars represent SEM.

3.2.4 Atherosclerosis-induced expansion of both CD11b$^+$ and CD103$^+$ DC subsets in apoE$^{-/-}$ mice

There are two mouse models of atherosclerosis, apoE$^{-/-}$ and Ldlr$^{-/-}$. In apoE$^{-/-}$ mice, atherosclerotic lesions develop spontaneously and development of disease is accelerated with feeding of high fat, rich cholesterol, diet. In contrast, atherosclerotic lesions only develop upon high fat feeding in the Ldlr$^{-/-}$ mice. Both models are widely used for studies in atherosclerosis. As mentioned previously, the study on DC subsets in atherosclerosis mainly focused on the Ldlr$^{-/-}$ mice. To determine if the same DC subsets exist in apoE$^{-/-}$ mice, flow cytometric analyses of aortic cell suspensions were performed.

Consistent with a previous report (Galkina et al., 2006), increased numbers of CD45$^+$ leukocytes and DCs can be observed in apoE$^{-/-}$ mice compared to WT controls (Figure 3.4 and 3.5A). Both CD11b$^+$ and CD103$^+$ DC subsets were found to be significantly increased as a percentage of CD45$^+$ leukocytes and absolute numbers in the apoE$^{-/-}$ mice (Figure 3.5B and 3.5C).

To determine the localization and assess the accumulation of DCs in aortic lesions during progression of atherosclerosis, mice were sacrificed at 10, 16 and 24 weeks of age and sections of aortas were stained with I-A, CD11c and CD11b. Accumulation of DCs mainly occurred in the intima of aorta (Figure 3.6). They were rarely detected in the adventitia. At 10 weeks of age, small foam cell atherosclerotic plaques can be found (Stary et al., 1994) with I-A$^+$

$CD11c^+$ $CD11b^+$ DCs dominating the plaque area (Figure 3.6A). With increasing duration of high fat diet feeding, the atherosclerotic lesions became larger and the localization of $CD11b^+$ DCs was altered. At 16 weeks of age, fatty streak lesions developed (Stary et al., 1994) and plaque $CD11b^+$ DCs were found at the outermost layer of intima (Figure 3.6B). At 24 weeks of age, atherosclerotic plaques that form are usually fibroatheromatous plaques with necrotic core and fibrous caps (Stary et al., 1995; Whitman, 2004). At this stage, plaque $CD11b^+$ DCs mainly localized on the top layer of fibrous plaques (Figure 3.6C) and the shoulder regions (Figure 3.6D).

The localization of plaque $CD11b^+$ DCs on the outermost layer of intima coupled with the observation that $CD11b^+$ DCs were rarely found in the adventitia, indicated that these cells are unlikely to migrate from the ablumenal-lumenal direction (Randolph et al., 1998). Instead, they are formed from newly-formed cells from the circulation. Plaque $CD11b^+$ DCs are also located in plaque shoulders which are sites predisposed to vulnerability and rupture in human atherosclerotic lesions (Finn et al., 2010), suggesting they may have a function in determining plaque vulnerability.

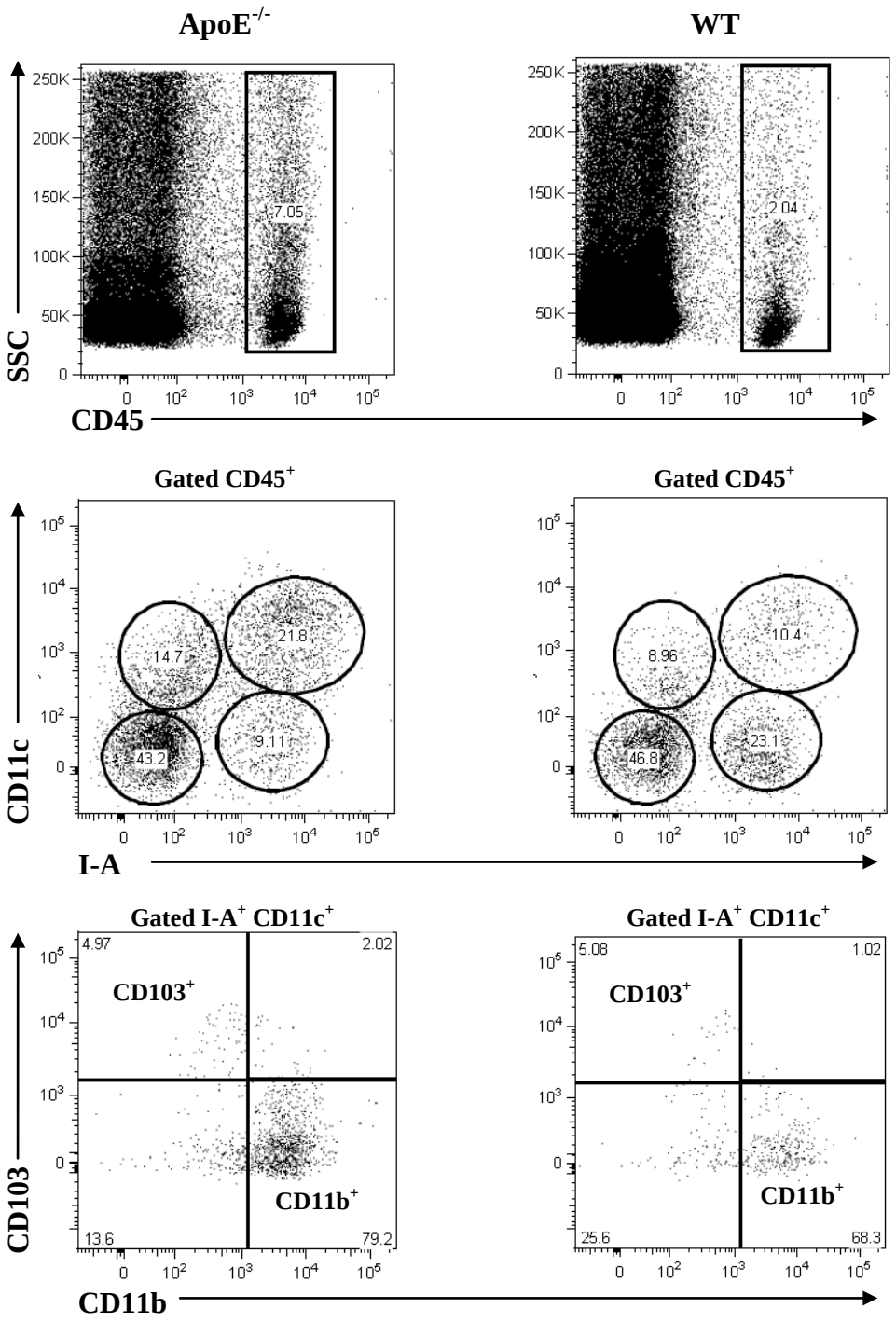

Figure 3.4. Atherosclerosis induced leukocyte infiltration and expansion of DCs in apoE$^{-/-}$ mice.

Representative flow cytometric plots showing increased percentages of leukocytes (CD45^{+}), DCs (I-A^{+} CD11c^{+}) and CD11b^{+} DC subset in apoE$^{-/-}$ mice compared to wild type controls.

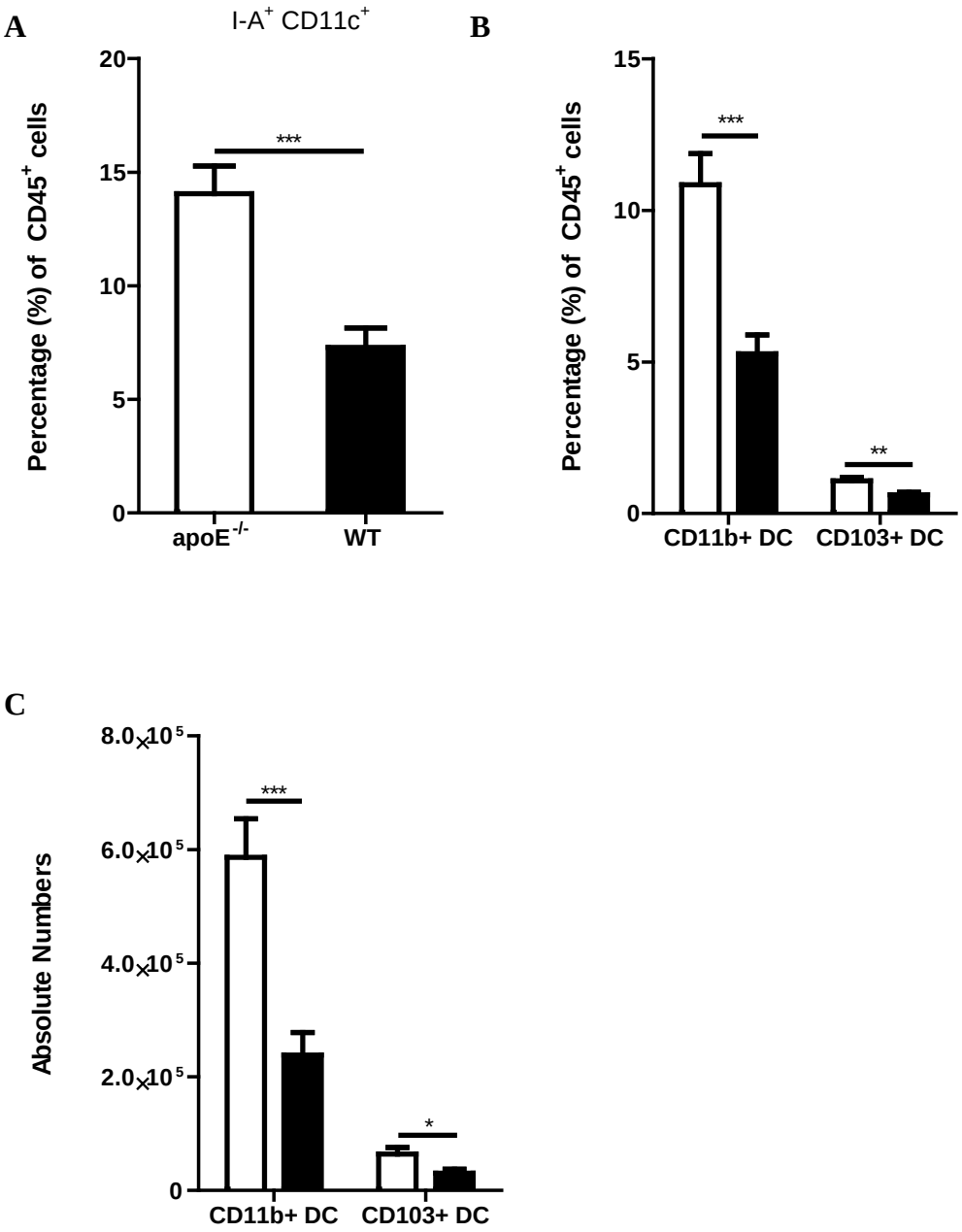

Figure 3.5 Expansion of DCs in apoE$^{-/-}$ mice was due to accumulation of both CD11b^{+} and CD103^{+} DC subsets.

(A) Bar graph showing percentage of I-A^{+} CD11c^{+} DCs in aortas of apoE$^{-/-}$ (white) and WT mice (black). (B and C) Bar graphs showing percentages of CD11b^{+} and CD103^{+} DC subsets as a percentage of total CD45^{+} leukocytes and their absolute numbers in aortas of apoE$^{-/-}$ (white) and WT mice (black) respectively. Data shown are representative of at least 3 independent experiments (n = 2-3) per group. Student's t test: *** $p<0.001$, **$p<0.05$, *$p<0.01$. Error bars represent SEM.

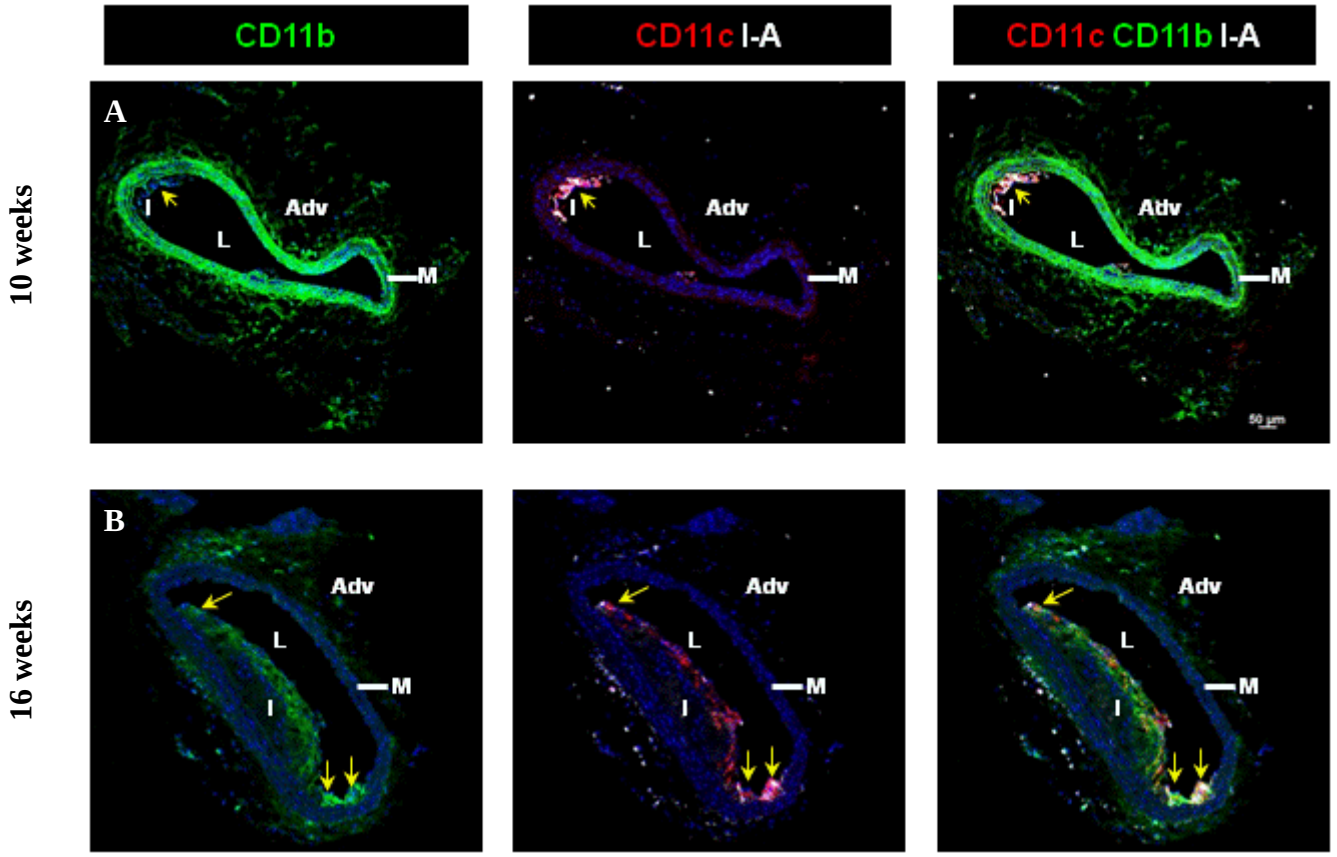

Figure 3.6. Accumulation of DCs occurred across disease progression.

Sections were stained with I-A (white), CD11c (red), CD11b (green) and DAPI (blue) to identify DCs, particularly $CD11b^{+}$ DCs. (A-D) Accumulation of $I\text{-}A^{+}$ $CD11c^{+}$ DCs can be seen across increasing weeks of high fat diet feeding. $CD11b^{+}$ DCs (yellow arrows) are mostly localized in the intima. L: lumen; I: intima; M: media; Adv: adventitia; Sh: shoulder. Magnification 100x. Scale bar represents 50µm.

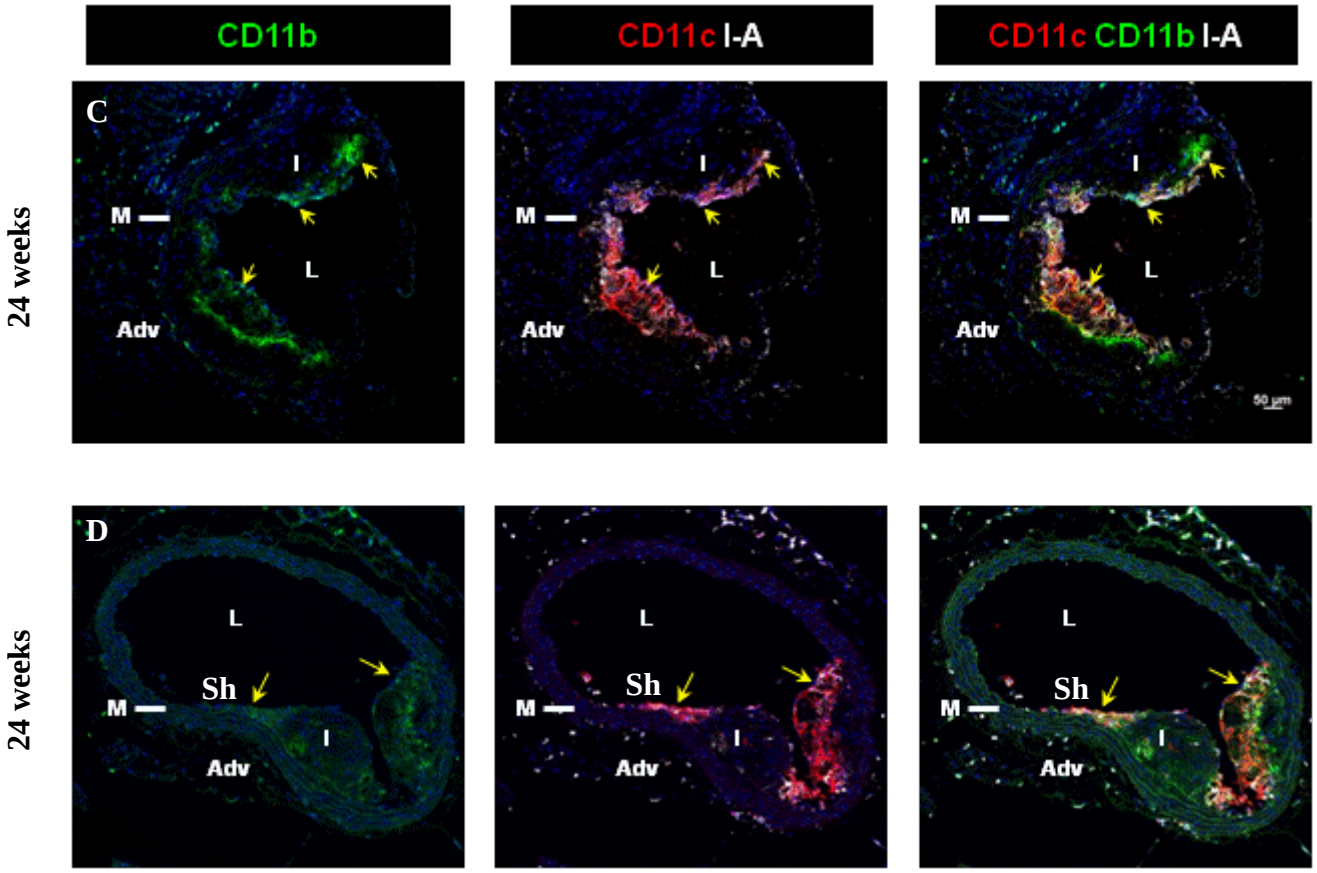
CD11b
CD11c I-A
CD11c CD11b I-A
C
24 weeks
M
I
L
Adv
50 µm
D
24 weeks
Sh

3.2.5 Atherosclerosis-induced expansion of DC subsets in Ldlr$^{-/-}$ mice

As Ldlr$^{-/-}$ mice do not spontaneously develop atherosclerotic lesions in contrast to apoE$^{-/-}$ mice, the progression of disease is much slower in this model (Sjoland et al., 2000; Whitman, 2004). To obtain similar advanced plaques in a 24 week old apoE$^{-/-}$ mice (18 weeks of high fat diet), Ldlr$^{-/-}$ mice used in this study were placed on at least 24 weeks of high fat diet.

Similar to apoE$^{-/-}$ mice, an accumulation of DCs (Figure 3.7A) was observed in Ldlr$^{-/-}$ mice. However, the accumulation of DCs in the Ldlr$^{-/-}$ mice (approximately 6%) was less severe compared to apoE$^{-/-}$ (approximately 15%), reflecting the differences in the two models. Contrary to a previous study (Choi et al., 2011) which reported an accumulation of both DC subsets in Ldlr$^{-/-}$ mice, only the CD11b^{+} DC subset was significantly increased (Figure 3.7B) in our study. The differences may be due to the duration of high fat diet feeding which was 16 weeks compared to 24 weeks in our study. In terms of absolute numbers, there was a modest but not statistically significant increase in CD11b^{+} DCs (Figure 3.7C).

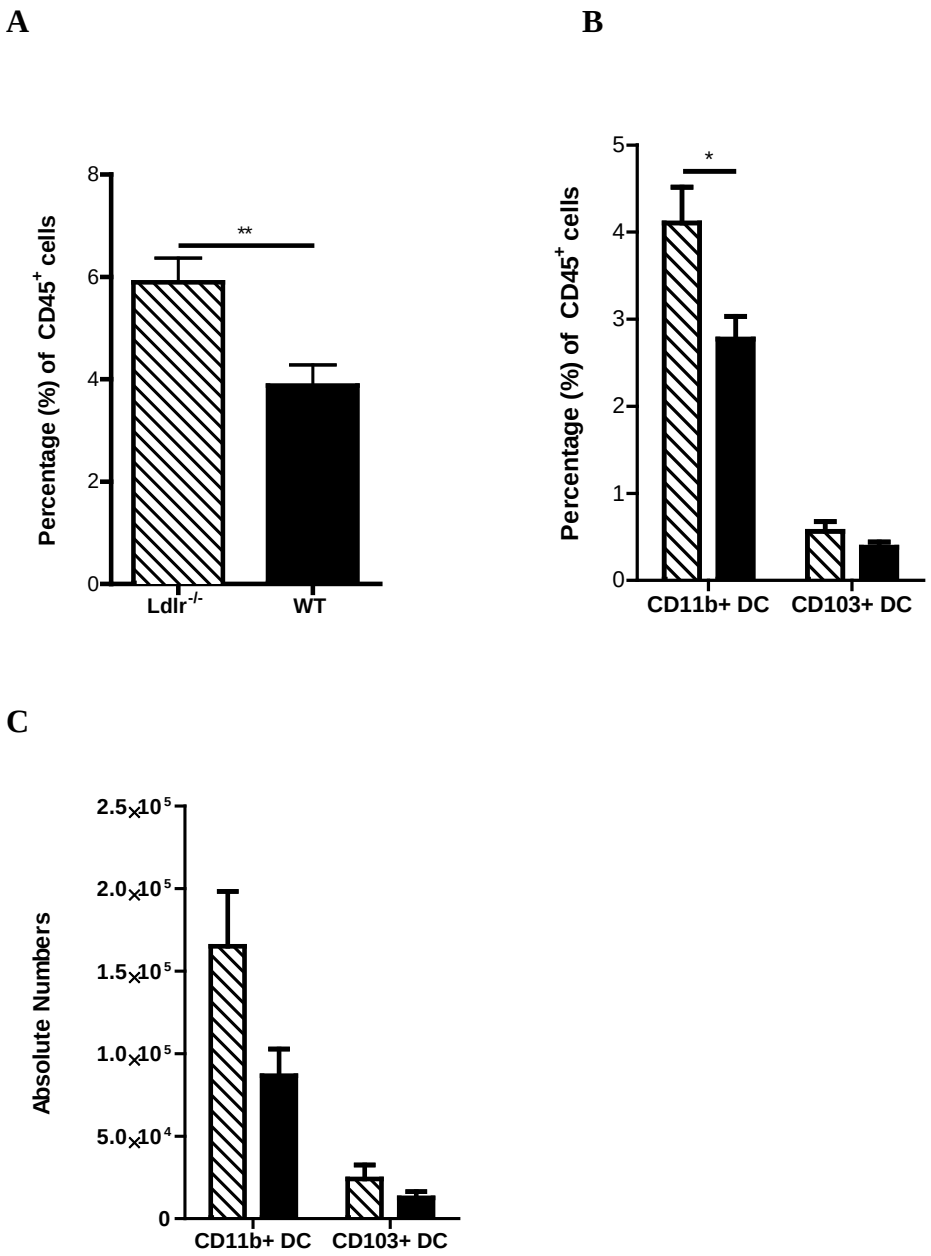

Figure 3.7. The expansion of DCs in Ldlr$^{-/-}$ mice was due to an accumulation of the CD11b^{+} DC subset rather than the CD103^{+} DC subset.

(A) Bar graph showing percentage of I-A^{+} CD11c^{+} DCs in aortas of Ldlr$^{-/-}$ (shaded) and WT mice (black). (B and C) Bar graphs showing percentages of CD11b^{+} and CD103^{+} DC subsets as a percentage of total CD45^{+} leukocytes and their absolute numbers in whole aortas of Ldlr$^{-/-}$ (shaded) and WT mice (black). Data shown are representative of at least 3 independent experiments (n = 2-3) per group. Student's t test: **p<0.05, *p<0.01. Error bars represent SEM.

3.3 Summary

In conclusion, we demonstrated the existence of two DC subsets: $CD11b^+$ and $CD103^+$ in the normal murine aorta whose phenotypes and proportions are analogous to other non-lymphoid tissues. These DC subsets are found in atherosclerosis-susceptible areas of the aorta. At steady state, both DC subsets come from bone marrow precursors as shown in the bone marrow transplantation experiment.

Under chronic inflammation conditions, such as atherosclerosis, studies have shown an accumulation of immune cells in plaque-laden areas. However, there are no studies available investigating the DC subsets in the $apoE^{-/-}$ mouse model of atherosclerosis. Our data indicated that when atherosclerotic plaques develop in the atherosclerotic $apoE^{-/-}$ mice, an expansion of both $CD11b^+$ and $CD103^+$ DC subsets is observed. Interestingly, the expansion is proportional such that the ratio of $CD11b^+$ and $CD103^+$ DC subsets remain unchanged (70% $CD11b^+$:10% $CD103^+$), implying that maintaining this distribution of DC subsets in the aorta is physiologically relevant.

In contrast, when a parallel study was conducted on the $Ldlr^{-/-}$ mice, a less severe model of atherosclerosis, only the $CD11b^+$ DCs were found to accumulate. Furthermore, the extent of accumulation of $CD11b^+$ DCs in the Ldlr-/- mice is smaller compared to $apoE^{-/-}$ mice. This suggests that the extent of disease severity may determine the amount of $CD11b^+$ DC accumulation and expansion of this subset is inflammation-dependent.

Chapter 4

Results

Origin of DCs in atherosclerosis

Chapter 4 – Origin of DCs in atherosclerosis

4.1 Introduction

Under inflammatory conditions, monocytes are known to be precursors of DCs (Dominguez and Ardavin, 2010). Since the origin of the $CD11b^+$ DC subset is not well-studied in atherosclerosis, we wanted to investigate whether the $CD11b^+$ DC subset in the atherosclerotic aorta comes from monocytes.

4.2 Results

4.2.1 Expression of CD64 distinguished monocyte-derived DCs

CD64, the high-affinity IgG receptor FcγRI in the mouse is largely expressed by myeloid cells involved in antigen presentation and processing such as macrophages and DCs (Tan et al., 2003). Interestingly, recent findings have shown that expression of CD64 is able to distinguish MoDCs from cDCs (Langlet et al., 2012; Plantinga et al., 2013) and is a good marker for monocyte-derived cells (Tamoutounour et al., 2012).

When we stained for CD64 by flow cytometry, we detected an increased percentage of $CD11b^{+}$ DCs expressing CD64 in the $apoE^{-/-}$ mice compared to WT controls (Figure 4.1). Moreover, $CD103^{+}$ DCs ($CD11b^{-}$) were CD64 negative in both $apoE^{-/-}$ and WT mice, suggesting that monocytes did not differentiate into $CD103^{+}$ DCs (Figure 4.1).

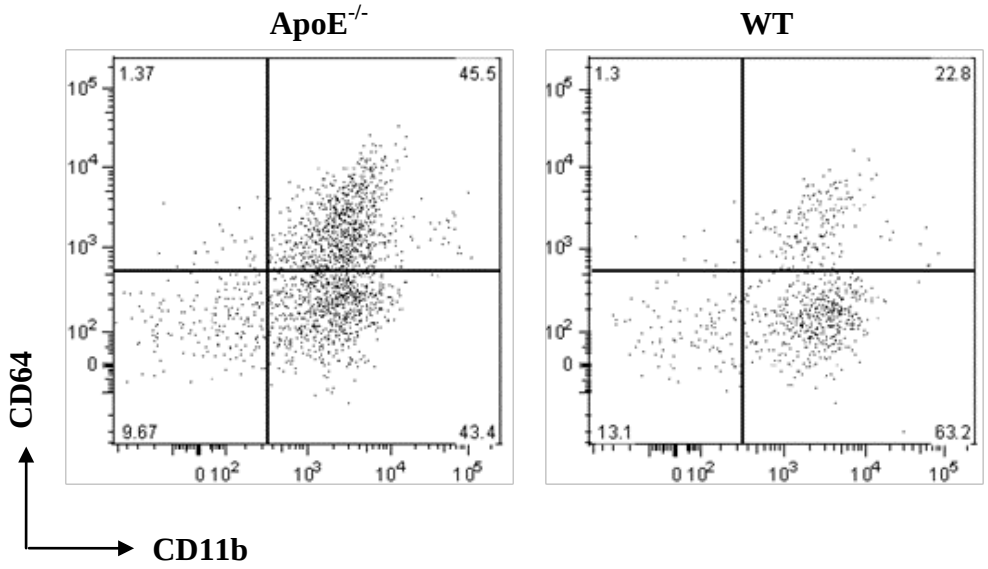

Figure 4.1 Expression of CD64 revealed expanded monocyte-derived DC population in apoE$^{-/-}$ mice compared to WT controls.

Dot plots show CD11b and CD64 expression by CD45^{+} I-A^{+} CD11c^{+} DCs. Representative plot of 2 independent experiments, n = 2 per group.

4.2.2 CD11b$^+$ DC subset arises from monocytes

To assess whether monocytes can give rise to CD11b$^+$ DCs during atherosclerosis, we adoptively transferred CD45.1 WT murine bone marrow monocytes into 24 weeks old CD45.2 apoE$^{-/-}$ recipients. Bone marrow monocytes were isolated by negative selection and purity of bone marrow monocytes was found to be 80-90% (Figure 4.2A). 1 day after transfer, we could detect 2-3% of blood monocytes in these recipients that are of CD45.1 donor origin (Figure 4.2B). 3 days after the transfer, the percentage of blood monocytes in the apoE$^{-/-}$ recipients dropped to less than 1% (Figure 4.2C), suggesting mobilization of these monocytes into peripheral tissues.

Indeed, when we looked at the aorta of these apoE$^{-/-}$ recipients, approximately 0.02% of cells in the aorta were from the donor. When we further looked at I-A and CD11c expression of these cells, approximately 5-6% of these cells were I-A$^+$ CD11c$^+$ DC, while the majority of the cells remained IA$^-$ CD11c$^-$ monocytes. Of I-A$^+$ CD11c$^+$ DCs that were CD45.1, all were CD11b$^+$ DCs, suggesting that monocytes definitely can differentiate into CD11b$^+$ DCs under atherosclerotic conditions (Figure 4.2D). These monocyte-derived CD11b$^+$ DCs were also all CD64 positive, further supporting CD64 as a good marker in detecting monocyte-derived cells. Since donor monocytes only give rise to CD11b$^+$ DCs *in vivo*, it also implied that CD103$^+$ DC subset (CD11b$^-$ CD24$^+$) in the aorta do not originate from monocytes under inflammatory conditions.

A

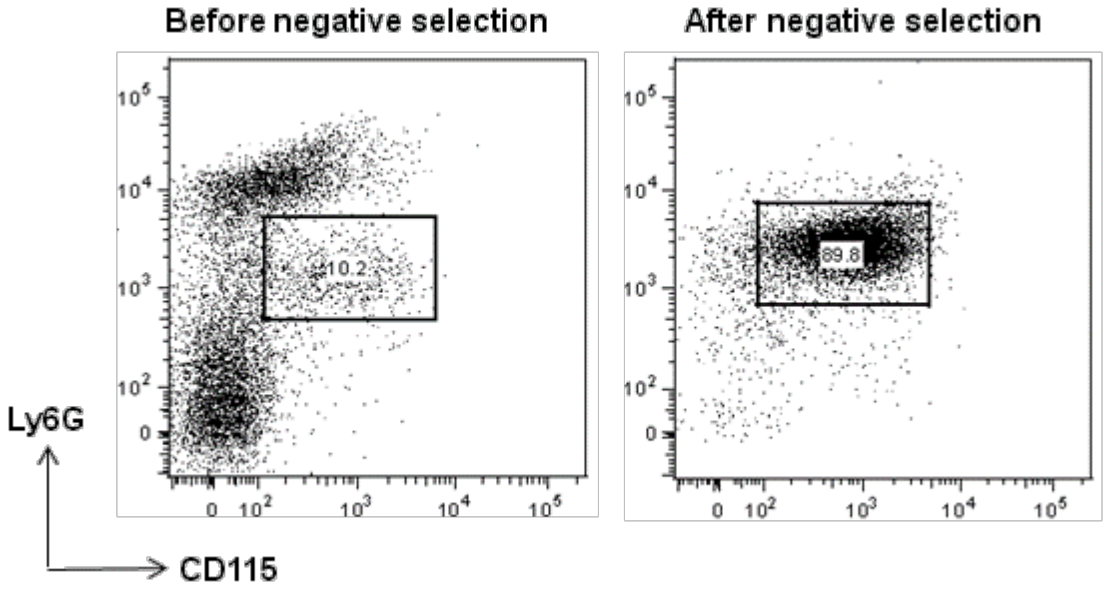
Before negative selection
After negative selection
10.2
89.8
Ly6G
CD115

B

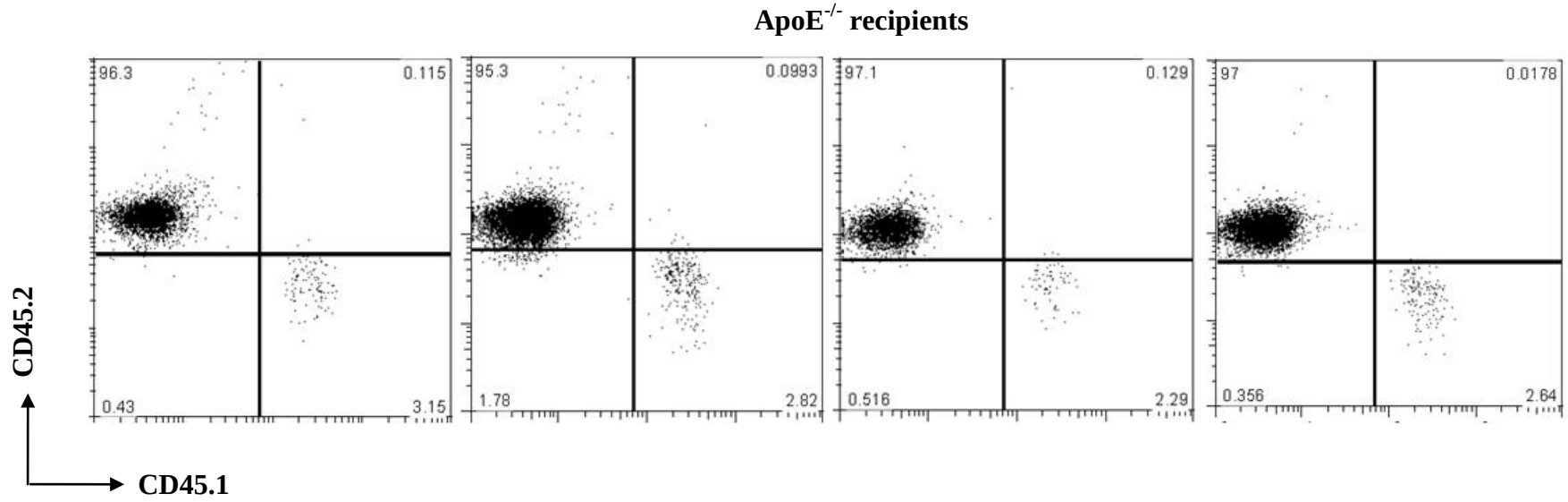
ApoE-/- recipients
96.3
0.115
0.43
3.15
95.3
0.0993
1.78
2.82
97.1
0.129
0.516
2.29
97
0.0178
0.356
2.64
CD45.2
CD45.1

C

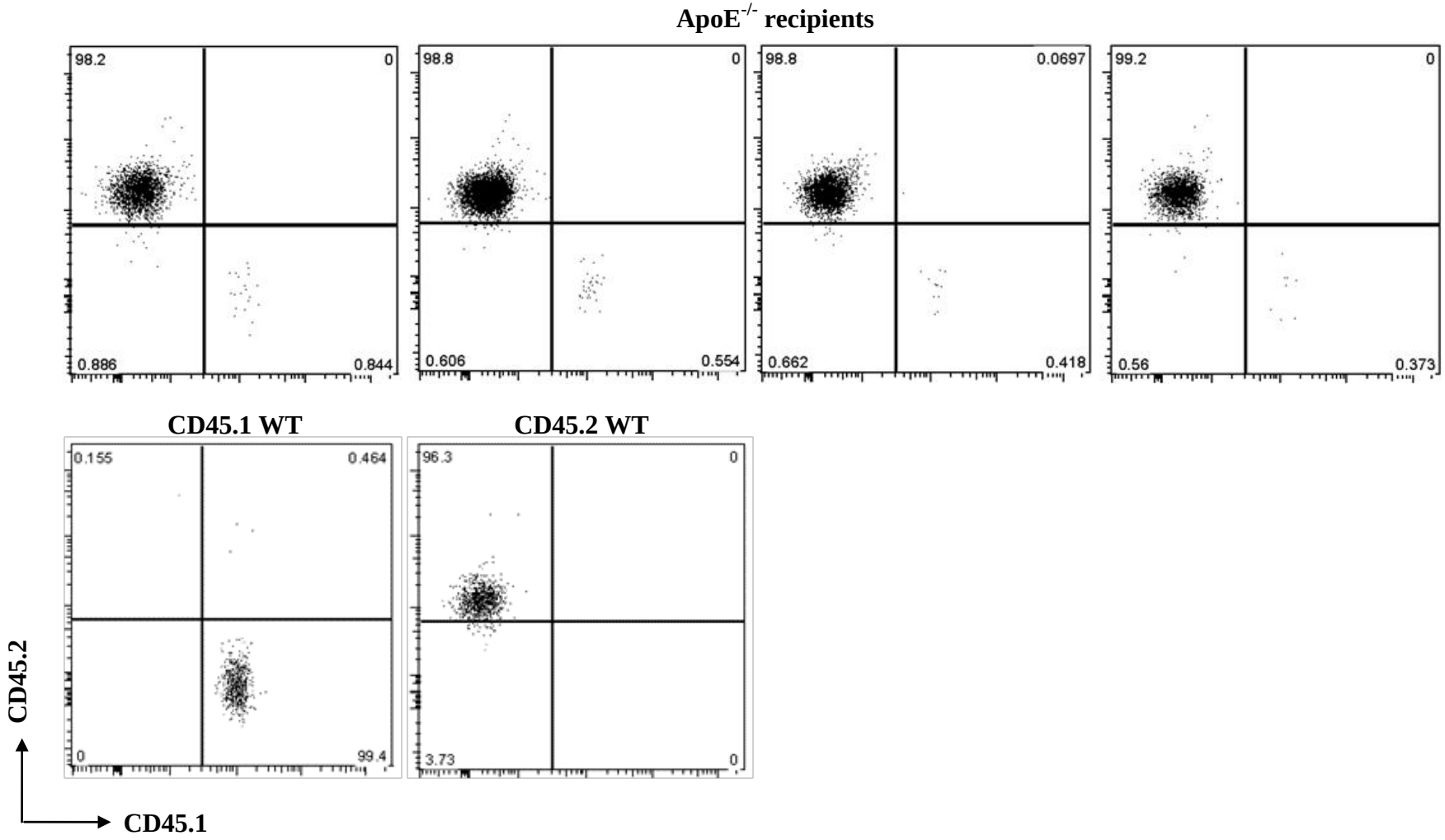
ApoE-/- recipients
98.2
0
0.886
0.844
98.8
0
0.606
0.554
98.8
0.0697
0.662
0.418
99.2
0
0.56
0.373
CD45.1 WT
CD45.2 WT
0.155
0.464
0
99.4
96.3
0
3.73
0
CD45.2
CD45.1

D

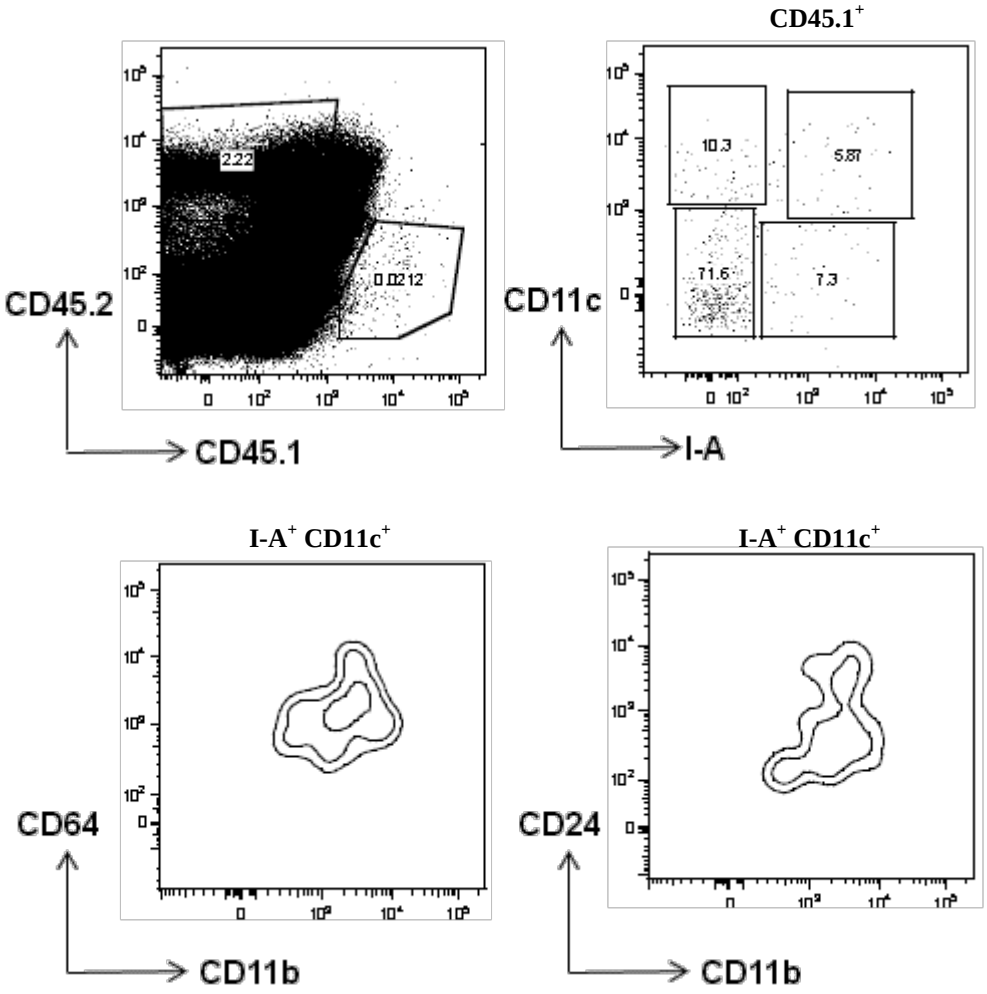

Figure 4.2. CD11b$^+$ DCs in the aorta were of monocyte origin.

CD45.1 WT monocytes were injected into apoE$^{-/-}$ mice at 24 weeks of age. (A) Dot plots showing percentages of monocytes (CD115$^+$ Ly6G$^-$) before (left) and after (right) negative selection. (B) Dot plots showing percentages of blood monocytes (CD11b$^+$ Low SSC, CD115$^+$ F4/80$^+$) that came from donor (CD45.1) and host (CD45.2) cells 1 day and (C) 3 days after adoptive transfer respectively with CD45.1 and CD45.2 WT controls. (D) CD45.1 donor cells were identified in aortic cell suspension of apoE$^{-/-}$ mice recipients and I-A$^+$ CD11c$^+$ DCs were further analyzed for CD11b, CD64 and CD24 expression. 4 aortas were pooled for this analysis.

4.3 Summary

Here, we show for the first time that CD64 expression is able to discriminate monocyte-derived cells in the murine aorta. Based on CD64 expression, there is an increasing amount of $CD11b^+$ DCs that differentiated from monocytes during atherosclerosis, consistent with literature that monocytes are a source of DCs during inflammatory conditions (Shortman and Naik, 2007).

We also provide evidence that monocytes adoptively transferred into $apoE^{-/-}$ recipients can differentiate into $CD11b^+$ DCs in the aorta *in vivo*. In contrast, adoptively transferred monocytes were shown to up-regulate F4/80 and MHC class II and suggesting that monocytes have differentiated into macrophages (Swirski et al., 2007). Of note, during both homeostasis and inflammation, $CD103^+$ DCs do not arise from monocytes as $CD103^+$ DCs are derived mainly from pre-cDCs (Ginhoux et al., 2009).

Chapter 5

Results

Mechanism(s) of DC accumulation in atherosclerosis

Chapter 5 – Mechanism(s) of DC accumulation in atherosclerosis

5.1 Introduction

Although the accumulation of DCs in atherosclerotic mice has been reported since 2006, there is still a lack of information on the potential mechanisms that could cause this process. Several hypotheses have been put forward to explain this accumulation. We have previously shown that hypercholesterolemia affects the ability of DCs to migrate from the skin to draining lymph nodes in the apoE$^{-/-}$ mice (Angeli et al., 2004), suggesting that aortic DCs may likewise have impaired emigration from atherosclerotic plaques to draining lymph nodes. Besides impaired emigration, accumulation of DCs in atherosclerotic aorta may be due to increased retention of these cells (Llodra et al., 2004) and the failure to up-regulate CCR7 (Trogan et al., 2006) in dyslipidemic conditions, supporting prolonged inflammation. Another probable explanation is an increased DC proliferation in nascent atherosclerotic lesions due to increased GM-CSF (Zhu et al., 2009). Lastly, GM-CSF is also known to promote DC survival in non-lymphoid tissues at steady state (Greter et al., 2012a) and this could account for the accumulation.

To date, none of these findings narrow down the mechanisms of accumulation for specific DC subsets. Earlier, we have determined that both CD11b^{+} and CD103^{+} DCs accumulated in apoE$^{-/-}$ mice and only CD11b^{+} DCs are derived from monocytes, suggesting different mechanisms for the accumulation of these two subsets. Indeed, it has been shown in a recent study that aortic CD103^{+} DCs originate from Flt3-dependent DC precursors whereas CD11b^{+}

DCs are Flt3-independent in $Ldlr^{-/-}$ mice (Choi et al., 2011). Herein, we sought to explore the potential mechanisms for the accumulation of $CD11b^{+}$ DCs in $apoE^{-/-}$ mice.

5.2 Results

5.2.1 Monocytosis occurs in the blood and aorta of apoE$^{-/-}$ mice

As seen from the adoptive transfer (Section 4.2.2), monocytes can give rise to CD11b^{+} DCs in apoE$^{-/-}$ mice and it is well known that monocytosis occurs in blood of these mice. We sought to verify in our model whether monocytosis possibly contributes to CD11b^{+} DC accumulation.

Blood monocytes are defined as CD11b^{+} with low side scatter and typically express CD115 and F4/80 (Sunderkotter et al., 2004). They can be divided into 2 subpopulations: Gr-1 high and Gr-1 low (Geissmann et al., 2003) (Figure 5.1A). In agreement with literature, an increase in total monocytes was observed in the apoE$^{-/-}$ mice compared to WT controls (Figure 5.1B). Moreover, as reported in recent studies (Swirski et al., 2007; Tacke et al., 2007), we observed a preferential Gr-1^{hi} monocytosis in the blood, leading to a reduction in Gr-1^{low} monocytes in apoE$^{-/-}$ mice (Figure 5.1C).

While blood monocytosis is recognized in apoE$^{-/-}$ mice, there were no reports on whether this occurs in the atherosclerotic plaques. In the same atherosclerotic animals in which we observed blood monocytosis and CD11b^{+} DC accumulation in aorta, we found that total monocytes (I-A^{-} CD11c^{-} CD11b^{+}) were also increased in aorta (Figure 5.2A). When we looked further into monocyte subsets in the aorta, we discovered that the increase could only be attributed to Gr-1^{hi} monocytes (Figure 5.2B and C). This increase was also reflected by higher absolute number of Gr-1^{hi} monocytes in the aorta (Figure 5.2D).

A

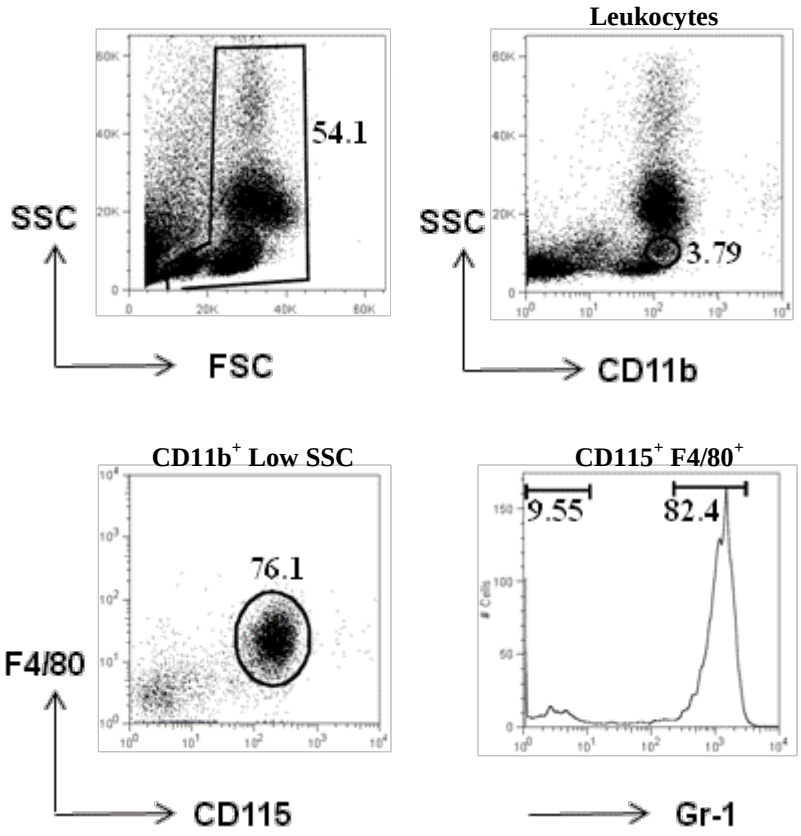
Leukocytes
54.1
SSC
FSC
SSC
3.79
CD11b
CD11b+ Low SSC
CD115+ F4/80+
76.1
F4/80
CD115
9.55
82.4
Gr-1

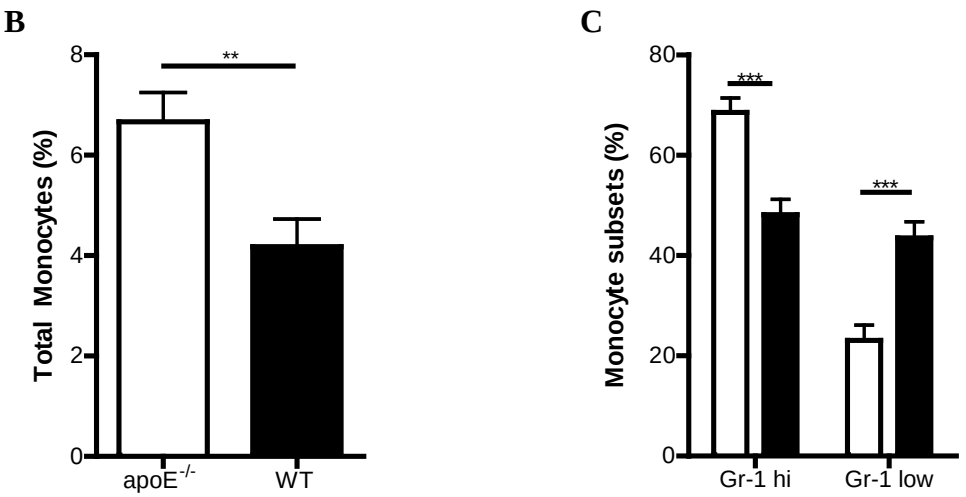

Figure 5.1. Monocytosis in the blood of apoE$^{-/-}$ mice.

(A) Monocytes in the blood are analyzed by flow cytometry. Leukocytes are gated followed by CD11b^{+} cells with low side scatter and CD115 and F4/80. Monocyte subsets are distinguished by Gr-1 expression. (B) Bar graphs showing percentage of total monocytes, Gr-1^{hi} and Gr-1^{low} monocytes of apoE$^{-/-}$ (white) and WT mice (black). These results are representative of at least 3 independent experiments (n = 4-6) per group. Student's t test: *** $p<0.001$, **$p<0.05$. Error bars represent SEM.

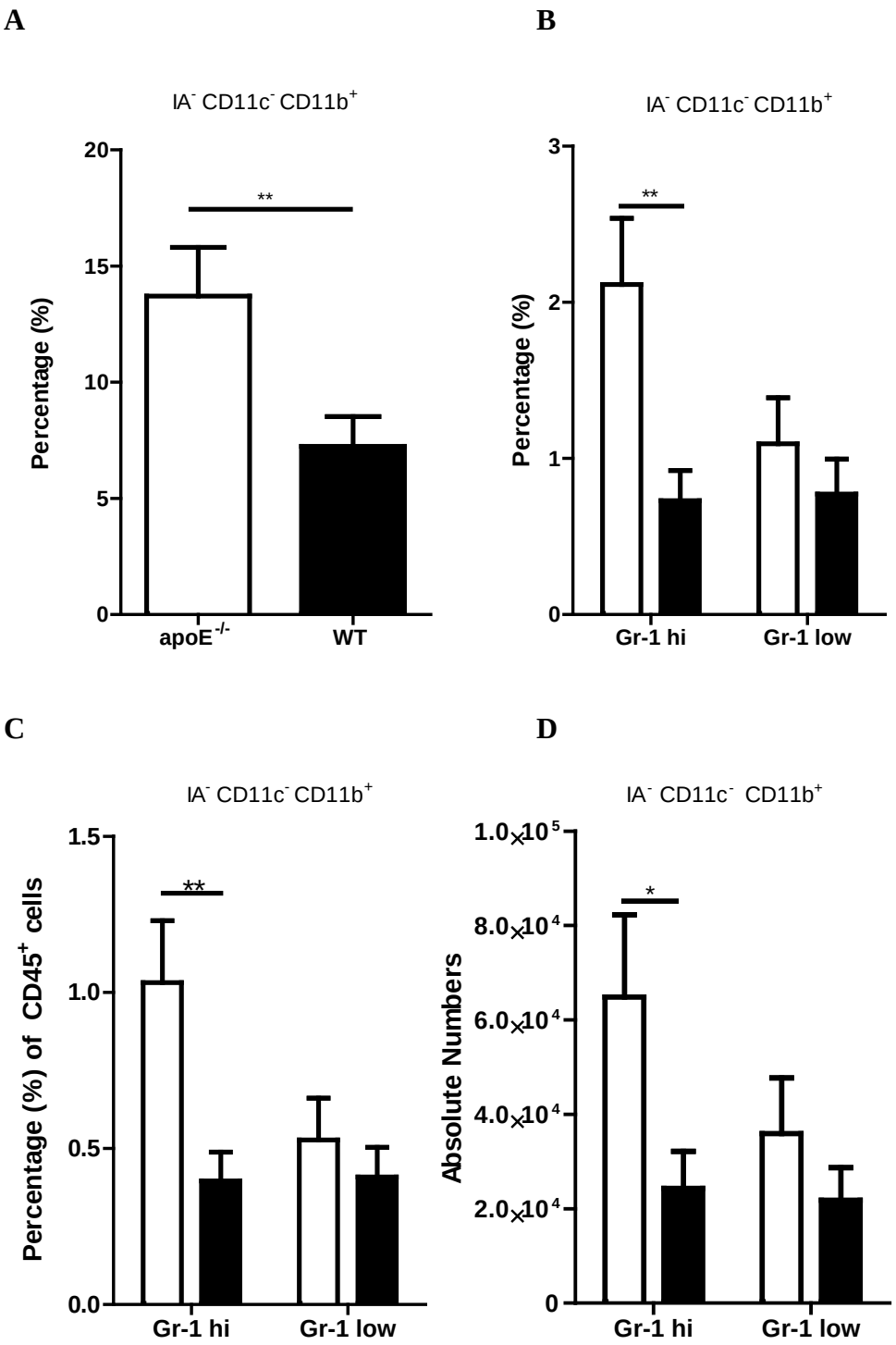

Figure 5.2. Monocytosis in the aorta of apoE$^{-/-}$ mice.

(A) Bar graph showing percentages of CD11b^{+} cells that are I-A^{-} CD11c^{-}. (B and C) Bar graphs showing percentages of Gr-1^{hi} and Gr-1^{low} monocyte subsets and their proportions in total leukocytes (CD45^{+}). (D) Bar graph showing absolute numbers of Gr-1^{hi} and Gr-1^{low} monocyte subsets. ApoE$^{-/-}$: white bar; WT: black bar. Data shown are representative of the same independent experiments (n = 2-3) per group as shown in Figure 4.2. Student's t test: **p<0.05, *p<0.01. Error bars represent SEM.

5.2.2 Ezetimibe abolished blood monocytosis in the blood and aorta of apoE$^{-/-}$ mice simultaneously with CD11b^{+} DC expansion in aorta

Although we have shown earlier that monocytosis in the blood and aorta occurred simultaneously with CD11b^{+} DC accumulation, there is no direct evidence that monocytosis plays a part in CD11b^{+} DC accumulation. To assess the relationship between monocytosis and CD11b^{+} DCs, we induced disease regression in apoE$^{-/-}$ mice by administering a cholesterol-lowering drug, Ezetimibe.

Ezetimibe is a cholesterol absorption inhibitor and has been shown to reduce atherosclerotic plaques in apoE$^{-/-}$ mice (Davis et al., 2001). After Ezetimibe treatment, blood monocytosis was reduced in apoE$^{-/-}$ mice (Figure 5.3A). Furthermore, Gr-1^{hi} monocytosis that was previously detected in apoE$^{-/-}$ mice was reversed and the proportion of monocyte subsets in treated apoE$^{-/-}$ mice became comparable to WT controls (Figure 5.3B). This effect was accompanied by a reduction in total monocytes in aorta (Figure 5.3C) of treated apoE$^{-/-}$ mice and was again attributed to a decrease in Gr-1^{hi} monocytes (Figure 5.3D).

Together with the reversal of monocytosis in treated apoE$^{-/-}$ mice, we detected a decrease in I-A^{+} CD11c^{+} DCs in the aorta (Figure 5.4A). Strikingly, there was a reduction in CD11b^{+} DC accumulation (Figure 5.4A) without any effect on CD103^{+} DCs in the treated apoE$^{-/-}$ mice. This was also evident by immunofluorescent staining (Figure 5.5). Hence, monocytosis may likely account for CD11b^{+} DC accumulation in atherosclerotic aorta.

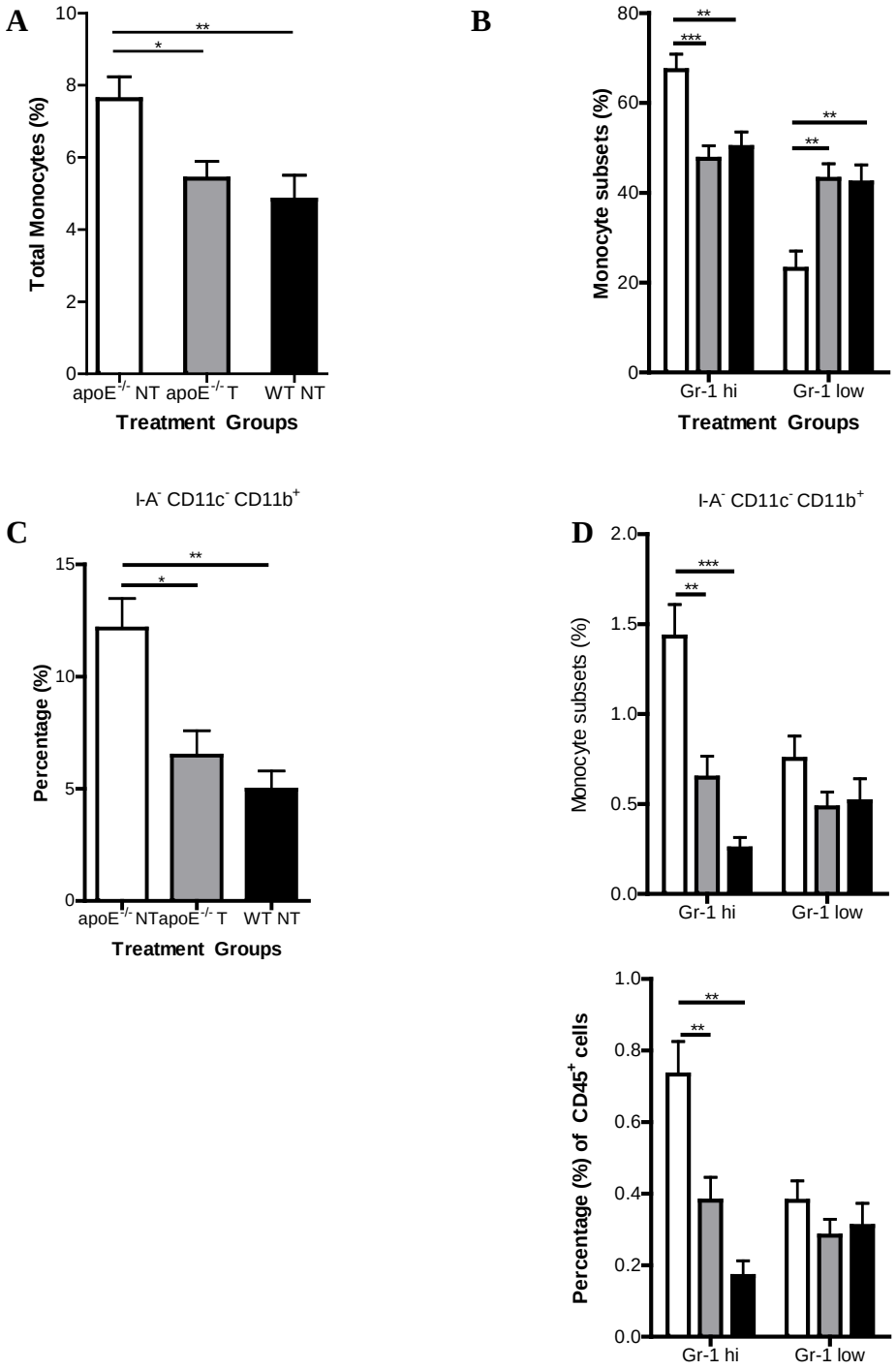

Figure 5.3. Ezetimibe reversed monocytosis in the blood and aorta of apoE$^{-/-}$ mice.

(A) Bar graphs showing percentages of total monocytes, (B) Gr-1^{hi} and Gr-1^{low} monocytes in the blood of apoE$^{-/-}$ non-treated (white), apoE$^{-/-}$ treated (grey) and WT non-treated (black) mice. (C) Percentage of total monocytes in aorta is displayed. (D) Bar graphs showing percentages of Gr-1 hi and Gr-1 low monocytes in the aorta as a proportion of total monocytes (top) and of CD45^{+} leukocytes (bottom) respectively. NT: non-treated; T: treated. Data shown are representative of 4 independent experiments (n = 2-3) per group. Student's t test: *** $p<0.001$, **$p<0.05$, *$p<0.01$. Error bars represent SEM.

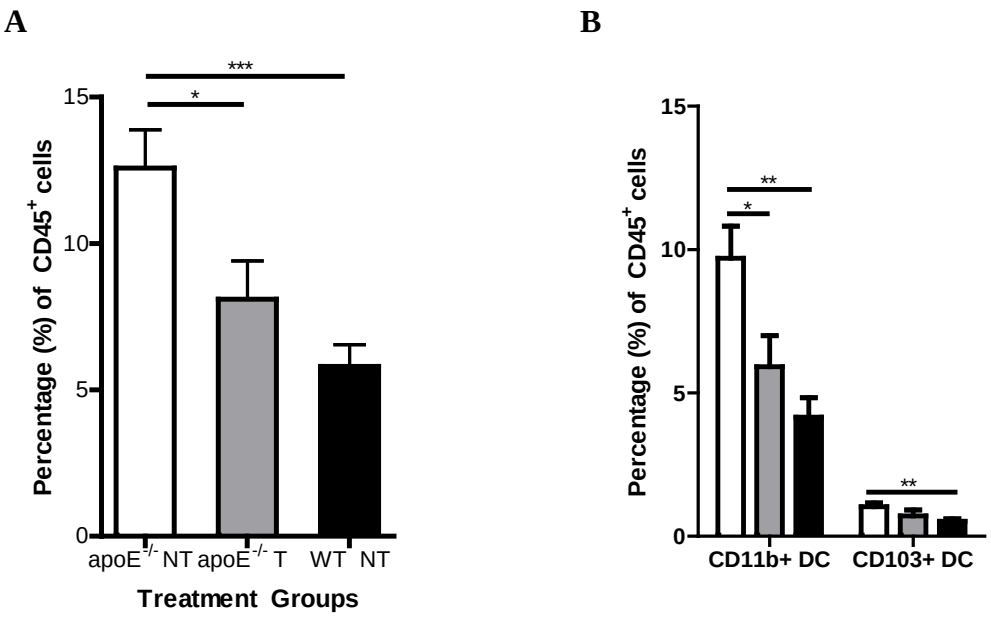

Figure 5.4. Ezetimibe abrogated CD11b^{+} DC accumulation in the aorta of apoE$^{-/-}$ mice.

(A) Bar graphs showing percentages of I-A^{+} CD11c^{+} DCs and (B) CD11b^{+} and CD103^{+} DC subsets respectively in aortas of apoE$^{-/-}$ non-treated (white), apoE$^{-/-}$ treated (grey) and WT non-treated (black) mice. NT: non-treated; T: treated. Data shown are representative of 4 independent experiments (n=2-3) per group. Student's t test: *** $p<0.001$, **$p<0.05$, *$p<0.01$. Error bars represent SEM.

A

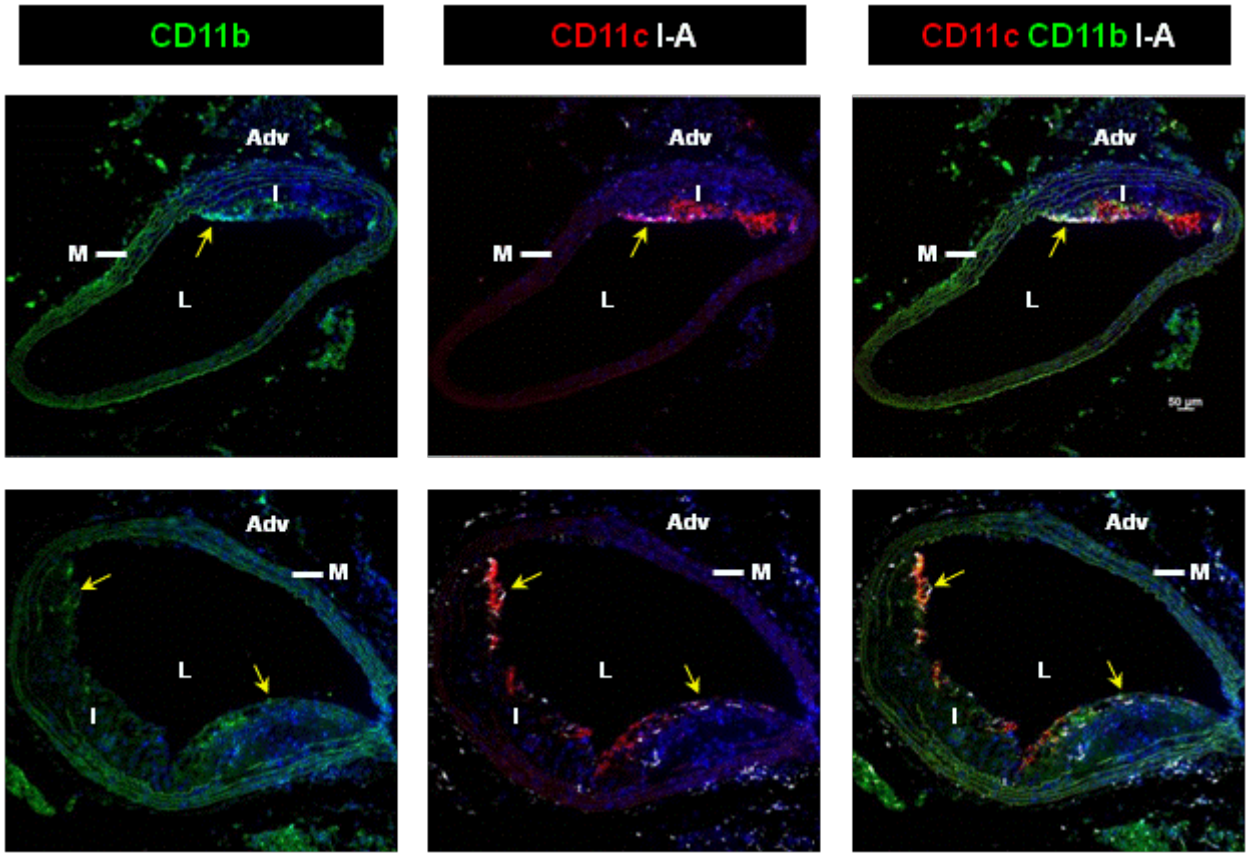

Figure 5.5. CD11b^{+} DCs are reduced together with plaque size after Ezetimibe.

Immunofluorescence analysis showed abolishment of CD11b^{+} DC accumulation after Ezetimibe treatment. (A) Panel of images show staining of CD11b^{+} DCs (yellow arrows) in apoE$^{-/-}$ mice treated with vehicle. L: lumen; I: intima; M: media; Adv: adventitia. Magnification 100x. Scale bar represents 50µm. (B) ApoE$^{-/-}$ mice treated with Ezetimibe for 12 weeks have reduced plaque size and abolishment of CD11b^{+} DC accumulation. L: lumen; I: intima; M: media; Adv: adventitia. Magnification 100x. Scale bar represents

B

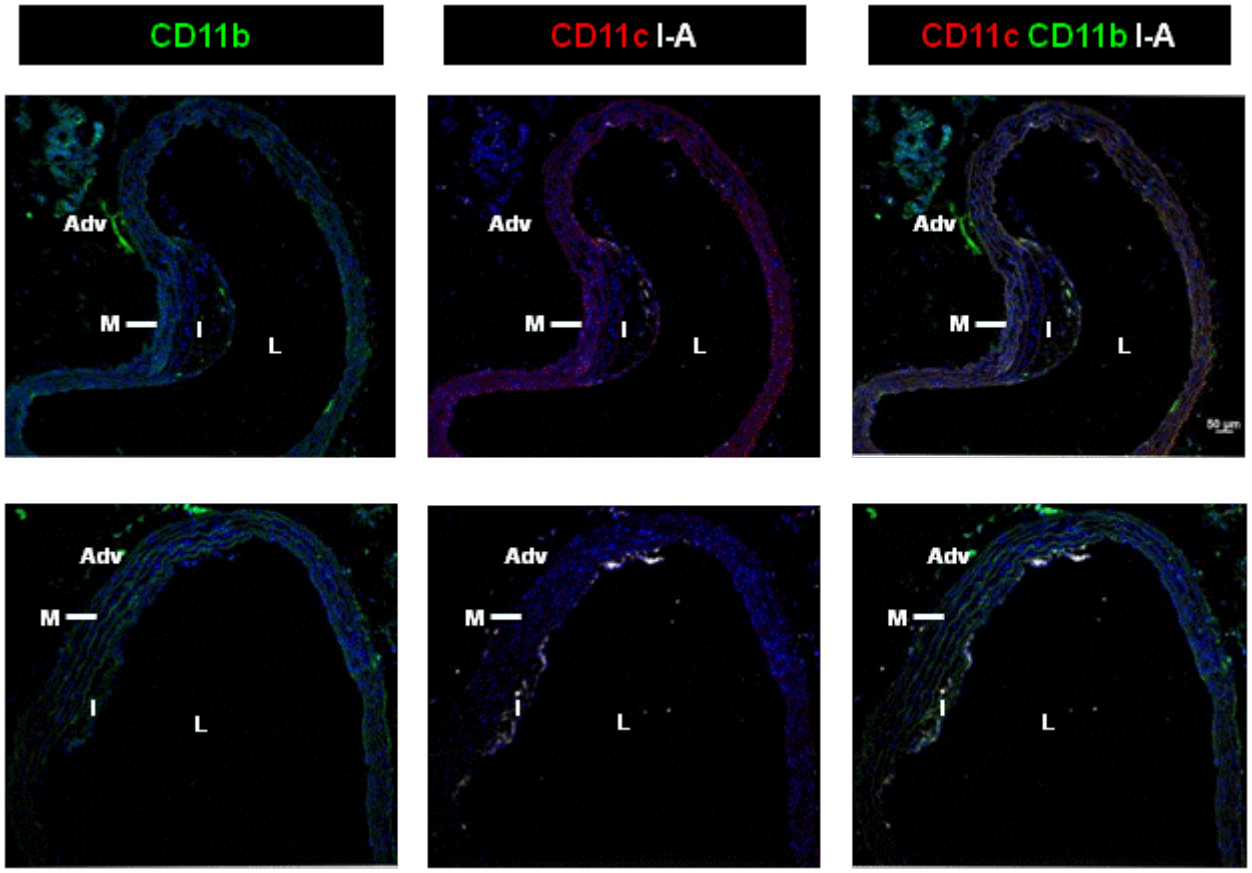
CD11b
CD11c I-A
CD11c CD11b I-A
Adv
M
I
L
Adv
M
I
L
Adv
M
I
L
Adv
M
I
L
Adv
M
I
L
Adv
M
I
L

5.2.3 Increase in bone marrow precursors does not account for CD11b$^+$ DC accumulation

Leukocytosis has been linked with proliferation and expansion of HSPCs in apoE$^{-/-}$ mice (Murphy et al., 2011). Therefore, we wondered whether DC precursors in the bone marrow are likewise expanded and eventually may account for CD11b$^+$ DC accumulation in the aorta during atherosclerosis.

In the bone marrow, there are two DC precursors: MDP and CDP. MDP gives rise to monocytes and CDP while CDP gives rise to pre-DCs. Both are known to differentiate into CD11b$^+$ and CD103$^+$ DC subsets in non-lymphoid tissues (Auffray et al., 2009a; Ginhoux et al., 2009). To define MDP and CDP in the bone marrow, mature hematopoietic cells which are lineage positive are excluded. Thereafter, Flt3$^+$ CD11c$^-$ CD115$^+$ and CD11b$^-$ cells were gated and analyzed for c-kit expression (Figure 5.6A) (Fogg et al., 2006; Onai et al., 2007) . MDPs are c-kit^{hi} whereas CDPs are c-kit^{low}. Comparing apoE$^{-/-}$ mice to WT controls, there were no significant differences in MDP and CDP in the bone marrow (Figure 5.6B), ruling out the possibility that DC precursors in the bone marrow contributed to CD11b$^+$ DC accumulation in the aorta.

Given that monocytosis occurs in peripheral blood of apoE$^{-/-}$ mice (Section 5.2.1), we also investigated whether bone marrow monocytes were expanded in apoE$^{-/-}$ mice. Interestingly, we did not detect any significant differences in total monocytes and monocyte subsets (Figure 5.6C). This is in contrast to an earlier study (Swirski et al., 2007) whereby the authors have observed an increase in bone marrow monocytes in apoE$^{-/-}$ mice over the duration of high

fat diet feeding. However, this study did not compare bone marrow monocytes to WT controls, explaining the differences in our observations.

In conclusion, bone marrow precursors: MDPs, CDPs and monocytes were not expanded in apoE$^{-/-}$ mice and are unlikely to provide for CD11b^{+} DC accumulation in the aorta. Also, since bone marrow monocytes are not expanded but peripheral blood monocytosis was observed indicated that there are factors in the periphery that encourage the development of monocytosis in the blood (Swirski et al., 2007). Otherwise, expansion of bone marrow monocytes might be occurring at earlier stages of atherosclerosis at 15-16 weeks of age as observed in this study (Combadiere et al., 2008), thereby giving rise to blood monocytosis in apoE$^{-/-}$ mice.

A

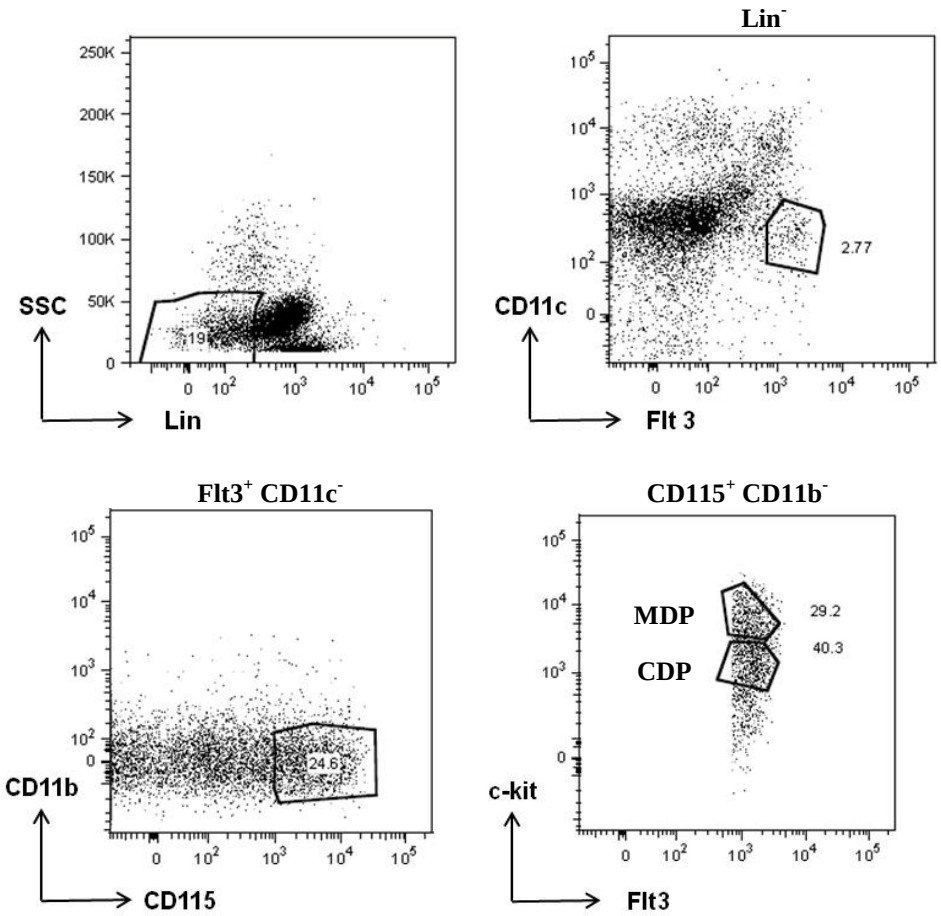
SSC
Lin
19.1
Lin-
CD11c
Flt 3
2.77
Flt3+ CD11c-
CD11b
CD115
24.6
CD115+ CD11b-
MDP
CDP
29.2
40.3
c-kit
Flt3

B

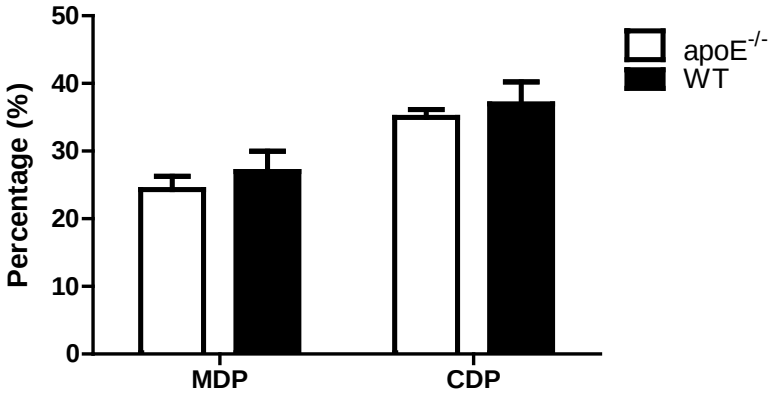
Percentage (%)
apoE-/-
WT
MDP
CDP

C

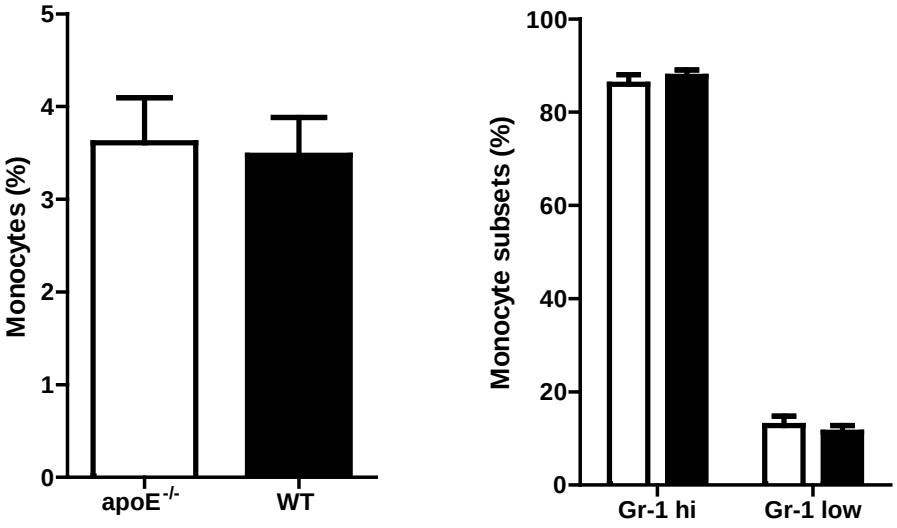

Figure 5.6. Bone marrow DC progenitors and monocytes do not contribute to DC accumulation in the apoE$^{-/-}$ mice.

(A) Gating strategy for DC progenitors, MDP and CDP is shown here. After selecting for live, aqua negative and singlet cells, lineage (lin) negative cells which are cells negative for B220, CD3, CD19, Gr-1, Ter-119, NK1.1 and Sca-1 are chosen. These cells are further gated based on CD11c, CD115, CD11b and Flt-3 expression. MDPs were c-kit^{hi} and CDPs were c-kit$^{low/int}$. (B) Bar graph shows percentage of MDPs and CDPs in the bone marrow. ApoE$^{-/-}$: white bar; WT: black bar (C) Bar graph shows percentage of monocytes and monocyte subsets: Gr-1^{hi} and Gr-1^{low}. ApoE$^{-/-}$: white bar; WT: black bar. Data shown here are from at least 3 independent experiments with n = 3-6 mice per group. Error bars represent SEM.

5.2.4 Extramedullary hematopoiesis does not play a role in CD11b^{+} DC accumulation

Emergency hematopoiesis has been known to be activated under inflammation and infection settings (Takizawa et al., 2012). In an earlier study (Swirski et al., 2009), the spleen has been identified to serve as a monocyte reservoir in myocardial infarction. This process known as extramedullary monocytopoiesis can sustain monocyte recruitment into infracted hearts, allowing resolution of inflammation (Leuschner et al., 2012). A recent study (Robbins et al., 2012) revealed that such a process occurs in apoE$^{-/-}$ mice and supplies monocytes to atherosclerotic lesions. Hence, we set out to determine whether this is also observed in our model.

Contrary to published reports, we do not observe any significant differences in total monocytes and monocyte subsets (Figure 5.7) between apoE$^{-/-}$ and WT control mice, that could account for CD11b^{+} DC accumulation in the aorta of apoE$^{-/-}$ mice. In the study that reported extramedullary hematopoiesis in apoE$^{-/-}$ mice, it was detected over weeks of high fat feeding and did not compare with age-matched WT control mice. In addition, the apoE$^{-/-}$ mice used were much older and on 30 weeks of high fat diet compared to 18 weeks of high fat diet in our experiments.

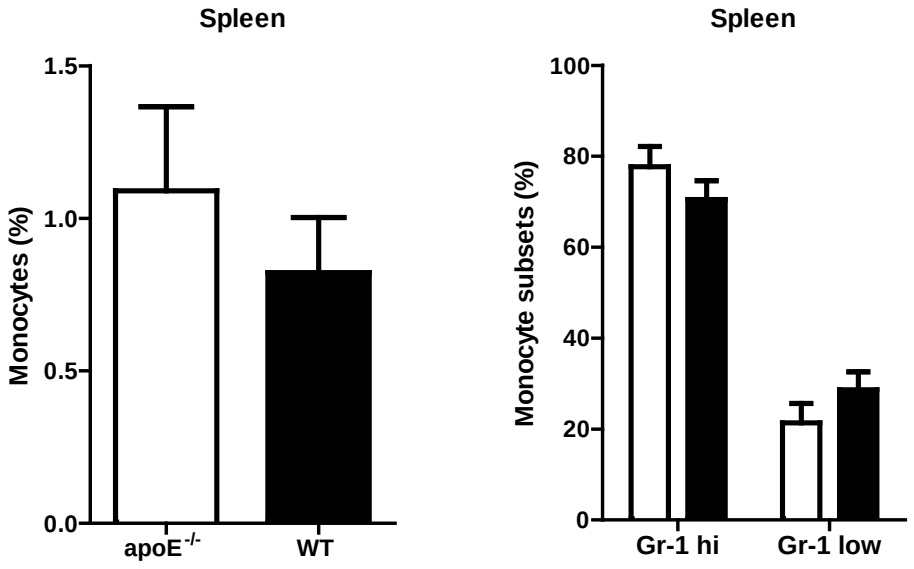

Figure 5.7. Extramedullary hematopoiesis does not contribute to DC accumulation in apoE$^{-/-}$ mice.

Splenic monocytes are defined as CD11b^{+} cells with low side scatter, CD115^{+} and F4/80 low. Bar graphs show percentage of total monocytes (left) and monocyte subsets (right) in spleens of apoE$^{-/-}$ (white bar) and WT controls (black bar). Data shown here are from 3 independent experiments with n = 4-5 mice per group. Error bars represent SEM.

5.2.5 CD11b$^+$ DCs proliferate in the aorta

Aside from increased precursors such as monocytes in the blood, one could also think that the expansion of DCs could occur through proliferation. In fact, during homeostasis, cDCs are known to replicate *in situ* (Diao et al., 2006) and non-lymphoid tissue DC subsets can proliferate *in vivo* (Ginhoux et al., 2009). Owing to these observations, a recent study showed that expansion of DCs in aeroallergen-induced airway inflammation was due to local proliferation of these cells instead of cell recruitment (Veres et al., 2013). In atherosclerotic Ldlr$^{-/-}$ mice, an intimal DC proliferation was demonstrated to contribute to the initiation of disease, although these DCs were resident 33D1$^+$ CD11b$^-$ DCs (Zhu et al., 2009). In this study, by comparing the kinetics of proliferation of blood monocytes and aortic DCs together with blocking monocyte recruitment, they have shown that aortic DCs proliferated independently of monocyte recruitment.

To study whether the expansion of CD11b$^+$ DCs in atherosclerotic aorta was a result of local proliferation, a thymidine analog, EdU was injected into the mice. By performing a similar kinetic experiment in blood and aorta as described by Zhu et al., (Zhu et al., 2009), we observed minimal proliferation of CD11b$^+$ DCs (approximately 1%) at 2 hours post-EdU injection when blood monocytes were not proliferating (data not shown). 12 hours after injecting EdU, consistent with literature (Swirski et al., 2007; Zhu et al., 2009), blood monocytes in apoE$^{-/-}$ mice were proliferating more than in WT mice (Figure 5.8), accounting for monocytosis in apoE$^{-/-}$ mice. In the aorta, we found that approximately 5% of CD11b$^+$ DCs were proliferating (EdU$^+$) in

apoE$^{-/-}$ mice (Figure 5.9). However, there was no difference in the percentage of proliferating CD11b^{+} DCs between apoE$^{-/-}$ and WT control mice, indicating that local CD11b^{+} DC proliferation in the aorta is unlikely accounting for the CD11b^{+} DC accumulation in atherosclerosis. Notably, the majority of CD11b^{+} DCs in the aorta were also non-proliferating cells (Figure 5.9).

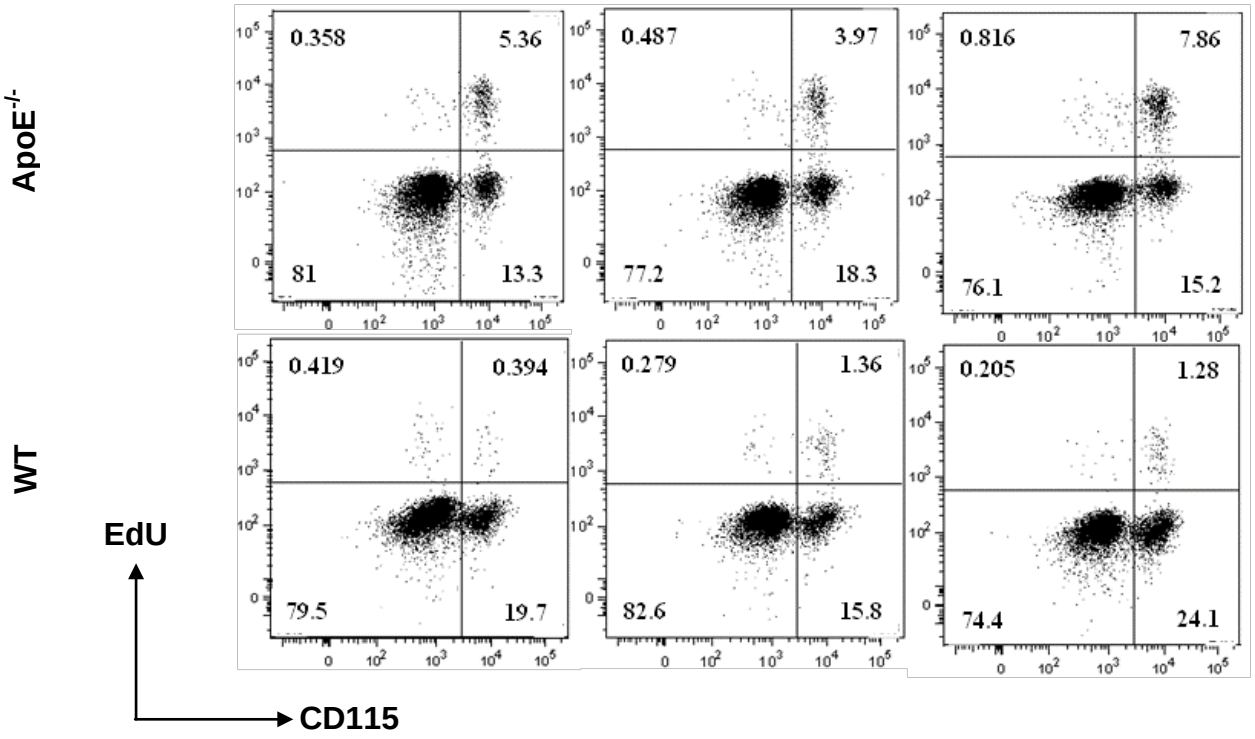

Figure 5.8. Increased proliferation of blood monocytes contributed to monocytosis in apoE$^{-/-}$ mice.

Dot plots show proliferating monocytes (CD115^{+} EdU^{+}) in apoE$^{-/-}$ (top row) and WT control (bottom row) mice measured 12 hours after a single dose of EdU injection. Data shown here are representative of 2 independent experiments, n = 4-6 per group.

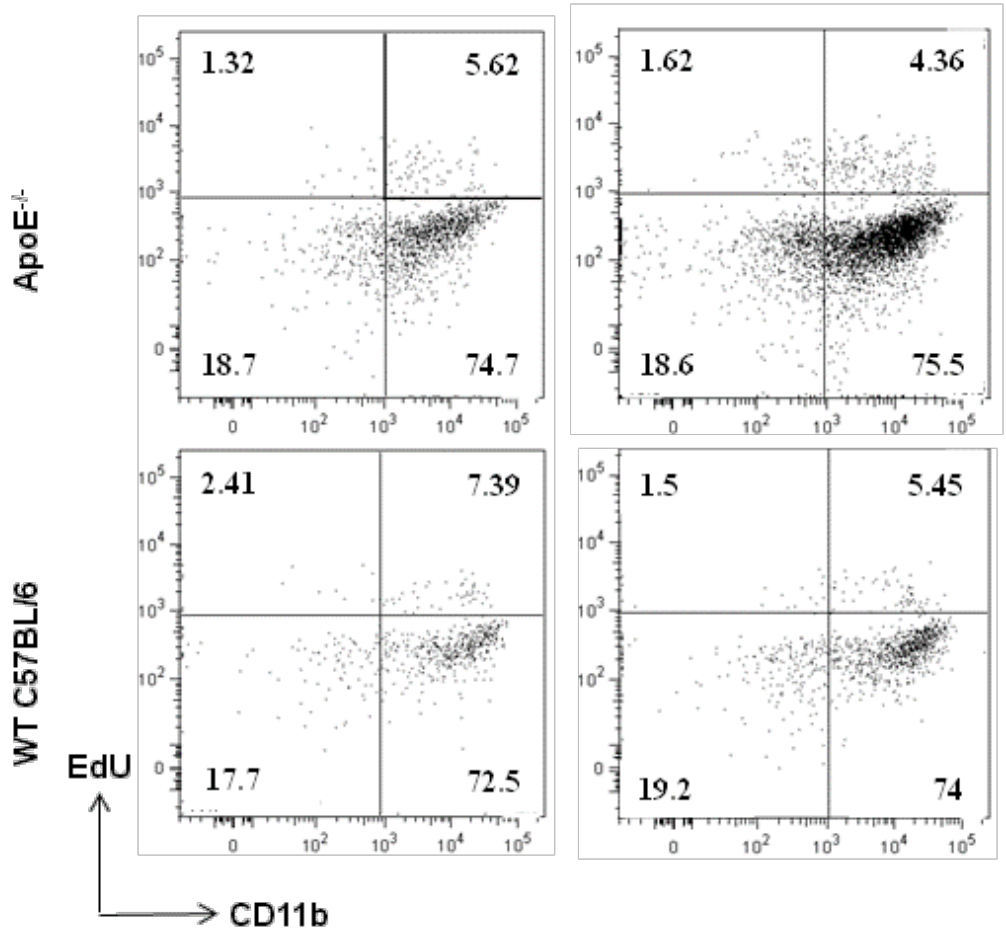

Figure 5.9. CD11b^{+} DC subset proliferated locally in the aorta.

After a single dose of EdU injection, mice were sacrificed 12 hours later and proliferation was measured by flow cytometry. Dot plots showing proliferation of CD11b^{+} DCs (I-A^{+} CD11c^{+}) measured by percentage of EdU^{+} DCs in apoE$^{-/-}$ (top panel) and WT (bottom panel) mice. Data shown here is representative of 3 independent experiments, n = 2-3 per group.

5.2.6 GM-CSF, a DC growth factor, is up-regulated and produced locally in atherosclerotic aorta

Classically, Flt3L and GM-CSF are DC growth factors that have been used to generate DC in cultures (Shortman and Naik, 2007). Flt3L is an essential factor for cDC and pDC development at steady state as $Flt3L^{-/-}$ mice have low numbers of DCs (McKenna et al., 2000). For non-lymphoid tissue DCs, Flt3 plays a more important role in the development of $CD103^+$ DCs in skin, lung, liver, kidney, (Ginhoux et al., 2009), pancreatic islet (Yin et al., 2012) and aorta (Choi et al., 2011).

In contrast, GM-CSF is thought to be a growth factor for DCs only under inflammatory conditions because development of lymphoid tissue DCs occur normally in mice deficient in GM-CSF or its receptor (Vremec et al., 1997). Importantly, GM-CSF levels are low under homeostatic conditions but increase during inflammation (Cheers et al., 1988; Hamilton, 2002). Yet, a recent report revealed that the absence of GM-CSF disrupts non-lymphoid tissue DC homeostasis particularly $CD103^+$ DCs while $CD11b^+$ DCs were unaffected except for $CD103^+$ $CD11b^+$ DCs in the lamina propia (Greter et al., 2012a).

Lastly, M-CSF (also known as CSF-1) is a growth factor for macrophage cultures but DCs also express the receptor for M-CSF and M-CSF deficient op/op mice are known to exhibit reduced pDCs and cDCs (MacDonald et al., 2005). Furthermore, another group has shown the ability of M-CSF to generate pDCs and cDCs both *in vitro* and *in vivo* independently of Flt3

(Fancke et al., 2008). IL-34, an alternative ligand for the M-CSF receptor (Chihara et al., 2010), has also been shown to be essential to the development of LCs, a unique DC subset in the skin (Greter et al., 2012b; Wang et al., 2012).

We hypothesized that DC growth factors might be elevated and contribute to the expansion of $CD11b^{+}$ DCs seen in $apoE^{-/-}$ mice. We went on to examine the mRNA expression of these growth factors in the aorta. Although the expression of Flt3L and M-CSF are increased in $apoE^{-/-}$ aorta, it is not statistically significant compared to WT aorta. Hence, among the four growth factors discussed above, only GM-CSF was significantly up-regulated (fold change ≈ 6.6) in $apoE^{-/-}$ aorta compared to WT aorta (Figure 5.10A). Likewise, GM-CSF was elevated in $Ldlr^{-/-}$ mice (fold change ≈ 4.8) (Figure 5.10B). Although GM-CSF was reported to preferentially increase in the spleen for extramedullary hematopoiesis to occur (Robbins et al., 2012), we did not detect this in our model (Figure 5.10C).

We also validated the increase of GM-CSF levels in atherosclerotic aorta by ELISA assay and found a 3-fold increase in GM-CSF protein levels (Figure 5.10D). There was no difference in GM-CSF levels in aortic draining lymph nodes (iliac lymph nodes) (Figure 5.10D). Furthermore, though circulating GM-CSF levels have been reported to increase in response to LPS-induced inflammation (Sheridan and Metcalf, 1972), both serum and plasma GM-CSF levels were undetectable by ELISA (data not shown).

Our findings indicated that during atherosclerosis, GM-CSF expression is increased and restricted to the aorta as it is not found in the spleen, circulation

and draining lymph nodes. This suggests that the production of GM-CSF in the aorta in apoE$^{-/-}$ mice may be involved in the expansion of CD11b^{+} DCs in the aorta. Comparing the difference in fold increase of GM-CSF between apoE$^{-/-}$ (fold change ≈ 6.6) and Ldlr$^{-/-}$ (fold change ≈ 4.8) with the percentage of CD11b^{+} DC expansion in these models (apoE$^{-/-}$: 2.04 fold; Ldlr$^{-/-}$: 1.48 fold) also imply that the amount of GM-CSF present in the aorta determined the extent of CD11b^{+} DC accumulation.

A

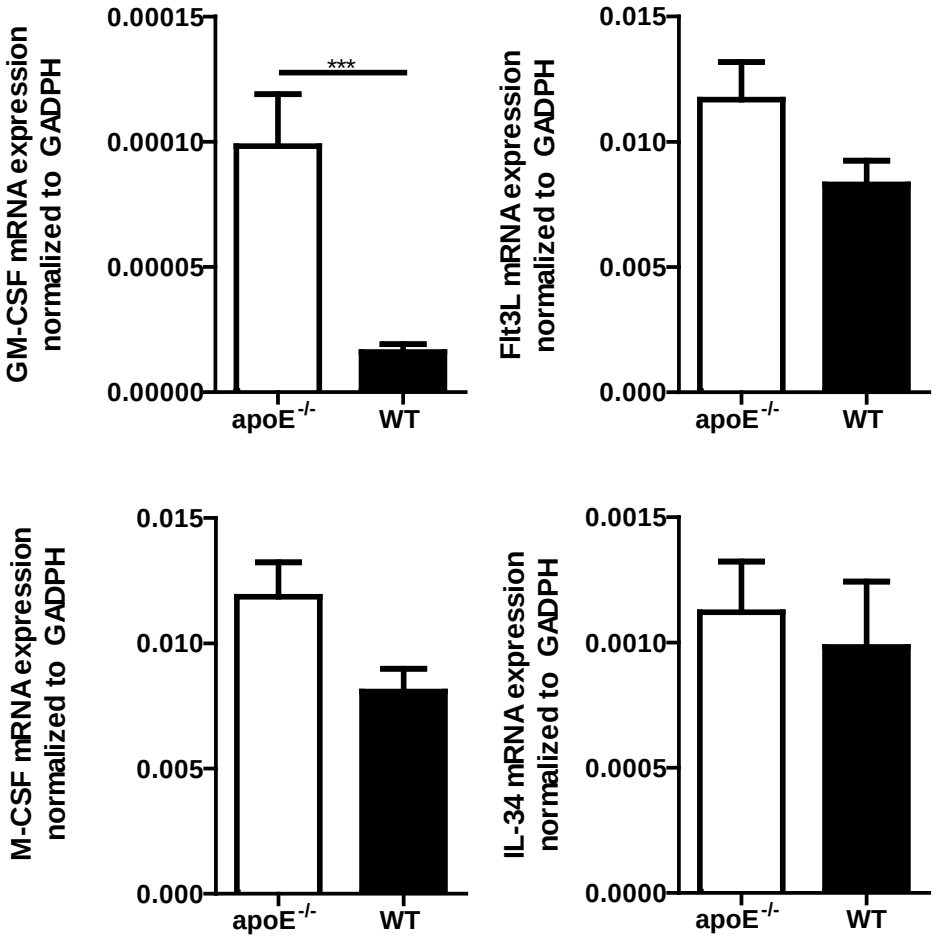
GM-CSF mRNA expression normalized to GADPH
0.00015
0.00010
0.00005
0.00000
***
apoE-/-
WT
Flt3L mRNA expression normalized to GADPH
0.015
0.010
0.005
0.000
apoE-/-
WT
M-CSF mRNA expression normalized to GADPH
0.015
0.010
0.005
0.000
apoE-/-
WT
IL-34 mRNA expression normalized to GADPH
0.0015
0.0010
0.0005
0.0000
apoE-/-
WT

B

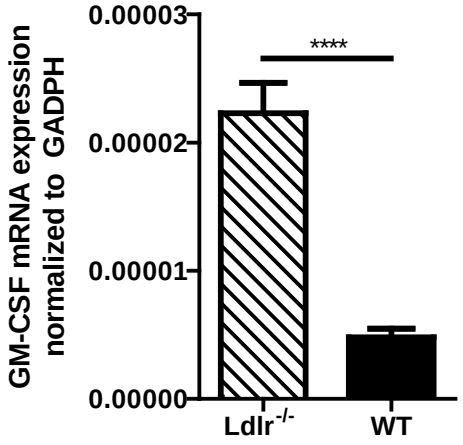
GM-CSF mRNA expression normalized to GADPH
0.00003
0.00002
0.00001
0.00000
****
Ldlr-/-
WT

C

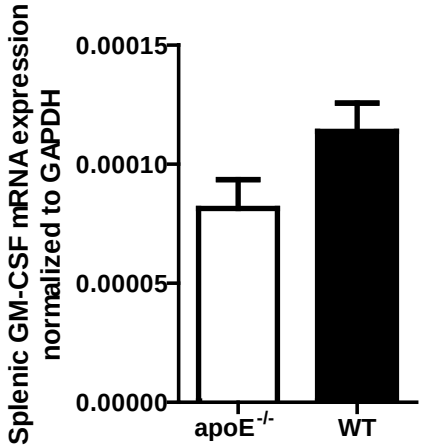
Splenic GM-CSF mRNA expression normalized to GAPDH
0.00015
0.00010
0.00005
0.00000
apoE-/-
WT

D

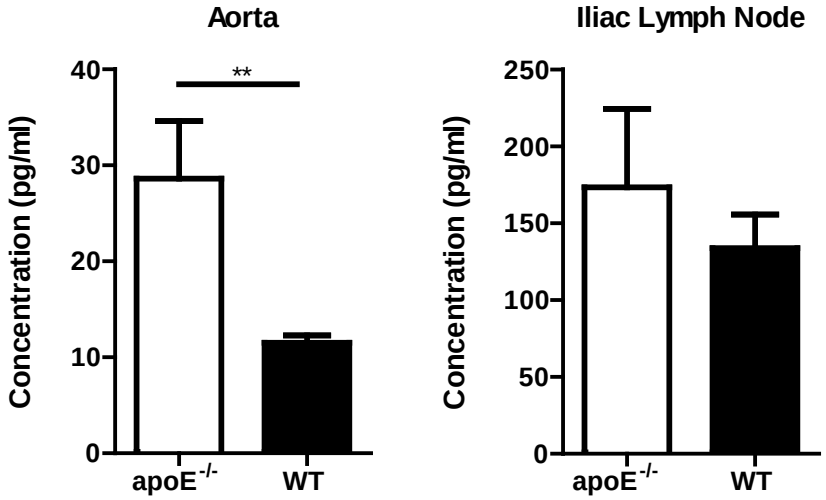

Figure 5.10. GM-CSF is the sole DC growth factor up-regulated in atherosclerotic plaques and its production is localized in the aorta.

(A) mRNA expression of GM-CSF, Flt3L, M-CSF and IL-34 in aorta of apoE$^{-/-}$ and WT mice. Data shown from one experiment, n = 5 per group. (B) mRNA expression of GM-CSF in aorta of Ldlr$^{-/-}$ (shaded bar) and WT mice. Data shown from one experiment, n = 5 per group. (C) Splenic GM-CSF mRNA expression between apoE$^{-/-}$ and WT mice. Data collected from one experiment, n = 5 per group. (D) GM-CSF protein expression was measured by ELISA in aorta and associated draining lymph node (iliac lymph node) in apoE$^{-/-}$ and WT mice. Data shown was from one experiment, n = 6 per group for aorta and n = 3 per group for iliac lymph node. ApoE$^{-/-}$: white bar; WT: black bar. Student's t test: *** $p<0.001$, **$p<0.05$. Error bars represent SEM.

5.2.7 Production of GM-CSF is decreased along with CD11b$^+$ DC accumulation in Ezetimibe-induced disease regression

Considering that elevated GM-CSF levels may be responsible for CD11b$^+$ DC accumulation in the aorta, we hypothesized that GM-CSF levels will be similarly affected as CD11b$^+$ DC accumulation in a disease regression model (Section 5.2.2). Thus, we assessed the amount of GM-CSF production in mice treated with Ezetimibe.

We found that Ezetimibe treatment induced a down-regulation of GM-CSF mRNA expression in apoE$^{-/-}$ mice (Figure 5.11A) and this drop was also significantly reflected at protein level (Figure 5.11B).

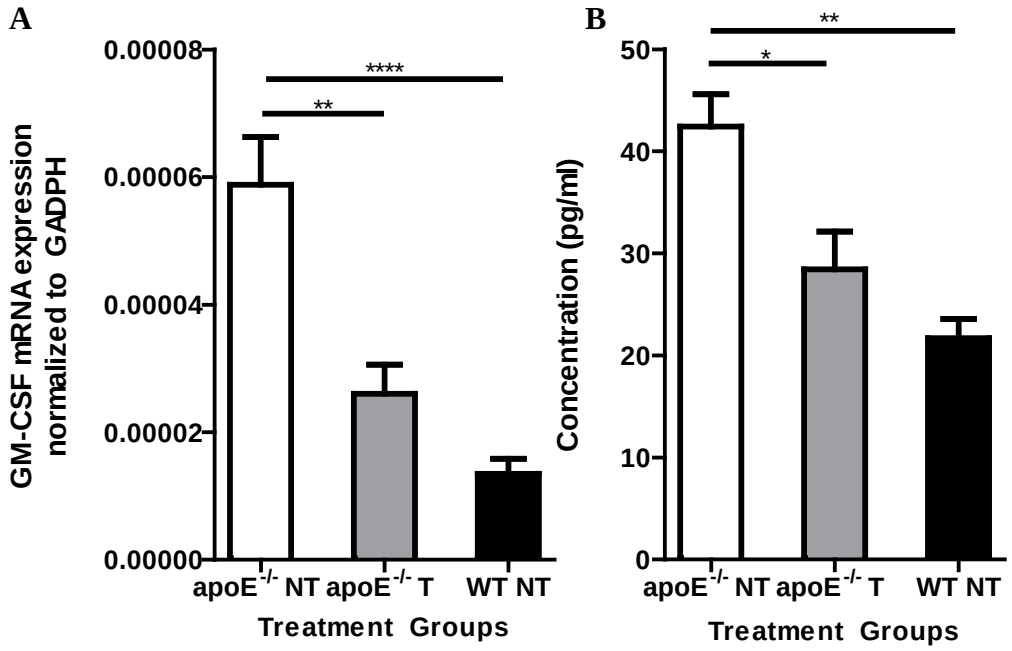

Figure 5.11. Ezetimibe treatment reduced production of GM-CSF.

(A) mRNA expression of GM-CSF in aorta. Data shown consists of n = 5 mice per group. (B) Protein expression of GM-CSF in aorta. Data shown from one experiment, n = 5-6 mice per group. $ApoE^{-/-}$ NT: white bar; $ApoE^{-/-}$ T: grey bar. WT NT: black bar. NT: non-treated; T: treated. Student's t test: **** $p<0.0001$, ** $p<0.05$, * $p<0.01$. Error bars represent SEM.

5.3 Summary

Earlier reports have established few theories behind the accumulation of DCs in atherosclerosis. Thus far, we have extended investigation into specifically $CD11b^+$ DCs. There are three possible mechanistic explanations for the expansion of $CD11b^+$ DCs. They are: increased precursors, increased *in situ* proliferation or increased differentiation and survival by growth factors.

We have clearly demonstrated that bone marrow precursors and extramedullary hematopoiesis do not play a role in the expansion of $CD11b^+$ DC in atherosclerotic aorta. Based on our earlier finding that monocytes give rise to $CD11b^+$ DCs (Chapter 4), we verified that monocytosis occurred in our model as shown by others. We confirmed that monocytosis is essential to the expansion of $CD11b^+$ DCs by reversing the process of hypercholesterolemia with a cholesterol-lowering drug, Ezetimibe, which eliminated monocytosis and $CD11b^+$ DC expansion in $apoE^{-/-}$ mice.

Though we showed that $CD11b^+$ DCs can proliferate *in situ* in the aorta, there was no difference in the proliferative ability of $CD11b^+$ DCs between $apoE^{-/-}$ and WT mice. More importantly, most of the $CD11b^+$ DCs in the aorta are actually non-proliferating cells, strongly suggesting that proliferation is not a major mechanism for $CD11b^+$ DC expansion.

Lastly, we showed that GM-CSF is the only DC poietin that is highly up-regulated and localized in the atherosclerotic aorta. We further confirmed that elevated GM-CSF levels accounted for $CD11b^+$ DC accumulation by

Ezetimibe treatment. The decrease of hypercholesterolemia by Ezetimibe treatment restored GM-CSF levels closer to homeostatic conditions and was accompanied by a reduction of monocytosis and $CD11b^+$ DC expansion.

Chapter 6

GM-CSF: a DC poietin

Chapter 6 – GM-CSF: a DC poietin

6.1 Introduction

Previously we demonstrated that elevated GM-CSF levels in the aorta accounted in part for $CD11b^+$ DC expansion in atherosclerosis. GM-CSF is a well-recognized cytokine for promoting DC differentiation and survival *in vitro* (Inaba et al., 1992; Ni and O'Neill, 2001). Yet, recent evidence showed that GM-CSF is not just a simple DC poietin.

GM-CSF and Flt3L are known to preferentially expand different DC subsets (Daro et al., 2000; Parajuli et al., 2001). DCs derived from GM-CSF resemble closely to inflammatory TipDCs whereas those derived from Flt3L represent steady state resident DCs (Xu et al., 2007). The presence of GM-CSF is also sufficient to divert committed Flt3L-derived DCs (pDCs and $CD8^+$ $Sirp\alpha^-$ DCs) into GM-CSF derived DCs ($CD8^-$ $Sirp\alpha^+$ DCs) (Zhan et al., 2012) and to prevent differentiation into DC-like regulatory macrophages (Diao et al., 2012).

Besides influencing the developmental outcome of DCs, an early study on a GM-CSF producing tumor cell vaccine implied an ability of GM-CSF to recruit DCs at vaccination sites through local release of MIP-1α (Kielian et al., 1999). GM-CSF was also found to be required for DC recruitment and survival *in vivo* as part of host response against an enteric bacterial pathogen infection (Hirata et al., 2010).

The role of GM-CSF is not well-studied in atherosclerosis. It has been proven that GM-CSF is pro-atherogenic in $Ldlr^{-/-}$ mice by promoting a DC accumulation (Shaposhnik et al., 2007) and intimal DC proliferation (Zhu et al., 2009). Conversely, the function of GM-CSF is less clear in the $apoE^{-/-}$ mice. While GM-CSF deficiency in $apoE^{-/-}$ mice was shown to increase atherosclerosis, indicating an anti-atherogenic role for GM-CSF (Ditiatkovski et al., 2006), supplementing GM-CSF to $apoE^{-/-}$ mice exacerbated disease, implying that GM-CSF is pro-atherogenic in this study (Haghighat et al., 2007).

Though we demonstrated that GM-CSF is required for $CD11b^{+}$ expansion in $Apoe^{-/-}$ mice, the identity of cells that are responsive to GM-CSF signaling and the source of GM-CSF are still unknown. Consequently, we decided to examine the expression of GM-CSF receptors and determine the source of GM-CSF in atherosclerotic plaques.

6.2 Results

6.2.1 GM-CSF Receptors are highly up-regulated in atherosclerotic aorta

GM-CSF receptor is a heterodimer made up of two subunits: α ligand-binding subunit and β common signaling subunit. While the α subunit is cytokine-specific, the GM-CSF βc subunit is shared with other cytokines, IL-3 and IL-5. In the mouse, IL-3 has an additional β chain subunit, $\beta_{IL\text{-}3}$ (GM-CSF receptor β2) which can bind to IL-3Rα in the absence of the common β subunit for IL-3 signaling to occur (Robb et al., 1995).

We first assessed the mRNA expression of GM-CSF receptors and observed that both α (fold change ≈ 7) (Figure 6.1A) and βc (fold change ≈ 4) (Figure 6.1B) subunits were up-regulated in apoE$^{-/-}$ mice compared to WT controls. Since the βc subunit is common to both the IL-3 and IL-5 receptors, to exclude a contribution of IL-3 and IL-5, we investigated the cytokine-specific α subunits for both receptors. There was no significant difference in the IL-5 receptor α subunit (Figure 6.1C) between apoE$^{-/-}$ and WT mice. However, there was an increase in IL-3 receptor α subunit (fold change ≈ 2) (Figure 6.1D) and $\beta_{IL\text{-}3}$ (fold change ≈ 22) (Figure 6.1E), implying that elevated amounts of IL-3 receptor complexes are formed in atherosclerosis.

Given that IL-3 together with GM-CSF can stimulate emergency hematopoiesis (Robbins et al., 2012) and IL-3 can generate myeloid DCs independently of GM-CSF (Baumeister et al., 2003), we assessed the

expression of this cytokine in the aorta. Surprisingly, there was no difference in IL-3 expression (Figure 6.1F) between apoE$^{-/-}$ and WT mice.

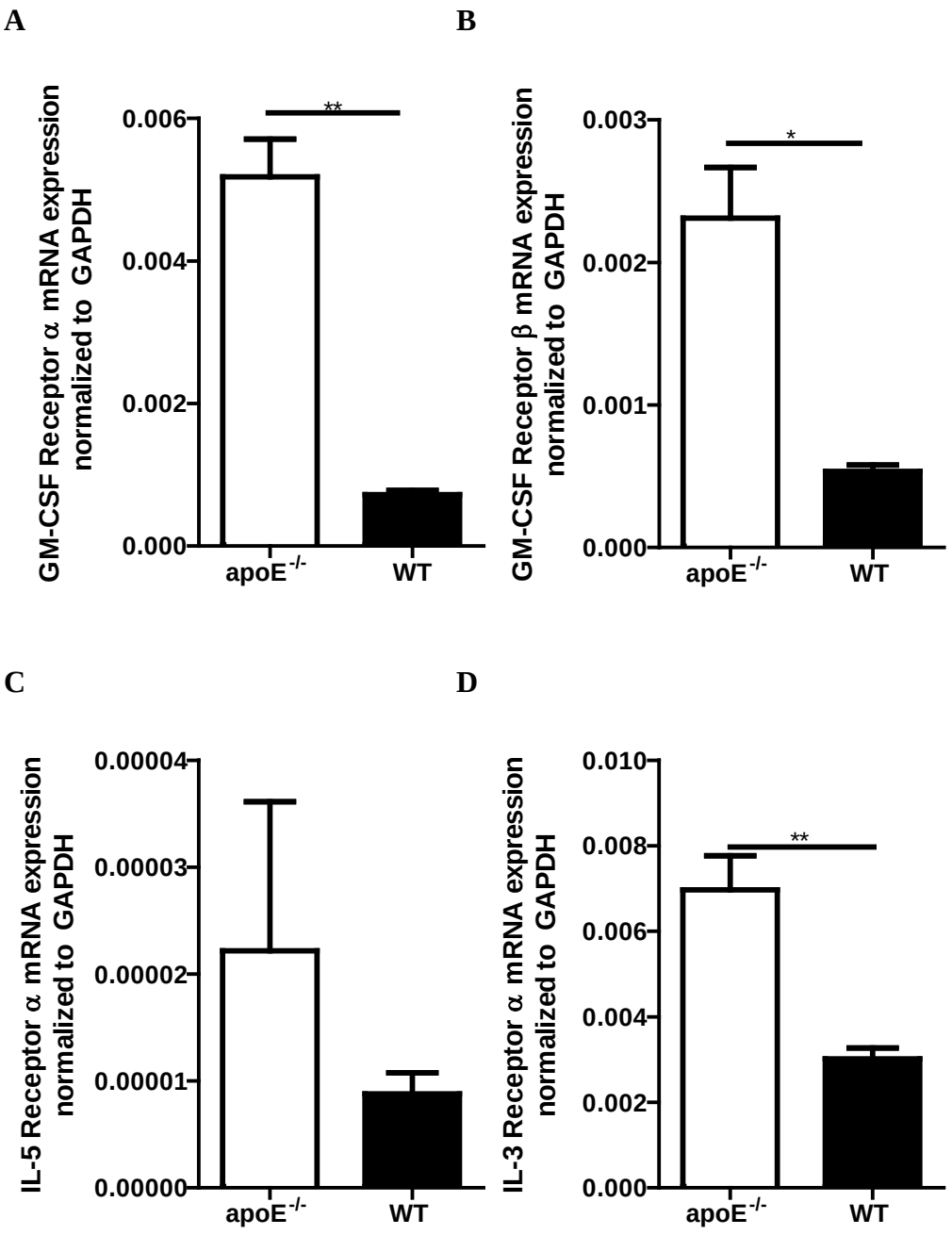
A
B
C
D
GM-CSF Receptor α mRNA expression normalized to GAPDH
GM-CSF Receptor β mRNA expression normalized to GAPDH
IL-5 Receptor α mRNA expression normalized to GAPDH
IL-3 Receptor α mRNA expression normalized to GAPDH
0.006
0.004
0.002
0.000
0.003
0.001
0.00004
0.00003
0.00002
0.00001
0.00000
0.010
0.008
0.006
0.004
0.002
0.000
**
*
**
apoE-/-
WT

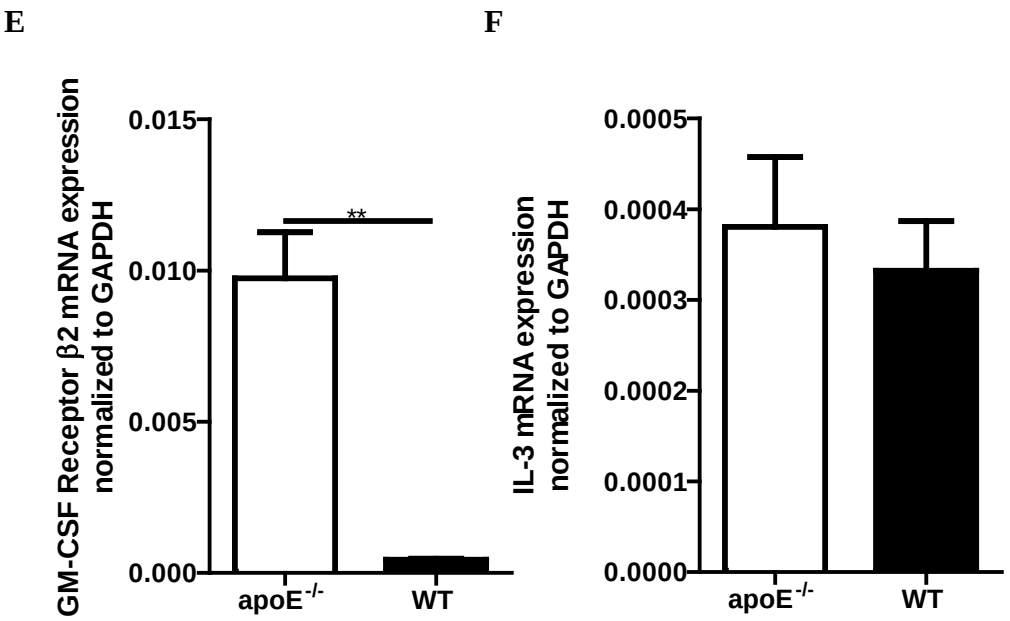

Figure 6.1. Both α and β subunit of GM-CSF receptor are elevated in atherosclerotic aorta.

(A and B) mRNA expression of α and βc subunits of GM-CSF receptor in aorta. (C) mRNA expression of IL-5 receptor α subunit in aorta. (D) mRNA expression of IL-3 receptor α subunit in aorta. (E) mRNA expression of additional IL-3 β subunit, β_{IL-3} (GM-CSF receptor β_2) in aorta. (F) mRNA expression of IL-3 in aorta. $ApoE^{-/-}$: white bars; WT: black bars. Data collected from one experiment, n = 5 per group. Student's t test: **$p<0.05$, *$p<0.01$. Error bars represent SEM.

6.2.2 Circulating monocytes expressed both subunits of GM-CSF receptor with βc subunit being up-regulated in atherosclerosis

Earlier we have shown that GM-CSF receptors were elevated in atherosclerosis without identifying the cells that express them. Expression of α subunit of GM-CSF receptor (GMRα) is mainly detected on myeloid cells and is highest in monocytes (Rosas et al., 2007). Thus far, expression of βc subunit (CD131) in mouse has been reported for neutrophils (Robb et al., 1995) and DC subsets (Greter et al., 2012a). However, the receptor subunits are always co-expressed on leukocytes (Hercus et al., 2009). Here, we sought to investigate the cells which express GM-CSF receptors by flow cytometry.

Circulating monocytes expressed both GMRα and CD131 with Gr-1^{hi} monocytes expressing higher levels than Gr-1^{low} monocytes (Figure 6.2A). In addition, monocytes in apo$E^{-/-}$ mice expressed higher levels of CD131 than WT mice (Figure 6.2B), while there is no difference in GMRα levels. To determine whether the expression level of CD131 is up-regulated due to atherosclerosis in apo$E^{-/-}$ mice, we further examined the expression level in apo$E^{-/-}$ mice treated with Ezetimibe. Indeed, we found that expression of CD131 on circulating monocytes is reduced in apo$E^{-/-}$ mice treated with Ezetimibe (Figure 6.2C), suggesting that expression of CD131 is likely regulated by inflammation.

A

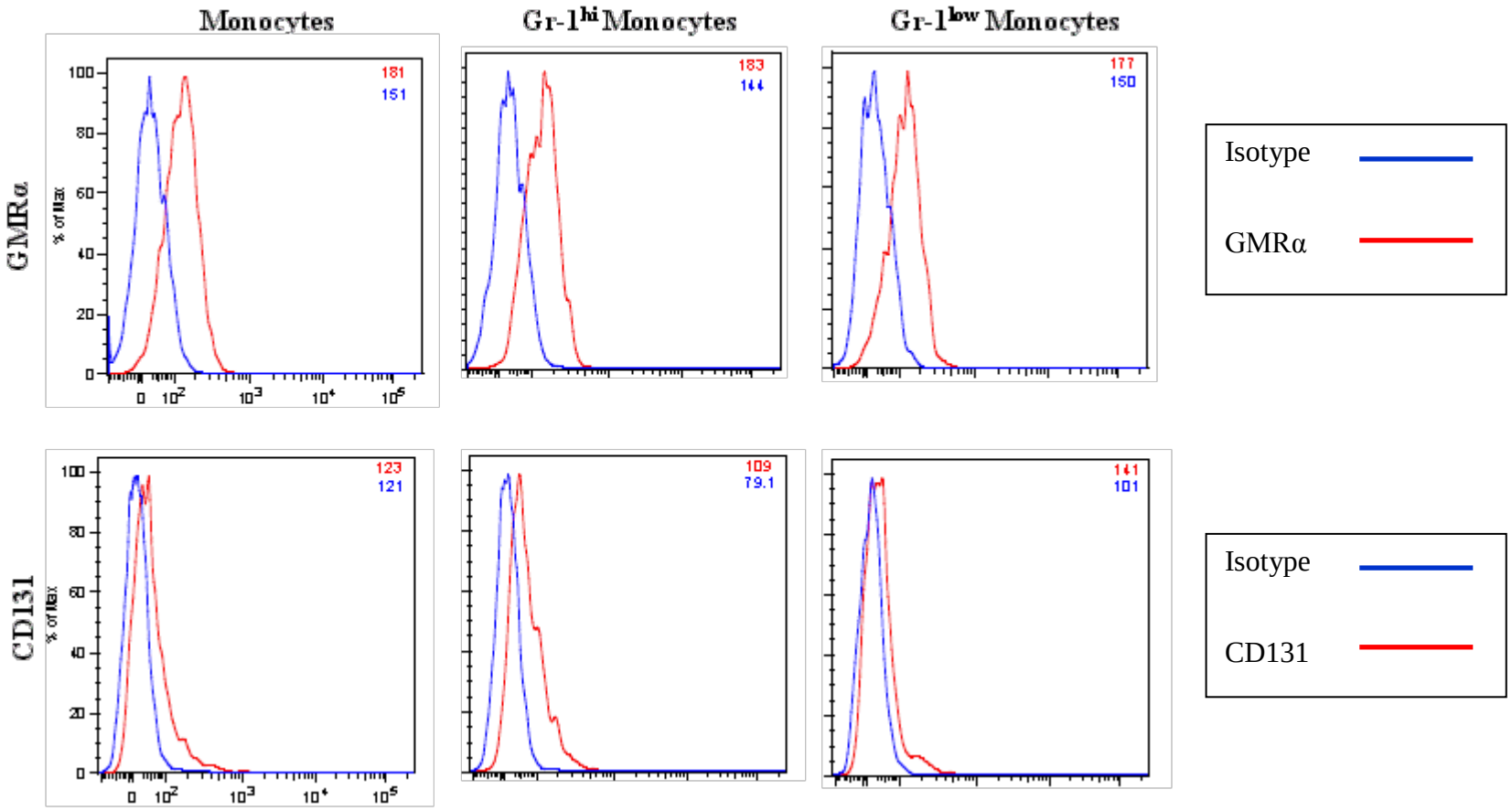
Monocytes
Gr-1hi Monocytes
Gr-1low Monocytes
GMRα
CD131
% of Max
181
151
183
144
177
150
123
121
109
79.1
141
101
Isotype
GMRα
Isotype
CD131

B

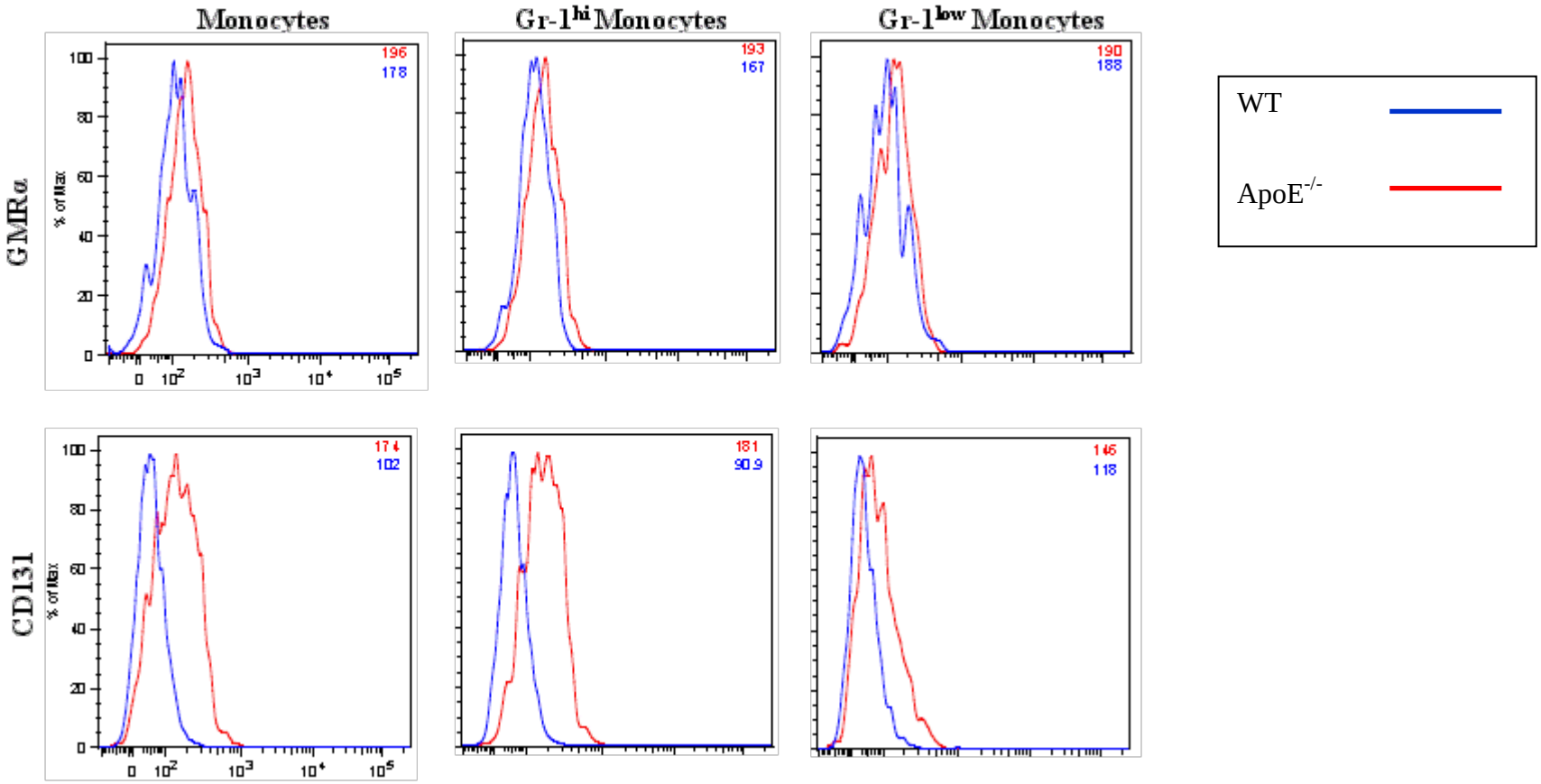
Monocytes
Gr-1hi Monocytes
Gr-1low Monocytes
GMRα
CD131
% of Max
196
178
193
167
190
188
174
102
181
90.9
145
118
WT
ApoE-/-

C

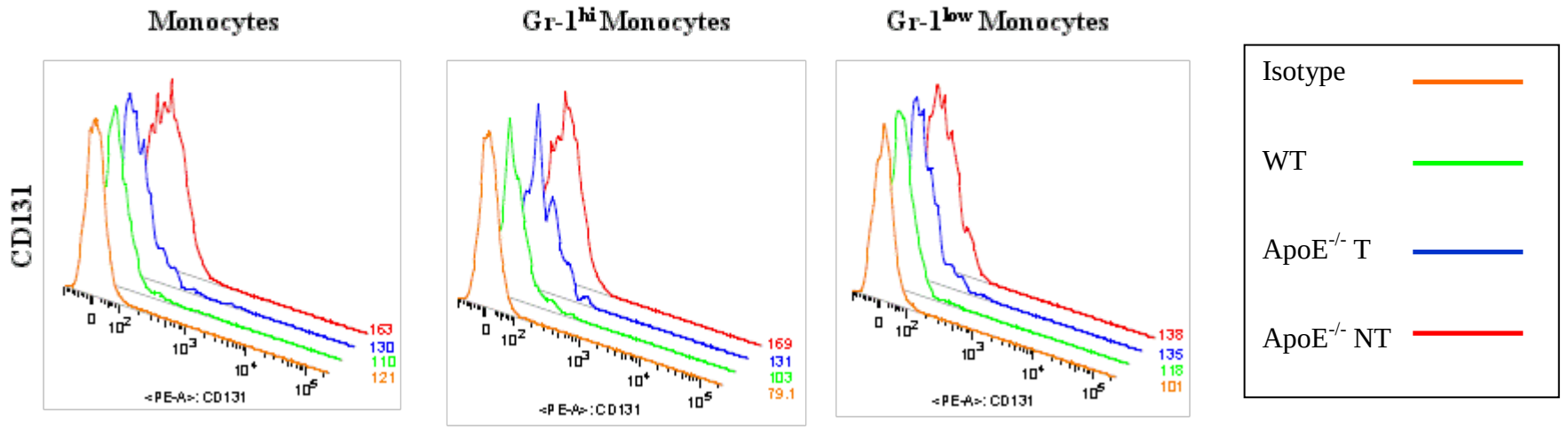

Figure 6.2. Circulating monocytes express both subunits of GM-CSF receptor with βc subunit being inflammation-dependent.

(A) Histograms show expression of GMRα (top) and CD131 (bottom) on circulating monocytes of WT mice. Numbers in the plot indicate geometric mean fluorescence intensity (GMFI). (B) Comparison of GMRα (top) and CD131 (bottom) expression level between apoE$^{-/-}$ and WT mice. Numbers in the plot represent GMFI. (C) Comparison of CD131 expression level in apoE$^{-/-}$ mice treated with Ezetimibe (ApoE$^{-/-}$ T), apoE$^{-/-}$ treated with vehicle (ApoE$^{-/-}$ NT) and WT mice. Numbers beside the histograms indicate GMFI. Data shown are representative of 2 independent experiments, n = 6-7 per group.

6.2.3 CD11b$^+$ DCs in the aorta expressed both subunits of GM-CSF receptors and βc subunit was increased in apoE$^{-/-}$ mice

Since we showed that GM-CSF contributes to CD11b$^+$ DC expansion in aorta, we hypothesized that CD11b$^+$ DCs express the receptors to be responsive to GM-CSF signaling. Consistent with a recent study (Greter et al., 2012a), CD11b$^+$ DCs expressed both GM-CSF receptors at steady state. Moreover, in the aorta, only DCs expressed GMRα with CD11b$^+$ DCs expressing a higher level of the receptor than CD103$^+$ DCs (Figure 6.3A). In contrast, expression of CD131 is not restricted to DCs in the aorta but was also detected on monocytes (Figure 6.3B). However, the Gr-1^{hi} monocytes expressed negligible or low level of CD131 while Gr-l^{low} monocytes expressed more.

As we have seen inflammation regulates the expression of CD131 on circulating monocytes (Section 6.2.2), we also investigated whether this is true for the aorta. Indeed, preliminary results show that expression of CD131 on CD11b$^+$ DCs is higher in apoE$^{-/-}$ mice compared to WT controls (Figure 6.4). Other than CD11b$^+$ DCs, the expression of CD131 remains unchanged between apoE$^{-/-}$ and WT mice for the other populations in the aorta such as CD103$^+$ DCs, monocytes and monocyte-derived cells (data not shown).

Functional GM-CSF receptors require both the α and β subunits. In the aorta, only the DCs possess both subunits, suggesting that they are the only ones responsive to GM-CSF signaling. Importantly, the CD11b$^+$ DCs up-regulate the signaling β subunit during atherosclerosis, implying that they have a higher capacity to respond to GM-CSF.

A

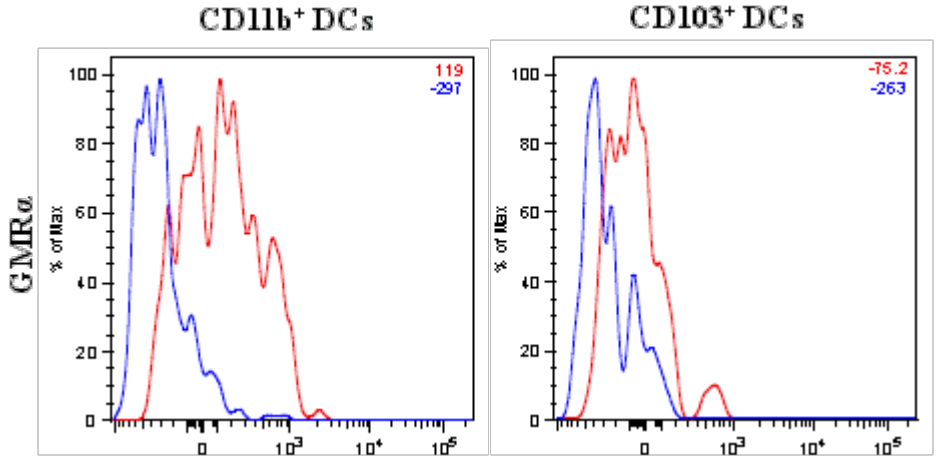

B

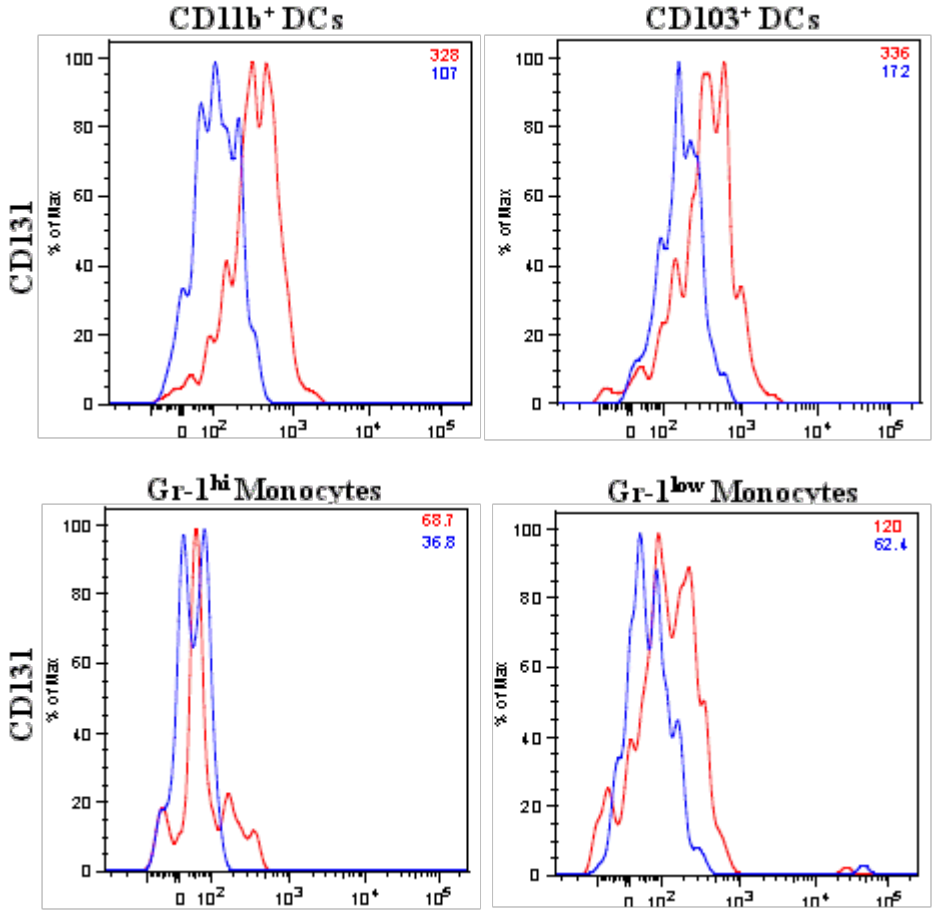

Figure 6.3. CD11b$^+$ DCs possessed GM-CSF receptor at steady state.

(A) Histograms show GMRα expression in CD11b$^+$ and CD103$^+$ DCs in aorta of WT mice. — Isotype; — GMRα. (B) Histograms depict CD131 expression on DC and monocyte subsets in aorta of WT mice. — Isotype; — CD131. Numbers shown inside histograms represent GMFI. Data shown are from n > 3.

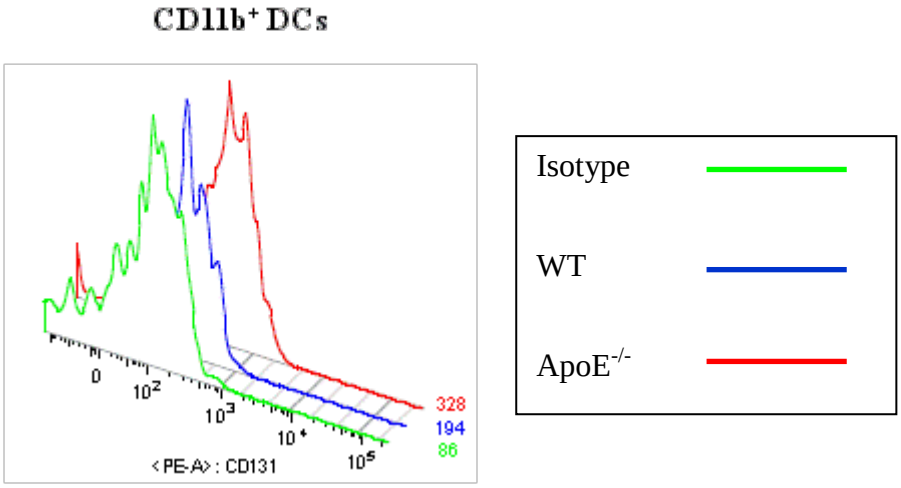

Figure 6.4. CD11b^{+} DCs expressed higher level of CD131 in atherosclerotic aorta.

Histogram comparing expression level of CD131 on CD11b^{+} DCs between apoE$^{-/-}$ and WT mice. Geometric mean fluorescence intensity (GMFI) is indicated beside histograms. Data shown are from 2 mice per group.

6.2.4 Sources of GM-CSF

GM-CSF can be produced by a myriad of cells such as T cells, macrophages, fibroblasts, endothelial cells and tumor cells (Shi et al., 2006). In atherosclerosis, GM-CSF can be produced by vascular smooth muscle cells (Plenz et al., 1997) and expression can be induced in endothelial cells (Rajavashisth et al., 1990) by modified lipoproteins. A recent study revealed GM-CSF as a $CD8^+$ T cell factor important for formation of potent effector DCs (Min et al., 2010). Based on these studies, we set out to evaluate the cells producing GM-CSF in atherosclerotic plaques with a focus on T cells.

Indeed, we could find $CD3^+$ T cells that produce GM-CSF (Figure 6.5). Interestingly, some $CD11b^+$ cells were found to colocalize with GM-CSF staining. In order to identify whether GM-CSF producing $CD11b^+$ cells are DCs, we stained serial sections with markers of DCs and looked at their localization. We saw that the area where $CD11b^+$ DCs were located, positive GM-CSF staining could be found in the subsequent section (Figure 6.6).

A preliminary study on aorta by flow cytometry confirmed that $CD11b^+$ DCs, $CD4^+$ and $CD8^+$ T cells produce GM-CSF (Figure 6.7). GM-CSF production could also be detected on other immune cells such as macrophages and monocytes (data not shown).

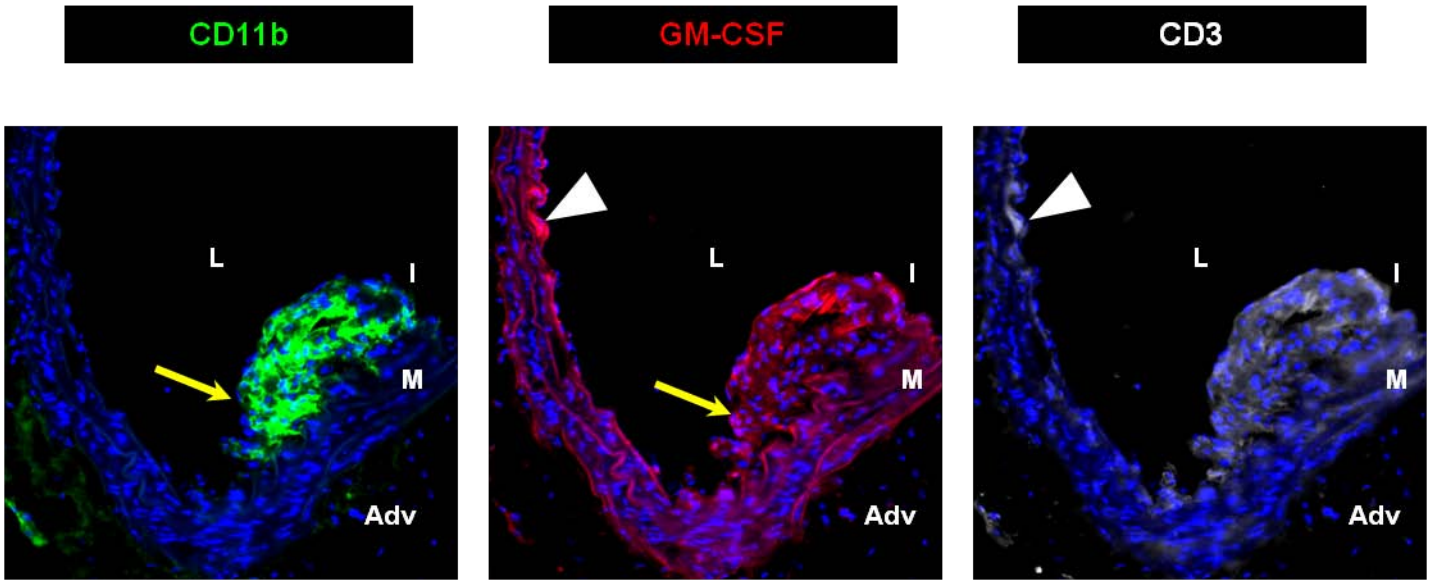

Figure 6.5. CD3 T cells and CD11b$^+$ cells are sources of GM-CSF in atherosclerotic plaque.

Immunofluorescence staining indicated CD3 T cells (triangle) and CD11b$^+$ cells (yellow arrow) produce GM-CSF. L: lumen; I: intima; M: media; Adv: adventitia. Magnification 200x. Scale bar represents 50µm.

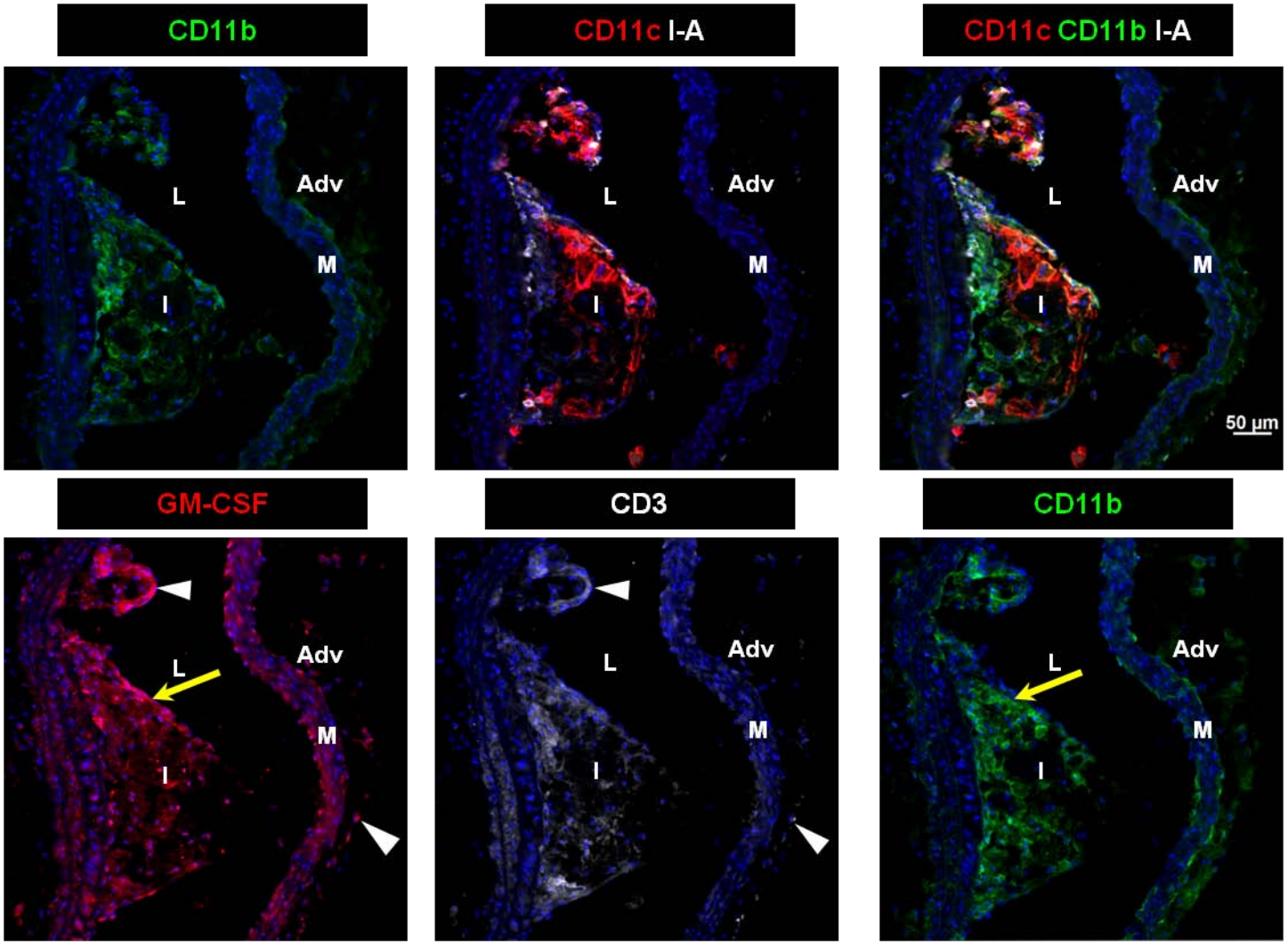

Figure 6.6. Serial sections showed CD11b^{+} cells are I-A^{+} CD11c^{+} DCs producing GM-CSF.

Colocalization of GM-CSF and CD11b is indicated by yellow arrows. CD3 T cells producing GM-CSF are present inside the plaque and outside in the adventitia (white arrows). L: lumen; I: intima; M: media; Adv: adventitia. Magnification 200x. Scale bar represents 50µm.

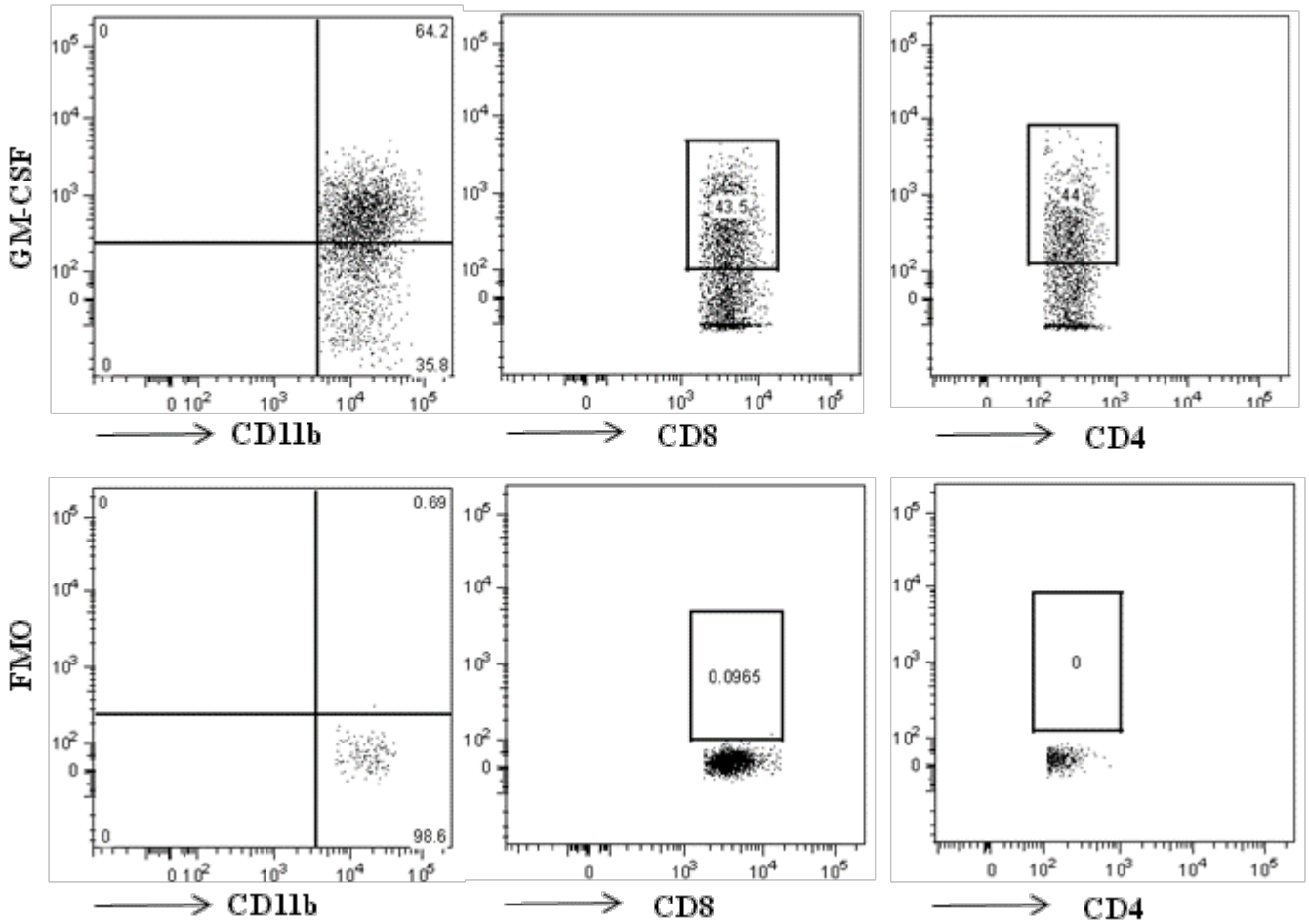

Figure 6.7. CD11b^{+} DCs, CD8^{+} and CD4^{+} T cells produced GM-CSF in the atherosclerotic aorta.

Monensin (1x) was added to aorta during digestion to block cytokine exocytosis. Thereafter, intracellular GM-CSF staining was performed directly ex vivo on aortic cells without re-stimulation. Dot plot show intracellular GM-CSF production (top) in CD11b^{+} DCs, CD8^{+} and CD4^{+} T cells in apoE$^{-/-}$ aorta. Bottom: FMO control. Fluorescence minus one (FMO) control was set up by staining for every antibody in the panel except for GM-CSF. Data shown is from a group of

6.2.5 Neutralizing GM-CSF diminished monocytosis and CD11b^{+} DC accumulation

Since CD11b^{+} DCs possess GM-CSF receptor (Section 6.2.3), produce GM-CSF themselves (Section 6.2.4) and are likely to expand under the influence of GM-CSF (Section 5.2.7), we postulated that neutralizing GM-CSF by intraperitoneal injection into apoE$^{-/-}$ mice should lower their expansion.

Preliminary results showed that blocking GM-CSF significantly reduced monocytosis in the blood (Figure 6.8A). This decrease was a result of a drop in Gr-1^{hi} monocytosis which was associated with a partial increase in the percentage of Gr-1^{low} monocytes (Figure 6.8B). Despite the reduction of blood monocytosis, monocytes in the aorta were unaffected by the treatment. Decreased blood monocytosis was accompanied by a decline in CD11b^{+} DC accumulation in aorta of apoE$^{-/-}$ mice treated with anti-GM-CSF antibody (Figure 6.8C), showing that aortic GM-CSF levels regulate the expansion of CD11b^{+} DC in apoE$^{-/-}$ mice.

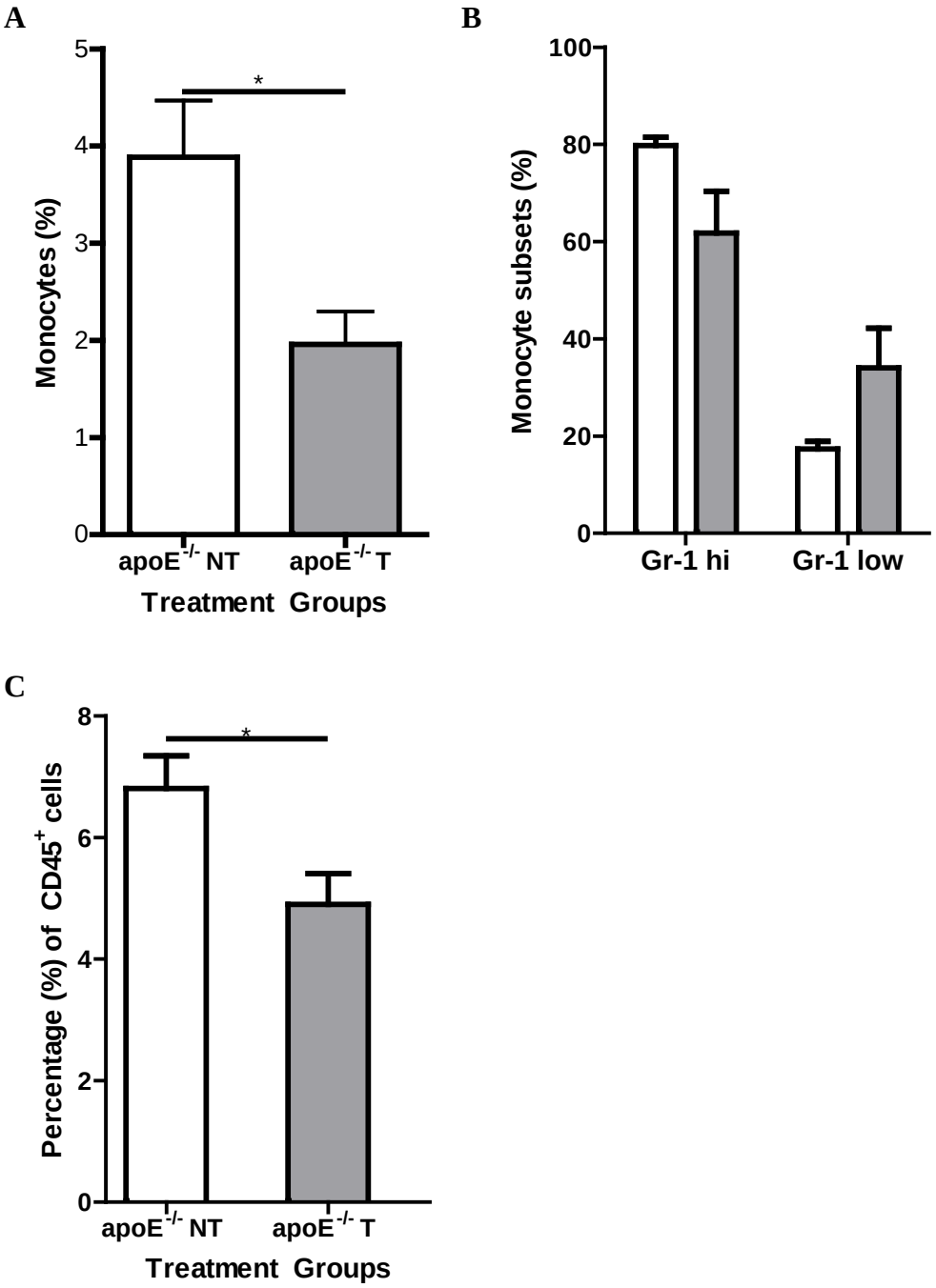

Figure 6.8. Blocking GM-CSF reduced blood monocytosis and CD11b$^+$ DC expansion in the aorta.

Anti-GM-CSF antibody was given by intraperitoneal injection consecutively for 4 days and mice were sacrificed on day 5. (A and B) Bar graphs depict percentage of monocytes and their subsets in the blood of apoE$^{-/-}$ NT and apoE$^{-/-}$ T respectively on day 5. Data shown consists of n = 6 mice per group. (C) Bar graph showing percentages of CD11b$^+$ DCs in terms of total CD45$^+$ leukocytes in apoE$^{-/-}$ NT and apoE$^{-/-}$ T mice after 4 days of anti-GM-CSF antibody administration. Data shown are from 2 independent experiments with n = 2-3 per group. NT: non-treated (white bar); T: treated (grey bar). Student's t test: *$p<0.01$. Error bars represent SEM.

6.2.6 BMDCs as model for CD11b^{+} DCs

As seen *in vivo*, CD11b^{+} DCs expressed GM-CSF receptors and produce GM-CSF themselves. The evidence of this autocrine loop implied that CD11b^{+} DCs may support their own survival. To test this hypothesis and to find an equivalent of CD11b^{+} DCs for *in vitro* studies, we freshly isolated bone marrow cells and cultured them with GM-CSF for 6 days (Inaba et al., 1992) before stimulation with LPS to mimick inflammatory conditions.

After stimulation with LPS, approximately 30-40% of DCs were I-A^{hi} CD11c^{hi}. Of this population, all were CD11b^{+} and CD24^{hi}. Most BMDCs were also Gr-1^{low} and F4/80^{+} with intermediate levels of CD115 (Figure 6.9A). About 60% of BMDCs were also CD64^{+} (Figure 6.9B). These BMDCs were markedly similar to aortic CD11b^{+} DCs with the exception that CD24 expression on CD11b^{+} DCs in the aorta ranged from low to high. Akin to aortic CD11b^{+} DCs, they expressed Sirpα and CD131 and these markers were up-regulated after stimulation with LPS (Figure 6.9C). Therefore, BMDCs cultured with GM-CSF resemble aortic CD11b^{+} DCs for *in vitro* studies.

A

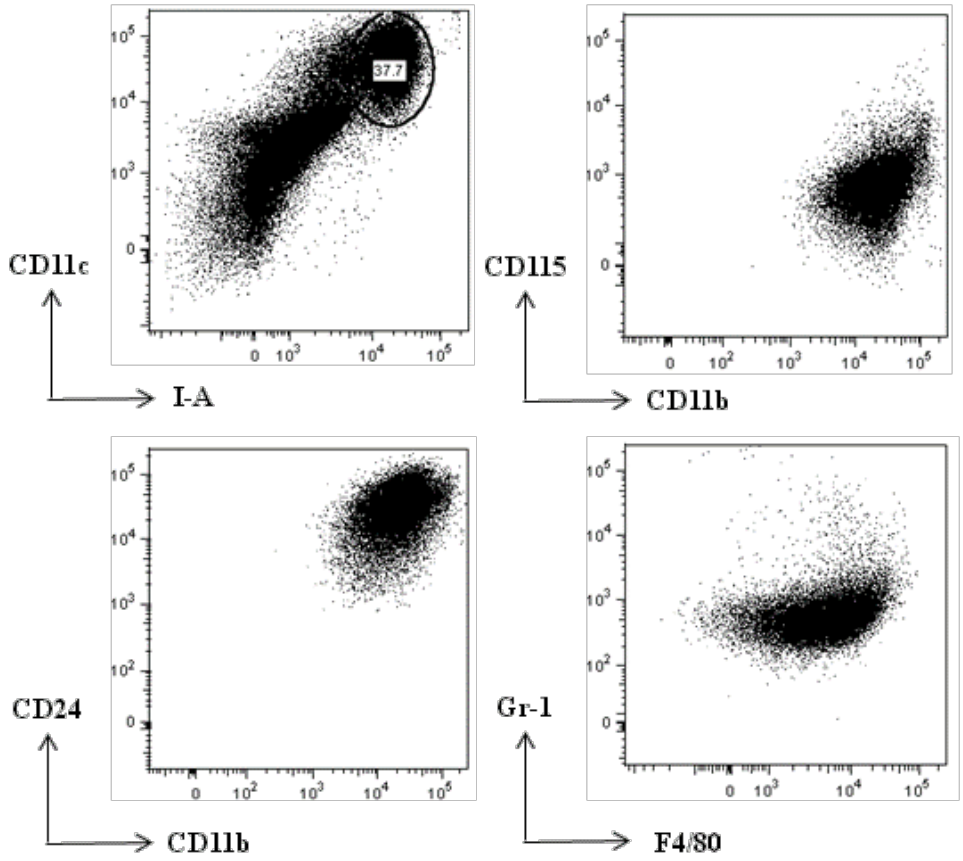
37.7
CD11c
I-A
CD115
CD11b
CD24
CD11b
Gr-1
F4/80

B

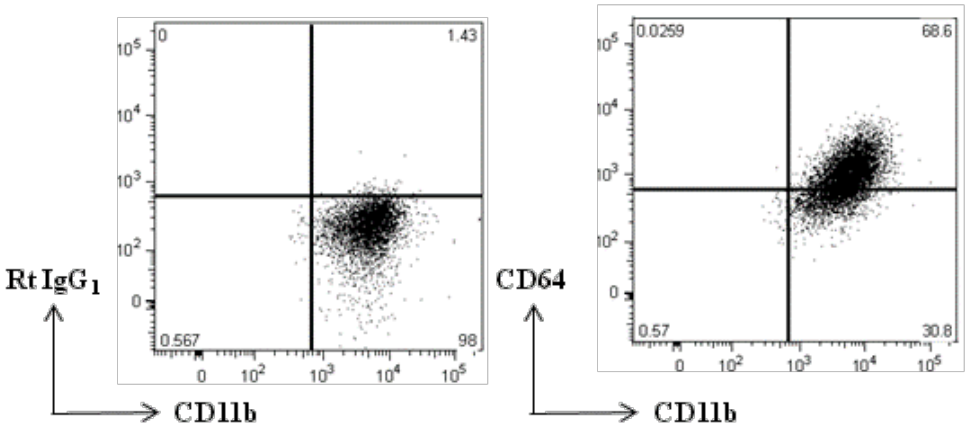
0
1.43
0.567
98
RtIgG1
CD11b
0.0259
68.6
0.57
30.8
CD64
CD11b

C

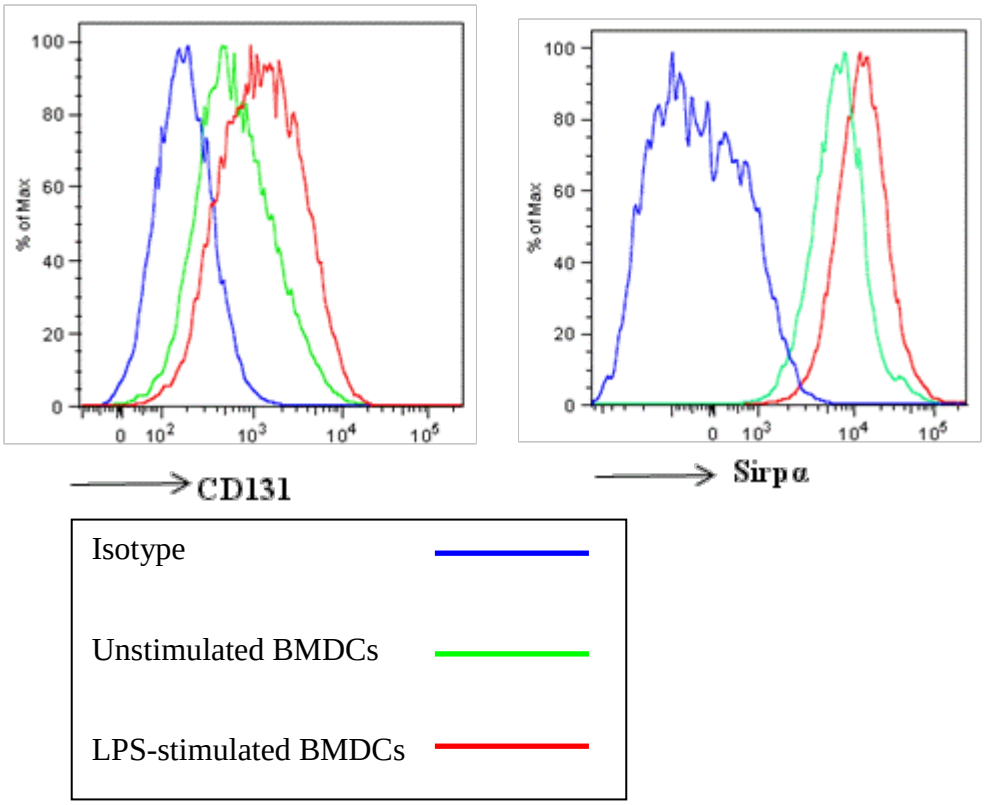

Figure 6.9. BMDCs cultured with GM-CSF are reminiscent of CD11b$^+$ DCs in aorta.

BMDCs derived from a culture of bone marrow cells with GM-CSF after 6 days were stimulated with 1µg/ml LPS. (A) Expression of I-A, CD11c, CD115, CD11b, F4/80, Gr-1 and CD24 was analyzed. (B) Dot plots show CD64 expression (right) on BMDCs against isotype control (left). (C) Histograms show expression of CD131 (left) and Sirpα (right) between unstimulated BMDCs and LPS-stimulated BMDCs with isotype control staining.

6.2.7 GM-CSF secretion by BMDCs promote their own survival

To examine whether autocrine production of GM-CSF by $CD11b^+$ DCs supports their own survival, we isolated and cultured BMDCs as before. However, on day 6 of culture, we deprived the cells of serum and exogenous GM-CSF to investigate the effects on their survival. For this, culture supernatants were collected for detection of GM-CSF protein by ELISA. Simultaneously, the cells were stained with Annexin and PI to assess their survival by flow cytometry.

Interestingly, endogenous secretion of GM-CSF by BMDCs increased over time (Figure 6.10A). The production of GM-CSF was increased slightly with LPS stimulation. Concurrent with this increase in GM-CSF production, we detected a decrease in late apoptotic ($Annexin^+$ PI^+) cells over time (Figure 6.10B).

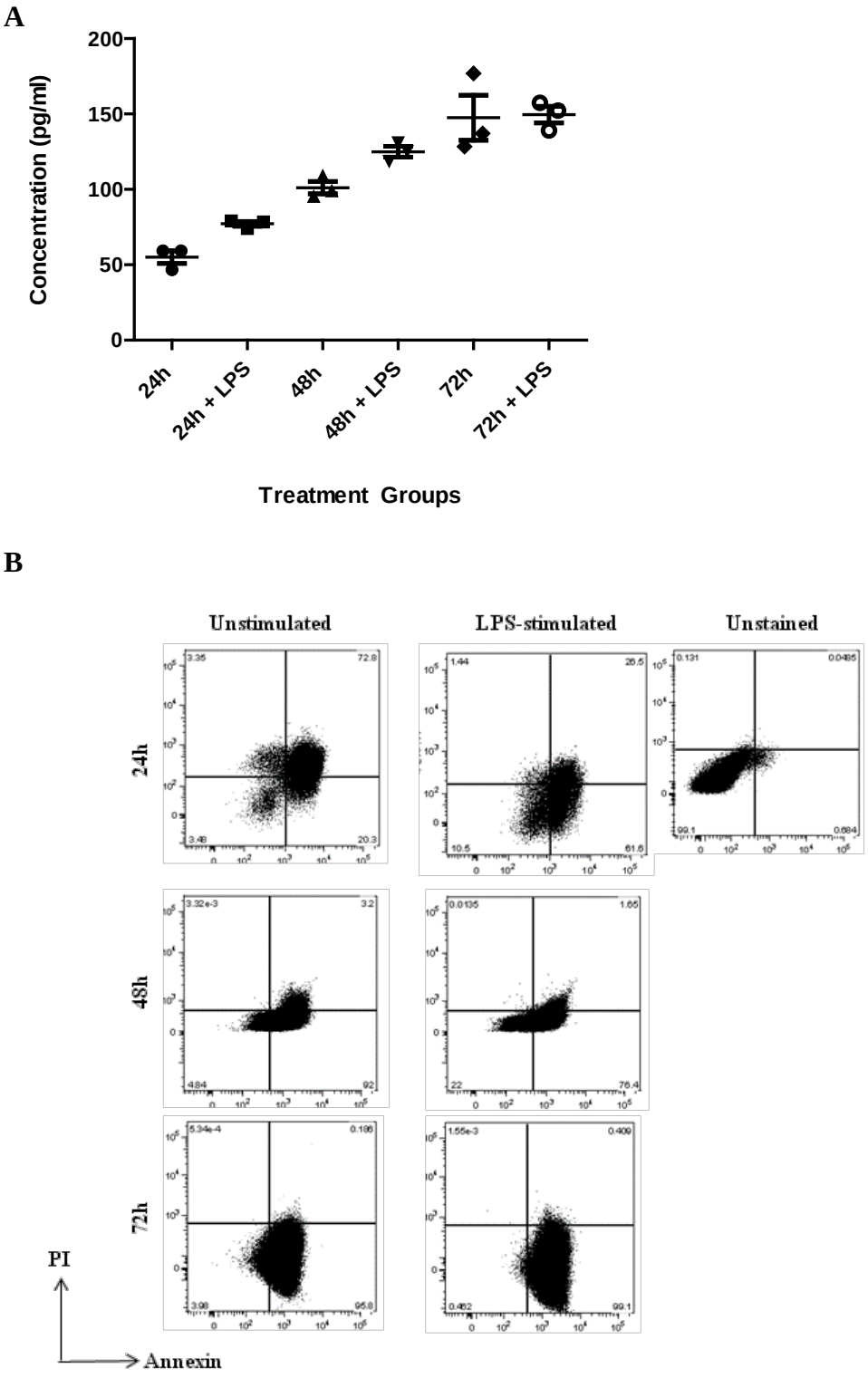

Figure 6.10. Secretion of GM-CSF coincides with survival of BMDCs.

BMDCs were deprived of serum and growth factor, GM-CSF on day 6 and were left unstimulated or stimulated with LPS for 24, 48 and 72 hours. (A) Culture supernatant was collected and assayed for GM-CSF protein concentration by ELISA. (B) Cell survival of BMDCs was analyzed by staining for Annexin and PI by flow cytometry.

6.3 Summary

Here, we showed that both the α and β subunits of the GM-CSF receptor were also increased at mRNA level with the ligand, GM-CSF. Although GM-CSF receptors are known to be expressed on monocytes, we demonstrated for the first time that circulating monocytes in apoE$^{-/-}$ mice expressed higher levels of CD131. This expression was also regulated by the extent of inflammation. Moreover, only DCs in the aorta possess both subunits, with CD11b^{+} DCs expressing higher levels of CD131, indicative of a higher ability to respond to GM-CSF.

We have also found T cells and DCs to be the source of GM-CSF in atherosclerotic plaques. It is not known that DCs produce GM-CSF themselves and this may be unique to the aorta. Blocking GM-CSF directly with a neutralizing antibody resulted in a partial reduction in monocytosis and CD11b^{+} DC expansion. This reinforced the fact that increased GM-CSF in the aorta participate in CD11b^{+} DC expansion.

Since CD11b^{+} DCs expressed GM-CSF receptor and produced GM-CSF themselves, we hypothesize that this autocrine loop affects their survival. We use BMDCs as models of CD11b^{+} DCs and observed that they produce increasing amounts of GM-CSF over time after serum-starvation and withdrawal of exogenous GM-CSF. This increase in production coincided with an increase in survival of BMDCs.

Chapter 7

Function of $CD11b^+$ DCs

Chapter 7 – Function of CD11b$^+$ DCs

7.1 Introduction

During inflammation, monocyte-derived DCs produced pro-inflammatory mediators such as TNF-α and iNOS that may contribute to disease pathogenesis (Chong et al., 2011; Serbina et al., 2003).We wondered if monocyte-derived CD11b$^+$ DCs in atherosclerotic aorta also produce these inflammatory mediators.

7.2 Results

7.2.1 CD11b$^+$ DCs produce TNF-α and iNOS

We first assessed the ability of CD11b$^+$ DCs to produce TNF-α and iNOS by intracellular flow cytometry. While we were able to detect TNF-α production by CD11b$^+$ DCs (Figure 7.1A), we were unable to observe any iNOS production by CD11b$^+$ DCs (data not shown). Interestingly, production of TNF-α was much higher in apoE$^{-/-}$ mice than in WT controls (Figure 7.1B).

While we were unable to detect iNOS production by CD11b$^+$ DCs using flow cytometry, we observed iNOS production by immunofluorescence. iNOS is mainly produced inside the plaque and in the shoulder regions when the plaque is advanced (Figure 7.2), suggesting that it may be involved in plaque stability. Importantly, serial sections showed colocalization of iNOS staining with I-A, CD11c and CD11b (Figure 7.2 A and B), indicating production by CD11b$^+$ DCs.

Often during inflammation, iNOS-derived NO is able to modify proteins through formation of peroxynitrite and this can be detected by its product, nitrotyrosine (Deeb et al., 2006). We speculated that CD11b$^+$ DCs may be involved in nitration of proteins by virtue of its production of iNOS. Consistent with literature (Beckmann et al., 1994; Parastatidis et al., 2007), extensive nitration could be found in atherosclerotic plaques. Interestingly, the site of nitration coincided with the location of CD11b$^+$ DCs (Figure 7.2C), suggesting that they may be involved in the modification of proteins in the

plaque. One of the proteins that could be possibly modified is vascular endothelial cell growth factor C (VEGFC) (unpublished observations).

A

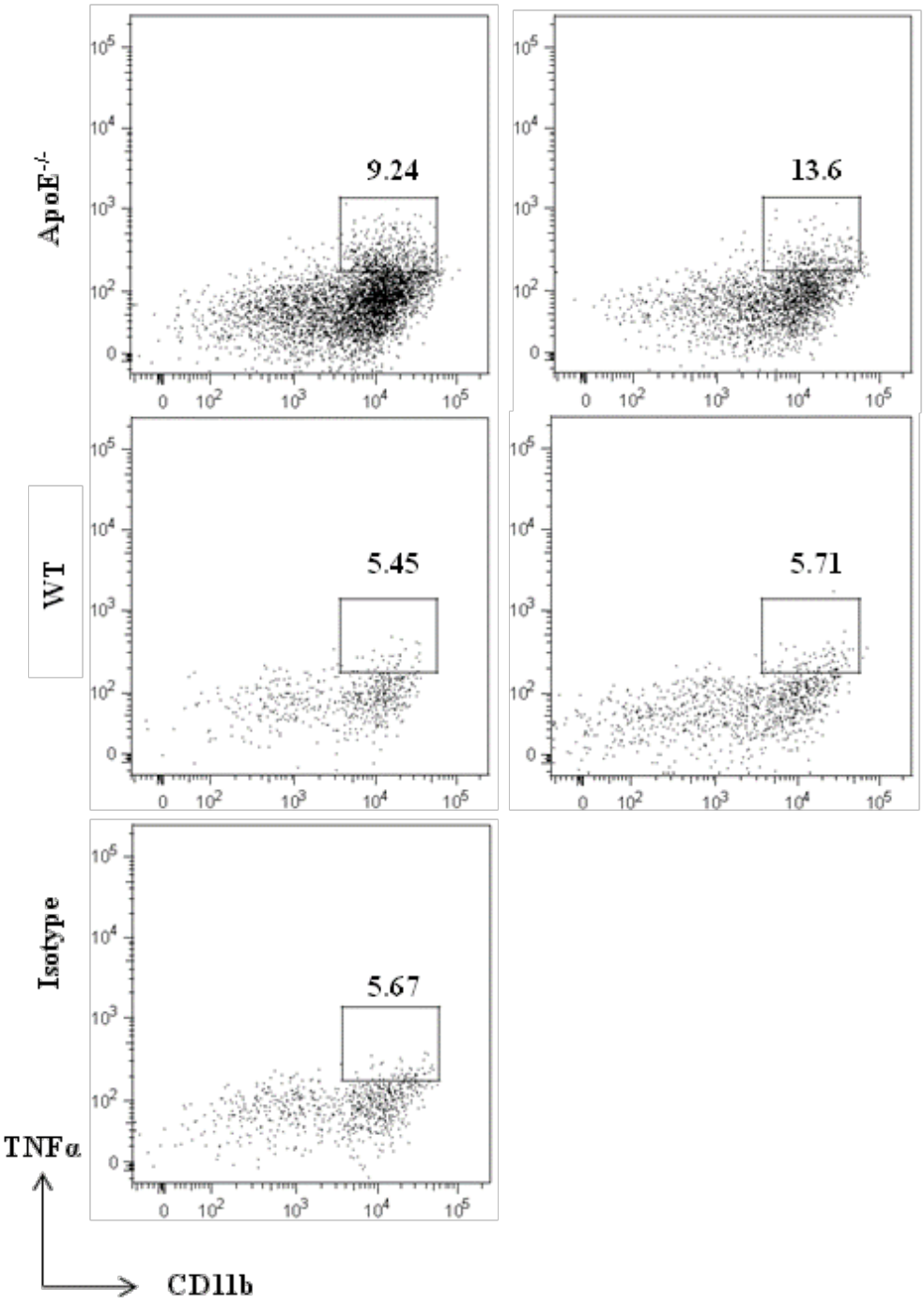

B

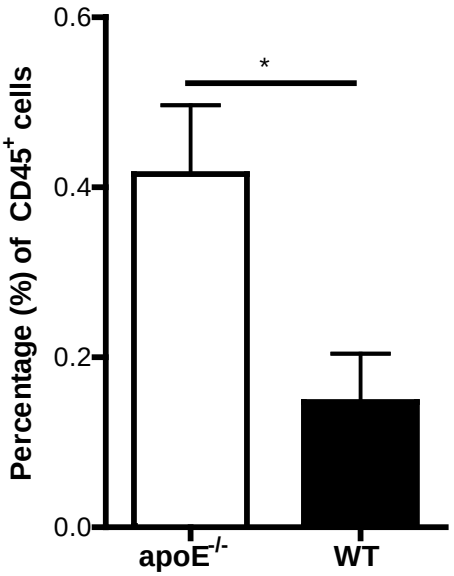

Figure 7.1. CD11b$^+$ DCs produced TNF-α in atherosclerotic aorta.

(A) Monensin (1x) was added to aorta during digestion to block cytokine exocytosis. Thereafter, intracellular TNF-α staining was performed directly ex vivo on aortic cells without re-stimulation. Dot plots show intracellular TNF-α production by I-A$^+$ CD11c$^+$ CD11b$^+$ DCs in apoE$^{-/-}$ and WT mice. (B) Bar graph comparing percentage of TNF-α-producing CD11b$^+$ DCs. Data shown from 2 independent experiments, n = 2-3 mice per group. Student's t-test: *p<0.01. Error bar represents SEM.

A

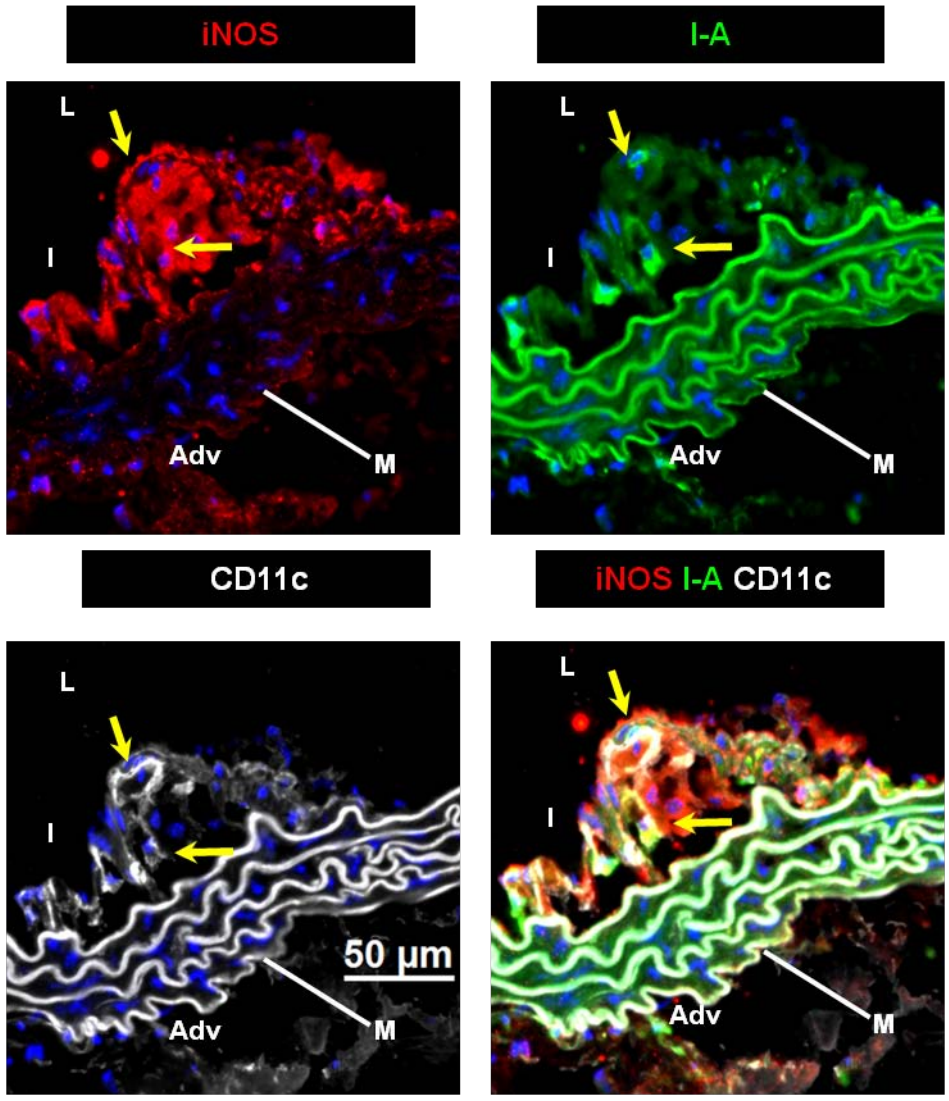

Figure 7.2. CD11b$^+$ DCs produce iNOS.

(A) I-A$^+$ CD11c$^+$ DCs colocalized with production of iNOS in the plaque area (yellow arrows). L: lumen; I: intima; M: media; Adv: adventitia. Scale bar represents 50µm.

B

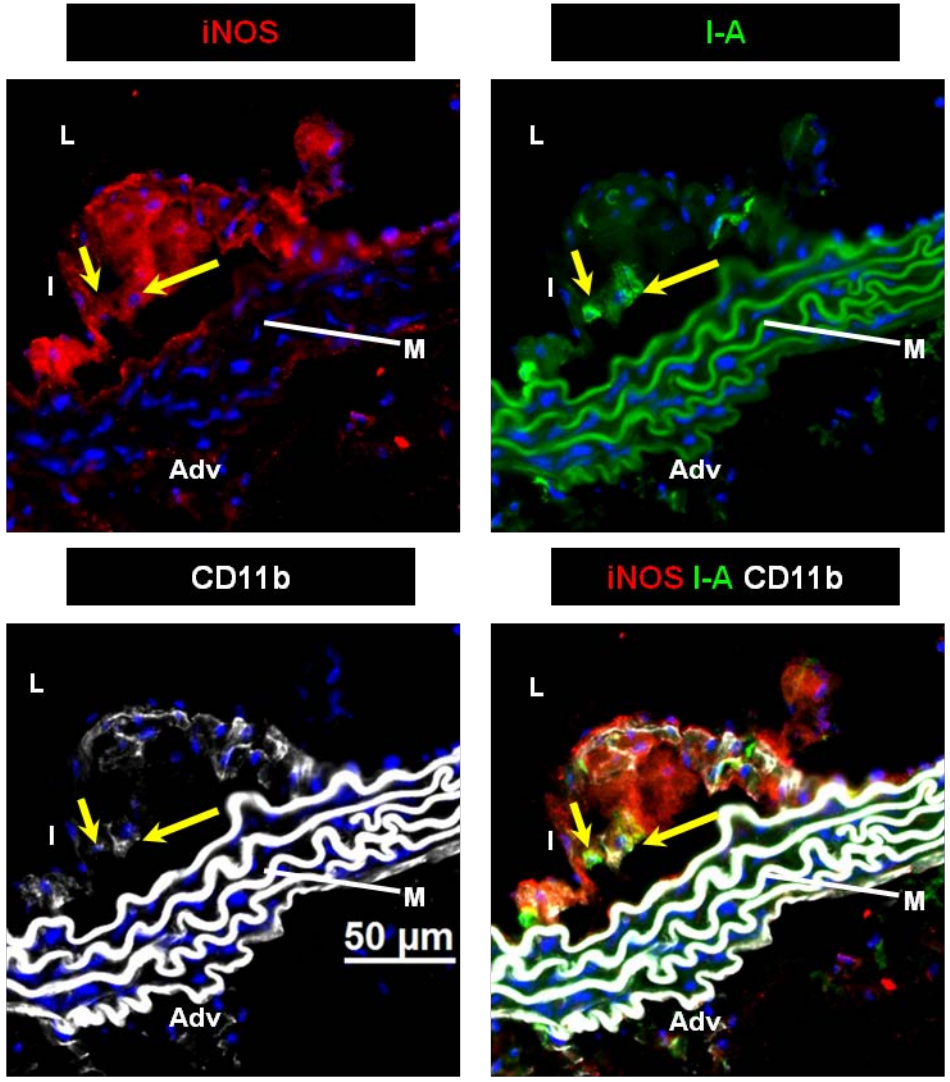

Figure 7.2. CD11b$^+$ DCs produce iNOS.

(B) Serial sections were stained with CD11b to verify DC population producing iNOS (yellow arrows). L: lumen; I: intima; M: media; Adv: adventitia. Scale bar represents 50µm.

C

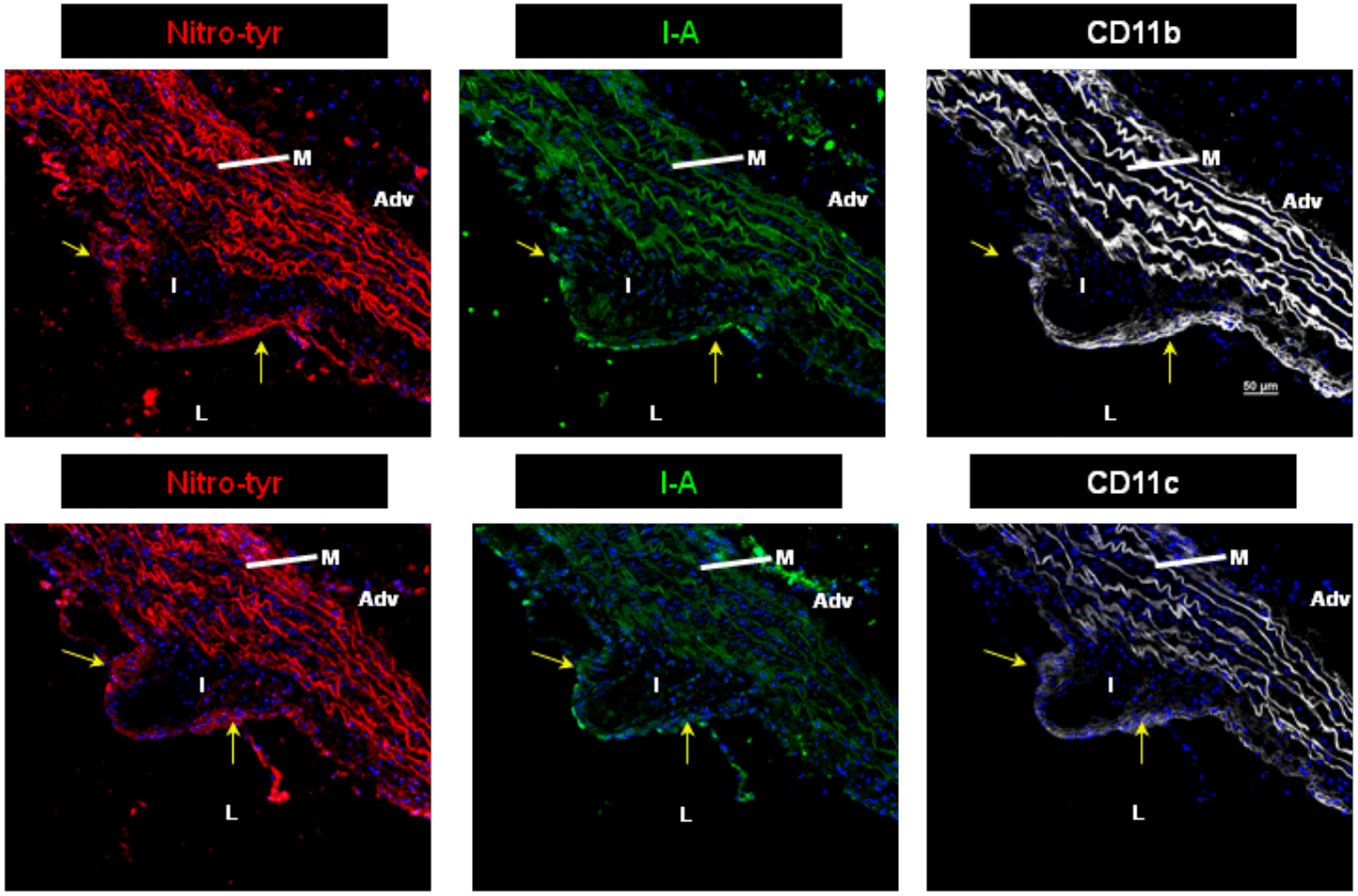

Figure 7.2. CD11b^{+} DCs produce iNOS.

(C) Serial sections showing nitrotyrosine staining with markers for DCs (yellow arrows). L: lumen; I: intima; M: media; Adv: adventitia. Scale bar represents 50µm.

7.3 Summary

To date, the function of $CD11b^+$ DCs in atherosclerotic plaques remains unknown. Here, we show that $CD11b^+$ DCs are major producers of TNF-α and iNOS. Since both TNF-α and iNOS are pro-inflammatory in nature and are involved in the pathogenesis of atherosclerosis (Branen et al., 2004; Detmers et al., 2000; Kuhlencordt et al., 2001), this suggests that $CD11b^+$ DCs are pro-inflammatory in nature.

Supporting this hypothesis, the site of protein nitration in atherosclerotic plaque, a process driven by iNOS, corresponded with the localization of $CD11b^+$ DCs. Notably, protein nitration is known to alter and inactivate proteins that will always ultimately result in amplification of the inflammatory response (Smythe et al., 2003; Zou et al., 1997) in atherosclerotic lesion.

Chapter 8

Discussion

Chapter 8 – Discussion

8.1 Expansion of aortic CD11b$^+$ DCs in atherosclerosis is supported by monocytosis and GM-CSF

Elucidating the origin and functional heterogeneity of aortic DC subsets during atherosclerosis is important for a better understanding of the pathogenesis of this deadly disease and for generation of suitable immunotherapy. Based on latest classification of non-lymphoid tissue DC subsets (Helft et al., 2010), we found that the aorta contains two non-lymphoid tissue DC subsets: CD103$^+$ and CD11b$^+$ DC subset which localized in atherosclerosis-susceptible regions of the aorta at steady state. Both DC subsets were replenished by hematopoietic cells and do not have the ability to self-renew like LCs (Helft et al., 2010; Merad et al., 2002). We went on to investigate these DC subsets in a mouse model of atherosclerosis, apoE$^{-/-}$mice. We show for the first time that accumulation of aortic DCs in apoE$^{-/-}$ mice was due to an expansion of both CD11b$^+$ and CD103$^+$ DC subsets in atherosclerotic aortas.

In terms of origin and function, the CD11b$^+$ DC subset in non-lymphoid tissues even in the aorta is the least well-studied DC subset as many studies on non-lymphoid tissue DC subsets focused on the CD103$^+$ DCs (Bachem et al., 2012; Bogunovic et al., 2009; Choi et al., 2011; Ginhoux et al., 2009; Schulz et al., 2009). The non-lymphoid tissue CD11b$^+$ DC subset is a heterogeneous population that is often described as macrophage-like (Denning et al., 2011), derived from circulating monocytes (Ginhoux et al., 2009; Varol et al., 2009)

and is found distributed between macrophage and cDC in a gene signature analysis (Miller et al., 2012). Hence, considering that this population was expanded in atherosclerosis implying a potential role for this DC subset in the disease, the $CD11b^+$ DC subset warranted further investigation.

The origin of the $CD11b^+$ DC subset accumulating in atherosclerotic aortas is unknown. However, accumulation of the $CD11b^+$ DC subset in other inflammatory conditions such as colitis (Rivollier et al., 2012), *Cryptococcus neoformans* fungal infection (Osterholzer et al., 2009) and diabetes (Yin et al., 2012) indicated a monocytic origin for $CD11b^+$ DCs. Furthermore, in the field of atherosclerosis, $Ly6C^{hi}$ monocytes and $Ly6C^{low}$ monocytes have been shown to give rise to macrophages (Swirski et al., 2007) and $CD11c^+$ DCs (Tacke et al., 2007), respectively.

To determine the origin of this population, we made use of a monocyte-derived cell marker, CD64 (Langlet et al., 2012; Plantinga et al., 2013; Tamoutounour et al., 2012). A higher proportion of the $CD11b^+$ DC subset in $apoE^{-/-}$ mice was $CD64^+$ compared to WT controls. This may imply that: 1) the $CD11b^+$ DC subset is increasingly monocyte-derived under atherosclerotic conditions; 2) a growth factor in $apoE^{-/-}$ may be involved in this differentiation; 3) not all $CD11b^+$ DCs are monocyte-derived, indicating other sources such as DC progenitors (Ginhoux et al., 2009); 4) $CD11b^+$ DC in aorta seems also heterogeneous in term of origin alike other non-lymphoid $CD11b^+$ DC subsets (Ginhoux et al., 2009).

We subsequently confirmed that the $CD11b^+$ subset arises from monocytes using adoptive transfer of monocytes. A proportion of adoptively transferred

WT monocytes into apoE$^{-/-}$ recipient mice were able to differentiate into CD11b^{+} DCs in the aorta. This was accompanied by a loss in detection of transferred monocytes in the blood circulation. Again, monocyte-derived CD11b^{+} DCs were CD64^{+}, affirming the use of CD64 as a monocyte-derived cell marker (Langlet et al., 2012; Plantinga et al., 2013; Tamoutounour et al., 2012).

Since the CD11b^{+} DC subset is monocyte-derived, we hypothesized that the expansion of this population in atherosclerosis is related to an increase in circulating monocytes. It is well established that hypercholesterolemia induced monocytosis in apoE$^{-/-}$ mice (Combadiere et al., 2008; Swirski et al., 2007; Tacke et al., 2007). Of note, Gr-1^{low} monocytes have been shown to express CD11c under hypercholesterolemic conditions in apoE$^{-/-}$ mice (Wu et al., 2009). In this study, CD11c expression was found to be regulated by oxLDL and expression of CD11c played a role in monocyte adhesion to the endothelium, an important step in atherogenesis.

We first verified that monocytosis occurred in our apoE$^{-/-}$ mice after 18 weeks of high fat diet feeding. To determine if monocytosis was a mechanism for the expansion of the CD11b^{+} DC subset in the aorta, we followed with a cholesterol-lowering drug treatment, Ezetimibe. Ezetimibe inhibits atherosclerosis development in apoE$^{-/-}$ mice (Davis et al., 2001; Kuhlencordt et al., 2009) and monocyte migration in a rabbit model of atherosclerosis (Gomez-Garre et al., 2009). Expectedly, when hypercholesterolemia was decreased with Ezetimibe treatment in apoE$^{-/-}$ mice, monocytosis in the blood and aorta was simultaneously abrogated with CD11b^{+} DC accumulation in the

aorta. Thus, monocytosis likely supports $CD11b^+$ DC accumulation in atherosclerotic aorta.

Since an increasing proportion of the $CD11b^+$ DC subset became monocyte-derived under atherosclerotic conditions and a portion of adoptively transferred monocytes were able to differentiate into this population, this prompted us to examine if certain growth factors were involved in this process. Out of the known four DC growth factors (M-CSF, Flt3-L, GM-CSF and IL-34), we discovered that GM-CSF was the only factor that was highly expressed and locally produced in atherosclerotic aorta from $apoE^{-/-}$ mice. In addition, expression of GM-CSF was reduced together with $CD11b^+$ DC expansion in Ezetimibe treated $apoE^{-/-}$ mice.

The delicate balance of colony-stimulating factors particularly GM-CSF and M-CSF in atherosclerosis has been known to modify and polarize macrophage populations: GM-CSF-derived macrophages produce inflammatory cytokines whereas M-CSF-derived macrophages are anti-inflammatory (Brocheriou et al., 2011; Di Gregoli and Johnson, 2012). GM-CSF has also been known to induce DC-like macrophages and promote MHC class II expression whereas M-CSF inhibits MHC class II expression (Willman et al., 1989). Furthermore, GM-CSF has the ability to divert committed DCs to change phenotype (Zhan et al., 2012). Hence, the cytokine milieu in atherosclerosis can determine the phenotype of cells present in the plaque. GM-CSF has been shown to promote inflammatory DC formation in experimental autoimmune myocarditis (Blyszczuk et al., 2013) and to increase differentiation of monocytes into DCs (Miller et al., 2002; Zhan et al., 2011). Drawing from these observations, the

predominant expression of GM-CSF in apoE$^{-/-}$ mice suggested that the balance is likely tipped towards inflammatory DC formation in atherosclerotic plaques.

We were then interested to know which cells were responsive to GM-CSF and the sources of GM-CSF in atherosclerotic plaques. We found that circulating monocytes express both the ligand binding (GMRα) and signaling subunit (CD131), with expression of CD131 being up-regulated in atherosclerotic conditions. In the aorta, we observed that only DCs expressed functional GM-CSF receptors, with the CD11b^{+} DC subset expressing the highest levels of the signaling subunit (CD131) in apoE$^{-/-}$ mice.

There are many potential cellular sources of GM-CSF in atherosclerotic plaques: T cells, monocytes, macrophages and even CD11b^{+} DCs. When we neutralized GM-CSF with an antibody, circulating monocytosis and CD11b^{+} DCs were decreased, demonstrating that GM-CSF contributed to CD11b^{+} DC accumulation in the atherosclerotic aorta. A couple of interesting observations emerged from this neutralization study. Firstly, although GM-CSF is not detectable in the circulation, neutralization of GM-CSF restored the ratio of monocyte subsets in the circulation and decreased monocytosis. GM-CSF may have a role in the release of monocytes from bone marrow (King et al., 2009) or prolonging the lifespan of monocytes by reducing apoptosis (Buschmann et al., 2001). Secondly, neutralization of GM-CSF reduced CD11b^{+} DCs but did not affect monocytes in the aorta. Also, circulating monocytes and CD11b^{+} DCs express functional GM-CSF receptors whereas aortic monocytes only express the signaling subunit CD131. Therefore, aortic monocytes may be incapable of responding to GM-CSF neutralization.

8.2 Pleiotrophic functions of GM-CSF in inflammation and autoimmunity

GM-CSF has diverse functions in inflammation and autoimmunity. In an endothelial injury mouse model, the lack of GM-CSF delayed neointimal formation which is an early event in atherogenesis (Harris et al., 2009). Tumor-derived GM-CSF regulated the recruitment and development of Gr-1^+ $CD11b^+$ myeloid derived suppressor cells (MDSCs) in pancreatic cancer (Bayne et al., 2012) which can inhibit $CD8^+$ T cell function (Bronte et al., 1999) by preventing the maturation of these APCs. GM-CSF also has the ability to drive the release of $Ly6C^{hi}$ monocytes from the bone marrow which differentiated into central nervous system DCs and macrophages, thereby contributing to the pathogenesis of autoimmune demyelinating disease (King et al., 2009).

On the other hand, GM-CSF is needed to confer protection from diabetes. Lack of GM-CSF promoted diabetes (Enzler et al., 2007) because GM-CSF is needed for the induction of IL-10 producing tolerogenic DCs that confer resistance to diabetes through maintenance of suppressive regulatory T cells (Gaudreau et al., 2007). The role of GM-CSF in immunosuppression is also evident in experimental autoimmune thyroiditis model (Vasu et al., 2003) and experimental autoimmune myasthenia gravis (Sheng et al., 2006).

8.3 How does GM-CSF exert its pleitrophic functions?

GM-CSF can be both immunostimulatory and immunosuppressive. So how does it achieve this? Different concentrations of GM-CSF can produce different types of DCs. DCs cultured with low concentrations of GM-CSF are immature, resistant to maturation and tolerogenic in nature whereas those cultured with high concentrations of GM-CSF can still mature in response to stimuli and become immunocompetent DCs (Lutz et al., 2000). Biochemically, low concentrations of GM-CSF only promote cell survival whereas high concentrations of GM-CSF support both cell survival and proliferation (Hercus et al., 2009). The role of GM-CSF in inflammation is also dependent on stimulus. Lack of GM-CSF in thioglycollate-induced peritonitis has no consequence. However, in antigen-specific methylated BSA-induced peritonitis, the lack of GM-CSF reduced peritonitis, inflammatory cells such as macrophages and inflammatory cytokines (Cook et al., 2004).

In apoE$^{-/-}$ mice, we observed autocrine production of this cytokine by CD11b^{+} DCs and suspected that GM-CSF has a role to play in the survival of CD11b^{+} DC. To demonstrate this, we used BMDCs cultured with exogenous GM-CSF as a model as they resemble CD11b^{+} DCs phenotypically. We found that GM-CSF prolonged BMDC survival and this may account for the CD11b^{+} DC accumulation in atherosclerotic aorta.

8.4 Function of CD11b$^+$ DCs in atherosclerotic plaques

GM-CSF derived DCs produced TNF-α and iNOS and are developmentally related to TipDCs (Xu et al., 2007). In colitis, monocyte-derived CD11b$^+$ DCs are also pro-inflammatory, producing cytokines such as IL-12, IL-23, TNF-α and iNOS (Rivollier et al., 2012). In our study, we observed that both TNF-α and iNOS were produced by CD11b$^+$ DCs in atherosclerotic plaques. TNF-α has been implicated in atherogenesis. The lack of this cytokine in apoE$^{-/-}$ mice reduced plaque size (Branen et al., 2004). This may be due to a decrease in adhesion molecules such as ICAM-1 and VCAM-1 and chemokine MCP-1, which are responsible for early recruitment of monocytes to atherosclerotic lesions (Ohta et al., 2005). Likewise, apoE$^{-/-}$ mice deficient in iNOS displayed reduced atherosclerotic lesion size but only at advanced stages (Detmers et al., 2000; Kuhlencordt et al., 2001; Miyoshi et al., 2006). Deficiency in iNOS led to a direct reduction in aortic cholesterol (Detmers et al., 2000) whereas the other two studies showed a reduction in plasma lipid peroxides (Kuhlencordt et al., 2001; Miyoshi et al., 2006). Therefore, being able to produce both TNF-α and iNOS, CD11b$^+$ DCs are undeniably playing a pro-inflammatory and pro-atherogenic function in atherosclerosis.

Moreover, nitric oxide (NO) produced by iNOS can lead to peroxynitrite formation which can lead to nitration of tyrosine residues. Protein tyrosine nitration was first detected in foam cells in human coronary arteries and hypothesized to contribute to the pathogenesis of atherosclerosis (Beckmann et al., 1994). Subsequently, massive protein nitration can be found in high-fat diet fed apoE$^{-/-}$ mice and this process was iNOS-dependent (Upmacis et al.,

2007). One of the targets of protein tyrosine nitration in atherosclerotic plaques is prostaglandin H_2 synthase. This enzyme is important for vascular homeostasis and nitration of its Tyr385 residue by iNOS led to its inactivation in $apoE^{-/-}$ mice (Deeb et al., 2006). In our study, we observed that $CD11b^{+}$ DCs colocalized with sites of nitration in $apoE^{-/-}$ plaques, suggesting that iNOS produced by $CD11b^{+}$ DCs may have resulted in nitration in atherosclerotic plaques. A proposed model of mechanisms governing the $CD11b^{+}$ expansion and their functions is shown in Figure 8.1.

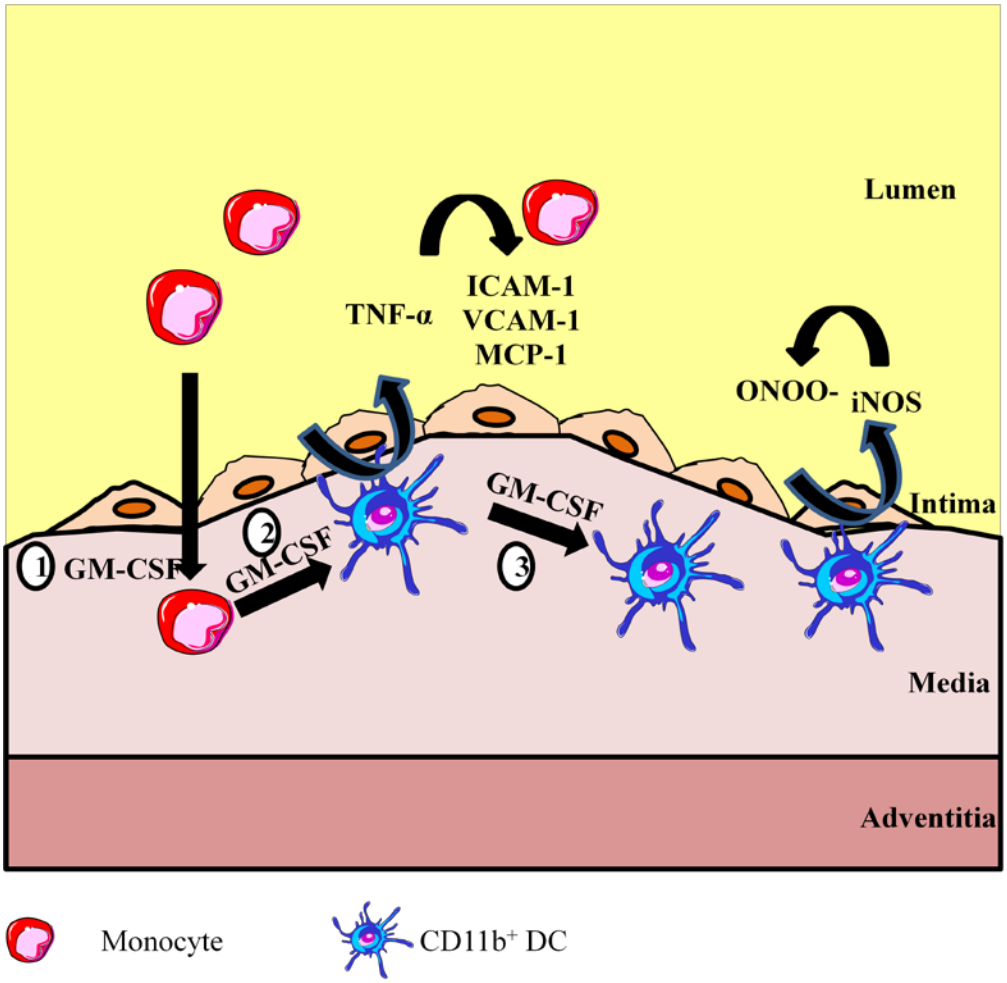

Figure 8.1. Proposed model for CD11b$^+$ DC expansion and their function in atherosclerosis.

Expansion of CD11b$^+$ DCs is governed by monocytosis and GM-CSF. High concentrations of GM-CSF in atherosclerotic plaques could function in (1) recruitment of monocytes; (2) differentiation of monocytes into CD11b$^+$ DCs; (3) survival and proliferation of CD11b$^+$ DCs. CD11b$^+$ DCs produce TNF-α and iNOS. Production of TNF-α upregulates ICAM-1, VCAM-1 and MCP-1 for monocyte adherence to endothelium. iNOS could generate peroxynitrite ($ONOO^-$) leading to nitration of proteins in atherosclerotic plaques. Art work adapted and modified from Servier Medical Art.

8.5 Limitations of our study

8.5.1 ApoE: Functions beyond a lipid transport protein

ApoE is not just involved in cholesterol metabolism. It can inhibit T cell proliferation in culture (Kelly et al., 1994). Lack of ApoE has been shown to enhance T cell stimulation and antigen presentation by an increase of co-stimulatory molecules on macrophages (Tenger and Zhou, 2003). Moreover, ApoE is needed for clearance of apoptotic bodies. $ApoE^{-/-}$ macrophages demonstrated a reduced ability to ingest apoptotic bodies resulting in massive accumulation of apoptotic bodies. This in turn prompted production of TNF-α and increased recruitment of macrophages in response to increased dying macrophages (Grainger et al., 2004). As a consequence, there is increased number of Th1 and Th17 cells as well as an up-regulation of pro-inflammatory cytokines (Wei et al., 2013). Considering the role of ApoE in antigen presentation and immune response, the accumulation of $CD11b^{+}$ DCs in

$apoE^{-/-}$ mice may be partially due to systemic inflammation in this mouse model. This may to some extent account for the more exaggerated accumulation of $CD11b^{+}$ DCs in $apoE^{-/-}$ compared to $Ldlr^{-/-}$ mice.

One limitation in using $apoE^{-/-}$ mice is transferring WT bone marrow into these mice results in reduction of hypercholesterolemia and atherosclerosis due to reconstitution of ApoE from WT cells (Boisvert et al., 1995; Llodra et al., 2004).

8.5.2 Relevance to human atherosclerosis

ApoE deficiency in humans is rare and manifests itself in type III hyperlipoproteinemia where only 1 in 5,000 individuals is affected and clinical symptoms are only apparent at adulthood (Rall et al., 1989). In addition, apoE is polymorphic in humans having three different isoforms: ε2, ε3 and ε4 and this polymorphism is absent in mice (Plump and Breslow, 1995). Nonetheless, this limitation could be overcome because of the relative ease of genetic manipulation of mice. For example, mice expressing human apoE isoforms are able to recapitulate similar lipid profiles as humans (Pendse et al., 2009). Atherosclerosis in humans is also confounded by other factors such as diabetes, hypertension etc (Bentzon and Falk, 2010). Based on a single gene knockout, apoE$^{-/-}$ mice are probably best at modeling homozygous familial hypercholesterolemia in humans. However, the levels of hypercholesterolemia and similar predilection sites for atherosclerosis development in this mouse model in comparison to its human counterparts are redeeming qualities of this mouse model for its use in studying human atherosclerosis.

As far as DC subsets in human atherosclerosis are concerned, four subtypes have been identified: classical myeloid DC (mDC) precursors (BDCA-1^{+}), pDC precursors (BDCA-2^{+}), mDCs (S100^{+} fascin^{+}) and pDCs (CD123^{+}). Both BDCA-1^{+} and BDCA-2^{+} DCs can be found in human atherosclerotic plaques with BDCA-1^{+} DCs being more predominant and both were shown to accumulate around neovessels (Van Vre et al., 2011). This observation coincided with a decrease of BDCA-1^{+} DCs in the circulation (Yilmaz et al., 2006). mDCs can be found in normal aorta and increased across

atherosclerosis progression (Bobryshev and Lord, 1995a). Activated mDCs ($CD83^+$) which accumulate in plaques are frequently found in contact with $CD3^+$ T cells suggesting a role in T cell activation (Yilmaz et al., 2007).

As the markers used in defining DC subsets in humans and mice markedly differ, it is difficult to relate studies from mouse models to human diseases. However, the equivalents of murine non-lymphoid tissue DC subsets to humans have been recently elucidated. Mouse $CD103^+$ DC subset and $CD11b^+$ $CD24^+$ DC subset correspond in humans to $CD141^+$ DC (Haniffa et al., 2012) and $CD1c^+$ DC ($BDCA\text{-}1^+$) (Schlitzer et al., 2013), respectively. It remains to be determined whether the $CD11b^+$ DCs in murine atherosclerotic plaques are functionally equivalent to $CD1c^+$ DCs or myeloid monocyte-derived $CD14^+$ DCs in human atherosclerotic plaques.

8.6 Developing therapeutic strategies for atherosclerosis

8.6.1 Targeting against CD64

CD64, which is Fc gamma receptor R I (FcγRI) is an activating receptor present on most myeloid cells such as monocytes, macrophages and DCs with a high affinity in binding immunoglobulins (van der Poel et al., 2011). Functions of CD64 include: 1) endocytosis of soluble IgG, 2) phagocytosis of immune complexes, 3) antibody-dependent cell-mediated cytotoxicity and 4) production of immune complex-induced inflammation (Barnes et al., 2002). A

lack of CD64 reduced the severity of cartilage damage in experimental antigen-induced arthritis (Ioan-Facsinay et al., 2002).

The uptake of LDL-immune complexes by human macrophages was shown to be favored by CD64 which may contribute to foam cell formation (Lopes-Virella et al., 1997). Moreover, deficiency of FcγR in apoE$^{-/-}$ mice displayed a reduction of atherosclerotic lesion size, macrophage and T cell content (Hernandez-Vargas et al., 2006). The immune mechanism behind this reduction of atherosclerotic size is attributed to decreased Th17 cell response and a shift towards regulatory T cell response (Ng et al., 2011). These findings imply that neutralization of Fcγ receptors may confer protection against atherosclerosis. Indeed, intravenous injection of immunoglobulin has been shown to attenuate atherosclerotic lesions in apoE$^{-/-}$ mice (Yuan et al., 2003) and induced anti-inflammatory effects resulting in improvement in chronic heart failure patients (Gullestad et al., 2001). Our finding that pro-inflammatory CD11b^{+} DCs express higher CD64 expression under atherosclerotic conditions suggests that neutralizing CD64 may limit the expansion of CD11b^{+} DCs and atherosclerosis.

8.6.2 Targeting against monocytosis

Monocyte recruitment and accumulation in atherosclerotic plaques is proportional to the severity of the disease (Swirski et al., 2006). Our study also demonstrated that monocytosis contributes to the accumulation of CD11b^{+}

DCs in atherosclerosis. Therefore, targeting monocytosis should ameliorate atherosclerosis.

Monocytes depend on chemokine receptors to migrate towards atherosclerotic plaques and inflammatory Gr-1^{hi} monocytes depend on CCR2 (Combadiere et al., 2008; Tacke et al., 2007). Inflammatory Gr-1^{hi} monocytes are detrimental to infarct healing (Nahrendorf et al., 2007). Nanoparticle-mediated silencing of CCR2 in myocardial infarction in $apoE^{-/-}$ mice displayed a reduction of monocytes and $CD11b^{+}$ myeloid cells, resolving inflammation in infarcted hearts (Majmudar et al., 2013).

Monocyte recruitment can also be blocked by a small molecule lecinoxoid, VB-201 *in vitro* (Feige et al., 2013). VB-201 was generated as an orally stable synthetic phospholipid analog, structurally similar to one of the oxidized phospholipid compound 1-pamitoyl-2-glutaryl phophatidylcholine (PGPC). Emerging data showed that not all oxidized phospholipids are pro-inflammatory. In fact, some of them are anti-inflammatory in nature (Feige et al., 2010). In the study (Feige et al., 2013), VB-201 demonstrated a specific inhibition of monocyte chemotaxis by regulating downstream signaling of chemokine receptors in monocytes. Moreover, it inhibited monocyte migration *in vivo* in a model of sterile inflammation. When given to young $apoE^{-/-}$ mice for 8 weeks, VB-201 was able to attenuate atherosclerosis development and accumulation of $CD68^{+}$ cells.

8.6.3 Targeting against GM-CSF

We found that GM-CSF was over expressed in atherosclerotic lesions and this governs the accumulation of $CD11b^+$ DCs. Although anti-GM-CSF therapy is still at its infant stage, its use in rheumatoid arthritis in Phase II clinical trials was efficacious and showed improved outcome for patients with mild adverse events (Nair et al., 2012). This is encouraging albeit more work still needs to be done to understand the consequences of GM-CSF over expression in atherosclerotic plaques.

8.7 Future Work

The role of GM-CSF in $CD11b^+$ DCs is still not fully understood. GM-CSF can act at various levels: 1) recruitment of monocytes to atherosclerotic plaque; 2) differentiation of monocytes into $CD11b^+$ DCs; 3) survival of $CD11b^+$ DCs. In order to understand whether GM-CSF plays a part in recruitment of monocytes, we intend to isolate bone marrow monocytes and study their chemotaxis *in vitro* in transwell assay towards GM-CSF. This can also be shown *in vivo* with an adoptive transfer of monocytes from

$GM\text{-}CSFR^{-/-}$ mice into $apoE^{-/-}$ recipients. If GM-CSF is not required for recruitment, the amount of monocytes arriving at atherosclerotic plaques should be similar as transferring WT monocytes into $apoE^{-/-}$ recipients. Examining the extent of $CD11b^+$ DC accumulation in this study will also

allow us to conclude whether GM-CSF on monocytes is required for their differentiation into $CD11b^+$ DCs *in vivo* during atherosclerosis. To evaluate if GM-CSF regulates the survival of $CD11b^+$ DCs *in vivo*, we intend to measure the proportion of Annexin V^+ $CD11b^+$ DCs after neutralizing GM-CSF in $apoE^{-/-}$ recipients.

GM-CSF is crucial to T_H1 and T_H17 responses in experimental autoimmune encephalomyelitis (Codarri et al., 2011; El-Behi et al., 2011). GM-CSF produced by T_H17 cells is required for the maintenance of neuro-inflammation by recruitment of myeloid cells into the central nervous system (Codarri et al., 2011). T_H17 cells are increased in $apoE^{-/-}$ mice in proportion to atherosclerotic plaque size (Gao et al., 2010; Smith et al., 2010). Neutralizing IL-17 reduced plaque burden, IL-6 and macrophage content (Smith et al., 2010). Genetic deletion of IL-17 in $apoE^{-/-}$ mice resulted in fewer dendritic cells and macrophages (Madhur et al., 2011). This was due to decreased monocyte migration to atherosclerotic aortas (Butcher et al., 2012). Since GM-CSF is produced by $CD11b^+$ DCs in atherosclerotic plaques, they may be involved in the maintenance of the T_H17 response whereby the atherosclerosis development is sustained and monocyte migration is promoted under the influence of IL-17. Hence, it will be interesting to explore this possibility by investigating whether T_H17 responses are affected when GM-CSF is neutralized in $apoE^{-/-}$ mice.

References

Abou-Raya, A., and Abou-Raya, S. (2006). Inflammation: a pivotal link between autoimmune diseases and atherosclerosis. Autoimmun Rev *5*, 331-337.

Aldridge, J.R., Jr., Moseley, C.E., Boltz, D.A., Negovetich, N.J., Reynolds, C., Franks, J., Brown, S.A., Doherty, P.C., Webster, R.G., and Thomas, P.G. (2009). TNF/iNOS-producing dendritic cells are the necessary evil of lethal influenza virus infection. Proc Natl Acad Sci U S A *106*, 5306-5311.

Angeli, V., Llodra, J., Rong, J.X., Satoh, K., Ishii, S., Shimizu, T., Fisher, E.A., and Randolph, G.J. (2004). Dyslipidemia associated with atherosclerotic disease systemically alters dendritic cell mobilization. Immunity *21*, 561-574.

Auffray, C., Fogg, D., Garfa, M., Elain, G., Join-Lambert, O., Kayal, S., Sarnacki, S., Cumano, A., Lauvau, G., and Geissmann, F. (2007). Monitoring of blood vessels and tissues by a population of monocytes with patrolling behavior. Science *317*, 666-670.

Auffray, C., Fogg, D.K., Narni-Mancinelli, E., Senechal, B., Trouillet, C., Saederup, N., Leemput, J., Bigot, K., Campisi, L., Abitbol, M., *et al.* (2009a). CX3CR1+ CD115+ CD135+ common macrophage/DC precursors and the role of CX3CR1 in their response to inflammation. J Exp Med *206*, 595-606.

Auffray, C., Sieweke, M.H., and Geissmann, F. (2009b). Blood monocytes: development, heterogeneity, and relationship with dendritic cells. Annu Rev Immunol *27*, 669-692.

Bachem, A., Hartung, E., Guttler, S., Mora, A., Zhou, X., Hegemann, A., Plantinga, M., Mazzini, E., Stoitzner, P., Gurka, S., *et al.* (2012). Expression

of XCR1 Characterizes the Batf3-Dependent Lineage of Dendritic Cells Capable of Antigen Cross-Presentation. Front Immunol *3*, 214.

Barnes, N., Gavin, A.L., Tan, P.S., Mottram, P., Koentgen, F., and Hogarth, P.M. (2002). FcgammaRI-deficient mice show multiple alterations to inflammatory and immune responses. Immunity *16*, 379-389.

Baumeister, T., Rossner, S., Pech, G., de Bruijn, M.F., Leenen, P.J., Schuler, G., and Lutz, M.B. (2003). Interleukin-3Ralpha+ myeloid dendritic cells and mast cells develop simultaneously from different bone marrow precursors in cultures with interleukin-3. J Invest Dermatol *121*, 280-288.

Bayne, L.J., Beatty, G.L., Jhala, N., Clark, C.E., Rhim, A.D., Stanger, B.Z., and Vonderheide, R.H. (2012). Tumor-derived granulocyte-macrophage colony-stimulating factor regulates myeloid inflammation and T cell immunity in pancreatic cancer. Cancer Cell *21*, 822-835.

Beckmann, J.S., Ye, Y.Z., Anderson, P.G., Chen, J., Accavitti, M.A., Tarpey, M.M., and White, C.R. (1994). Extensive nitration of protein tyrosines in human atherosclerosis detected by immunohistochemistry. Biol Chem Hoppe Seyler *375*, 81-88.

Bentzon, J.F., and Falk, E. (2010). Atherosclerotic lesions in mouse and man: is it the same disease? Curr Opin Lipidol *21*, 434-440.

Berillis, P. (2013). The Role of Collagen in the Aorta's Structure. The Open Circulation and Vascular Journal *6*, 1-8.

Bierly, A.L., Shufesky, W.J., Sukhumavasi, W., Morelli, A.E., and Denkers, E.Y. (2008). Dendritic cells expressing plasmacytoid marker PDCA-1 are Trojan horses during Toxoplasma gondii infection. J Immunol *181*, 8485-8491.

Blasi, C. (2008). The autoimmune origin of atherosclerosis. Atherosclerosis *201*, 17-32.

Blasius, A.L., Cella, M., Maldonado, J., Takai, T., and Colonna, M. (2006a). Siglec-H is an IPC-specific receptor that modulates type I IFN secretion through DAP12. Blood *107*, 2474-2476.

Blasius, A.L., Giurisato, E., Cella, M., Schreiber, R.D., Shaw, A.S., and Colonna, M. (2006b). Bone marrow stromal cell antigen 2 is a specific marker of type I IFN-producing cells in the naive mouse, but a promiscuous cell surface antigen following IFN stimulation. J Immunol *177*, 3260-3265.

Blyszczuk, P., Behnke, S., Luscher, T.F., Eriksson, U., and Kania, G. (2013). GM-CSF promotes inflammatory dendritic cell formation but does not contribute to disease progression in experimental autoimmune myocarditis. Biochim Biophys Acta *1833*, 934-944.

Bobryshev, Y.V., and Lord, R.S. (1995a). S-100 positive cells in human arterial intima and in atherosclerotic lesions. Cardiovasc Res *29*, 689-696.

Bobryshev, Y.V., and Lord, R.S. (2001). Vascular-associated lymphoid tissue (VALT) involvement in aortic aneurysm. Atherosclerosis *154*, 15-21.

Bobryshev, Y.V., and Lord, R.S.A. (1995b). S-100 positive cells in human arterial intima and in atherosclerotic lesions. Cardiovascular Research *29*, 689-696.

Bobryshev, Y.V., Taksir, T., Lord, R.S., and Freeman, M.W. (2001). Evidence that dendritic cells infiltrate atherosclerotic lesions in apolipoprotein E-deficient mice. Histol Histopathol *16*, 801-808.

Bogunovic, M., Ginhoux, F., Helft, J., Shang, L., Hashimoto, D., Greter, M., Liu, K., Jakubzick, C., Ingersoll, M.A., Leboeuf, M., *et al.* (2009). Origin of the lamina propria dendritic cell network. Immunity *31*, 513-525.

Boisvert, W.A., Spangenberg, J., and Curtiss, L.K. (1995). Treatment of severe hypercholesterolemia in apolipoprotein E-deficient mice by bone marrow transplantation. J Clin Invest *96*, 1118-1124.

Branen, L., Hovgaard, L., Nitulescu, M., Bengtsson, E., Nilsson, J., and Jovinge, S. (2004). Inhibition of tumor necrosis factor-alpha reduces atherosclerosis in apolipoprotein E knockout mice. Arterioscler Thromb Vasc Biol *24*, 2137-2142.

Brocheriou, I., Maouche, S., Durand, H., Braunersreuther, V., Le Naour, G., Gratchev, A., Koskas, F., Mach, F., Kzhyshkowska, J., and Ninio, E. (2011). Antagonistic regulation of macrophage phenotype by M-CSF and GM-CSF: implication in atherosclerosis. Atherosclerosis *214*, 316-324.

Brode, S., and Macary, P.A. (2004). Cross-presentation: dendritic cells and macrophages bite off more than they can chew! Immunology *112*, 345-351.

Bronte, V., Chappell, D.B., Apolloni, E., Cabrelle, A., Wang, M., Hwu, P., and Restifo, N.P. (1999). Unopposed production of granulocyte-macrophage colony-stimulating factor by tumors inhibits CD8+ T cell responses by dysregulating antigen-presenting cell maturation. J Immunol *162*, 5728-5737.

Burnett, S.H., Kershen, E.J., Zhang, J., Zeng, L., Straley, S.C., Kaplan, A.M., and Cohen, D.A. (2004). Conditional macrophage ablation in transgenic mice expressing a Fas-based suicide gene. J Leukoc Biol *75*, 612-623.

Bursch, L.S., Wang, L., Igyarto, B., Kissenpfennig, A., Malissen, B., Kaplan, D.H., and Hogquist, K.A. (2007). Identification of a novel population of Langerin+ dendritic cells. J Exp Med *204*, 3147-3156.

Buschmann, I.R., Hoefer, I.E., van Royen, N., Katzer, E., Braun-Dulleaus, R., Heil, M., Kostin, S., Bode, C., and Schaper, W. (2001). GM-CSF: a strong arteriogenic factor acting by amplification of monocyte function. Atherosclerosis *159*, 343-356.

Butcher, M.J., Gjurich, B.N., Phillips, T., and Galkina, E.V. (2012). The IL-17A/IL-17RA axis plays a proatherogenic role via the regulation of aortic myeloid cell recruitment. Circ Res *110*, 675-687.

Cheers, C., Haigh, A.M., Kelso, A., Metcalf, D., Stanley, E.R., and Young, A.M. (1988). Production of colony-stimulating factors (CSFs) during infection: separate determinations of macrophage-, granulocyte-, granulocyte-macrophage-, and multi-CSFs. Infect Immun *56*, 247-251.

Chihara, T., Suzu, S., Hassan, R., Chutiwitoonchai, N., Hiyoshi, M., Motoyoshi, K., Kimura, F., and Okada, S. (2010). IL-34 and M-CSF share the receptor Fms but are not identical in biological activity and signal activation. Cell Death Differ *17*, 1917-1927.

Choi, J.H., Cheong, C., Dandamudi, D.B., Park, C.G., Rodriguez, A., Mehandru, S., Velinzon, K., Jung, I.H., Yoo, J.Y., Oh, G.T., and Steinman, R.M. (2011). Flt3 signaling-dependent dendritic cells protect against atherosclerosis. Immunity *35*, 819-831.

Choi, J.H., Do, Y., Cheong, C., Koh, H., Boscardin, S.B., Oh, Y.S., Bozzacco, L., Trumpfheller, C., Park, C.G., and Steinman, R.M. (2009). Identification of

antigen-presenting dendritic cells in mouse aorta and cardiac valves. J Exp Med *206*, 497-505.

Chong, S.Z., Wong, K.L., Lin, G., Yang, C.M., Wong, S.C., Angeli, V., Macary, P.A., and Kemeny, D.M. (2011). Human CD8(+) T cells drive Th1 responses through the differentiation of TNF/iNOS-producing dendritic cells. Eur J Immunol *41*, 1639-1651.

Chow, A., Brown, B.D., and Merad, M. (2011). Studying the mononuclear phagocyte system in the molecular age. Nat Rev Immunol *11*, 788-798.

Codarri, L., Gyulveszi, G., Tosevski, V., Hesske, L., Fontana, A., Magnenat, L., Suter, T., and Becher, B. (2011). RORgammat drives production of the cytokine GM-CSF in helper T cells, which is essential for the effector phase of autoimmune neuroinflammation. Nat Immunol *12*, 560-567.

Combadiere, C., Potteaux, S., Rodero, M., Simon, T., Pezard, A., Esposito, B., Merval, R., Proudfoot, A., Tedgui, A., and Mallat, Z. (2008). Combined inhibition of CCL2, CX3CR1, and CCR5 abrogates Ly6C(hi) and Ly6C(lo) monocytosis and almost abolishes atherosclerosis in hypercholesterolemic mice. Circulation *117*, 1649-1657.

Cook, A.D., Braine, E.L., and Hamilton, J.A. (2004). Stimulus-dependent requirement for granulocyte-macrophage colony-stimulating factor in inflammation. J Immunol *173*, 4643-4651.

Daissormont, I.T., Christ, A., Temmerman, L., Sampedro Millares, S., Seijkens, T., Manca, M., Rousch, M., Poggi, M., Boon, L., van der Loos, C., *et al.* (2011). Plasmacytoid dendritic cells protect against atherosclerosis by tuning T-cell proliferation and activity. Circ Res *109*, 1387-1395.

Daro, E., Pulendran, B., Brasel, K., Teepe, M., Pettit, D., Lynch, D.H., Vremec, D., Robb, L., Shortman, K., McKenna, H.J., *et al.* (2000). Polyethylene glycol-modified GM-CSF expands CD11b(high)CD11c(high) but notCD11b(low)CD11c(high) murine dendritic cells in vivo: a comparative analysis with Flt3 ligand. J Immunol *165*, 49-58.

Davis, H.R., Jr., Compton, D.S., Hoos, L., and Tetzloff, G. (2001). Ezetimibe, a potent cholesterol absorption inhibitor, inhibits the development of atherosclerosis in ApoE knockout mice. Arterioscler Thromb Vasc Biol *21*, 2032-2038.

Deeb, R.S., Shen, H., Gamss, C., Gavrilova, T., Summers, B.D., Kraemer, R., Hao, G., Gross, S.S., Laine, M., Maeda, N., *et al.* (2006). Inducible nitric oxide synthase mediates prostaglandin h2 synthase nitration and suppresses eicosanoid production. Am J Pathol *168*, 349-362.

del Rio, M.L., Rodriguez-Barbosa, J.I., Bolter, J., Ballmaier, M., Dittrich-Breiholz, O., Kracht, M., Jung, S., and Forster, R. (2008). CX3CR1+ c-kit+ bone marrow cells give rise to CD103+ and CD103- dendritic cells with distinct functional properties. J Immunol *181*, 6178-6188.

Denning, T.L., Norris, B.A., Medina-Contreras, O., Manicassamy, S., Geem, D., Madan, R., Karp, C.L., and Pulendran, B. (2011). Functional specializations of intestinal dendritic cell and macrophage subsets that control Th17 and regulatory T cell responses are dependent on the T cell/APC ratio, source of mouse strain, and regional localization. J Immunol *187*, 733-747.

Detmers, P.A., Hernandez, M., Mudgett, J., Hassing, H., Burton, C., Mundt, S., Chun, S., Fletcher, D., Card, D.J., Lisnock, J., *et al.* (2000). Deficiency in

inducible nitric oxide synthase results in reduced atherosclerosis in apolipoprotein E-deficient mice. J Immunol *165*, 3430-3435.

Di Gregoli, K., and Johnson, J.L. (2012). Role of colony-stimulating factors in atherosclerosis. Curr Opin Lipidol *23*, 412-421.

Diao, J., Mikhailova, A., Tang, M., Gu, H., Zhao, J., and Cattral, M.S. (2012). Immunostimulatory conventional dendritic cells evolve into regulatory macrophage-like cells. Blood *119*, 4919-4927.

Diao, J., Winter, E., Cantin, C., Chen, W., Xu, L., Kelvin, D., Phillips, J., and Cattral, M.S. (2006). In situ replication of immediate dendritic cell (DC) precursors contributes to conventional DC homeostasis in lymphoid tissue. J Immunol *176*, 7196-7206.

Ditiatkovski, M., Toh, B.H., and Bobik, A. (2006). GM-CSF deficiency reduces macrophage PPAR-gamma expression and aggravates atherosclerosis in ApoE-deficient mice. Arterioscler Thromb Vasc Biol *26*, 2337-2344.

Dominguez, P.M., and Ardavin, C. (2010). Differentiation and function of mouse monocyte-derived dendritic cells in steady state and inflammation. Immunol Rev *234*, 90-104.

Drechsler, M., Megens, R.T., van Zandvoort, M., Weber, C., and Soehnlein, O. (2010). Hyperlipidemia-triggered neutrophilia promotes early atherosclerosis. Circulation *122*, 1837-1845.

El-Behi, M., Ciric, B., Dai, H., Yan, Y., Cullimore, M., Safavi, F., Zhang, G.X., Dittel, B.N., and Rostami, A. (2011). The encephalitogenicity of T(H)17 cells is dependent on IL-1- and IL-23-induced production of the cytokine GM-CSF. Nat Immunol *12*, 568-575.

Enzler, T., Gillessen, S., Dougan, M., Allison, J.P., Neuberg, D., Oble, D.A., Mihm, M., and Dranoff, G. (2007). Functional deficiencies of granulocyte-macrophage colony stimulating factor and interleukin-3 contribute to insulitis and destruction of beta cells. Blood *110*, 954-961.

Erbel, C., Sato, K., Meyer, F.B., Kopecky, S.L., Frye, R.L., Goronzy, J.J., and Weyand, C.M. (2007). Functional profile of activated dendritic cells in unstable atherosclerotic plaque. Basic Research in Cardiology *102*, 123-132.

Fancke, B., Suter, M., Hochrein, H., and O'Keeffe, M. (2008). M-CSF: a novel plasmacytoid and conventional dendritic cell poietin. Blood *111*, 150-159.

Fawcett, D.W. (1986). Bloom and Fawcett: A Textbook of Histology, 11th edn (Saunders, Philadelphia).

Feige, E., Mendel, I., George, J., Yacov, N., and Harats, D. (2010). Modified phospholipids as anti-inflammatory compounds. Curr Opin Lipidol *21*, 525-529.

Feige, E., Yacov, N., Salem, Y., Levi, I., Mendel, I., Propheta-Meiran, O., Shoham, A., Hait-Darshan, R., Polonsky, O., George, J., *et al.* (2013). Inhibition of monocyte chemotaxis by VB-201, a small molecule lecinoxoid, hinders atherosclerosis development in ApoE(-/-) mice. Atherosclerosis *229*, 430-439.

Finn, A.V., Nakano, M., Narula, J., Kolodgie, F.D., and Virmani, R. (2010). Concept of vulnerable/unstable plaque. Arterioscler Thromb Vasc Biol *30*, 1282-1292.

Fogg, D.K., Sibon, C., Miled, C., Jung, S., Aucouturier, P., Littman, D.R., Cumano, A., and Geissmann, F. (2006). A clonogenic bone marrow progenitor specific for macrophages and dendritic cells. Science *311*, 83-87.

Frostegard, J. (2002). Autoimmunity, oxidized LDL and cardiovascular disease. Autoimmun Rev *1*, 233-237.

Galkina, E., Kadl, A., Sanders, J., Varughese, D., Sarembock, I.J., and Ley, K. (2006). Lymphocyte recruitment into the aortic wall before and during development of atherosclerosis is partially L-selectin dependent. Journal of Experimental Medicine *203*, 1273-1282.

Gao, Q., Jiang, Y., Ma, T., Zhu, F., Gao, F., Zhang, P., Guo, C., Wang, Q., Wang, X., Ma, C., *et al.* (2010). A critical function of Th17 proinflammatory cells in the development of atherosclerotic plaque in mice. J Immunol *185*, 5820-5827.

Gaudreau, S., Guindi, C., Menard, M., Besin, G., Dupuis, G., and Amrani, A. (2007). Granulocyte-macrophage colony-stimulating factor prevents diabetes development in NOD mice by inducing tolerogenic dendritic cells that sustain the suppressive function of CD4+CD25+ regulatory T cells. J Immunol *179*, 3638-3647.

Gautier, E.L., Huby, T., Saint-Charles, F., Ouzilleau, B., Pirault, J., Deswaerte, V., Ginhoux, F., Miller, E.R., Witztum, J.L., Chapman, M.J., and Lesnik, P. (2009). Conventional dendritic cells at the crossroads between immunity and cholesterol homeostasis in atherosclerosis. Circulation *119*, 2367-2375.

Geissmann, F., Jung, S., and Littman, D.R. (2003). Blood monocytes consist of two principal subsets with distinct migratory properties. Immunity *19*, 71-82.

Gerrity, R.G. (1981). The role of the monocyte in atherogenesis: I. Transition of blood-borne monocytes into foam cells in fatty lesions. Am J Pathol *103*, 181-190.

Getz, G.S. (2000). Mouse model of unstable atherosclerotic plaque? Arterioscler Thromb Vasc Biol *20*, 2503-2505.

Getz, G.S., and Reardon, C.A. (2012). Animal models of atherosclerosis. Arterioscler Thromb Vasc Biol *32*, 1104-1115.

Gimbrone, M.A., Jr., and Garcia-Cardena, G. (2013). Vascular endothelium, hemodynamics, and the pathobiology of atherosclerosis. Cardiovasc Pathol *22*, 9-15.

Ginhoux, F., Liu, K., Helft, J., Bogunovic, M., Greter, M., Hashimoto, D., Price, J., Yin, N., Bromberg, J., Lira, S.A., *et al.* (2009). The origin and development of nonlymphoid tissue CD103+ DCs. J Exp Med *206*, 3115-3130.

Gomez-Garre, D., Munoz-Pacheco, P., Gonzalez-Rubio, M.L., Aragoncillo, P., Granados, R., and Fernandez-Cruz, A. (2009). Ezetimibe reduces plaque inflammation in a rabbit model of atherosclerosis and inhibits monocyte migration in addition to its lipid-lowering effect. Br J Pharmacol *156*, 1218-1227.

Gordon, S., and Taylor, P.R. (2005). Monocyte and macrophage heterogeneity. Nat Rev Immunol *5*, 953-964.

Grainger, D.J., Reckless, J., and McKilligin, E. (2004). Apolipoprotein E modulates clearance of apoptotic bodies in vitro and in vivo, resulting in a systemic proinflammatory state in apolipoprotein E-deficient mice. J Immunol *173*, 6366-6375.

Grassia, G., MacRitchie, N., Platt, A.M., Brewer, J.M., Garside, P., and Maffia, P. (2013). Plasmacytoid dendritic cells: biomarkers or potential therapeutic targets in atherosclerosis? Pharmacol Ther *137*, 172-182.

Greter, M., Helft, J., Chow, A., Hashimoto, D., Mortha, A., Agudo-Cantero, J., Bogunovic, M., Gautier, E.L., Miller, J., Leboeuf, M., *et al.* (2012a). GM-CSF controls nonlymphoid tissue dendritic cell homeostasis but is dispensable for the differentiation of inflammatory dendritic cells. Immunity *36*, 1031-1046.

Greter, M., Lelios, I., Pelczar, P., Hoeffel, G., Price, J., Leboeuf, M., Kundig, T.M., Frei, K., Ginhoux, F., Merad, M., and Becher, B. (2012b). Stroma-derived interleukin-34 controls the development and maintenance of langerhans cells and the maintenance of microglia. Immunity *37*, 1050-1060.

Grotenhuis, H.B., and de Roos, A. (2011). Structure and function of the aorta in inherited and congenital heart disease and the role of MRI. Heart *97*, 66-74.

Gullestad, L., Aass, H., Fjeld, J.G., Wikeby, L., Andreassen, A.K., Ihlen, H., Simonsen, S., Kjekshus, J., Nitter-Hauge, S., Ueland, T., *et al.* (2001). Immunomodulating therapy with intravenous immunoglobulin in patients with chronic heart failure. Circulation *103*, 220-225.

Haghighat, A., Weiss, D., Whalin, M.K., Cowan, D.P., and Taylor, W.R. (2007). Granulocyte colony-stimulating factor and granulocyte macrophage colony-stimulating factor exacerbate atherosclerosis in apolipoprotein E-deficient mice. Circulation *115*, 2049-2054.

Hamilton, J.A. (2002). GM-CSF in inflammation and autoimmunity. Trends Immunol *23*, 403-408.

Han, J.W., Shimada, K., Ma-Krupa, W., Johnson, T.L., Nerem, R.M., Goronzy, J.J., and Weyand, C.M. (2008). Vessel wall-embedded dendritic cells induce T-cell autoreactivity and initiate vascular inflammation. Circ Res *102*, 546-553.

Haniffa, M., Shin, A., Bigley, V., McGovern, N., Teo, P., See, P., Wasan, P.S., Wang, X.N., Malinarich, F., Malleret, B., *et al.* (2012). Human tissues contain CD141hi cross-presenting dendritic cells with functional homology to mouse CD103+ nonlymphoid dendritic cells. Immunity *37*, 60-73.

Hansson, G.K., and Hermansson, A. (2011). The immune system in atherosclerosis. Nat Immunol *12*, 204-212.

Hansson, G.K., Jonasson, L., Lojsthed, B., Stemme, S., Kocher, O., and Gabbiani, G. (1988). Localization of T lymphocytes and macrophages in fibrous and complicated human atherosclerotic plaques. Atherosclerosis *72*, 135-141.

Hansson, G.K., and Libby, P. (2006). The immune response in atherosclerosis: a double-edged sword. Nat Rev Immunol *6*, 508-519.

Harris, A.K., Shen, J., Radford, J., Bao, S., and Hambly, B.D. (2009). GM-CSF deficiency delays neointima formation in a normolipidemic mouse model of endoluminal endothelial damage. Immunol Cell Biol *87*, 122-130.

Hart, D.N. (1997). Dendritic cells: unique leukocyte populations which control the primary immune response. Blood *90*, 3245-3287.

Havel, R.J., and Kane, J.P. (1973). Primary dysbetalipoproteinemia: predominance of a specific apoprotein species in triglyceride-rich lipoproteins. Proc Natl Acad Sci U S A *70*, 2015-2019.

Helft, J., Ginhoux, F., Bogunovic, M., and Merad, M. (2010). Origin and functional heterogeneity of non-lymphoid tissue dendritic cells in mice. Immunol Rev *234*, 55-75.

Henri, S., Vremec, D., Kamath, A., Waithman, J., Williams, S., Benoist, C., Burnham, K., Saeland, S., Handman, E., and Shortman, K. (2001). The dendritic cell populations of mouse lymph nodes. J Immunol *167*, 741-748.

Hercus, T.R., Thomas, D., Guthridge, M.A., Ekert, P.G., King-Scott, J., Parker, M.W., and Lopez, A.F. (2009). The granulocyte-macrophage colony-stimulating factor receptor: linking its structure to cell signaling and its role in disease. Blood *114*, 1289-1298.

Hernandez-Vargas, P., Ortiz-Munoz, G., Lopez-Franco, O., Suzuki, Y., Gallego-Delgado, J., Sanjuan, G., Lazaro, A., Lopez-Parra, V., Ortega, L., Egido, J., and Gomez-Guerrero, C. (2006). Fcgamma receptor deficiency confers protection against atherosclerosis in apolipoprotein E knockout mice. Circ Res *99*, 1188-1196.

Hirata, Y., Egea, L., Dann, S.M., Eckmann, L., and Kagnoff, M.F. (2010). GM-CSF-facilitated dendritic cell recruitment and survival govern the intestinal mucosal response to a mouse enteric bacterial pathogen. Cell Host Microbe *7*, 151-163.

Hobbs, H.H., Russell, D.W., Brown, M.S., and Goldstein, J.L. (1990). The LDL receptor locus in familial hypercholesterolemia: mutational analysis of a membrane protein. Annu Rev Genet *24*, 133-170.

Hochleitner, B.W., Hochleitner, E.O., Obrist, P., Eberl, T., Amberger, A., Xu, Q., Margreiter, R., and Wick, G. (2000). Fluid shear stress induces heat shock

protein 60 expression in endothelial cells in vitro and in vivo. Arterioscler Thromb Vasc Biol *20*, 617-623.

Huo, Y., Guo, X., and Kassab, G.S. (2008). The flow field along the entire length of mouse aorta and primary branches. Ann Biomed Eng *36*, 685-699.

Inaba, K., Inaba, M., Romani, N., Aya, H., Deguchi, M., Ikehara, S., Muramatsu, S., and Steinman, R.M. (1992). Generation of large numbers of dendritic cells from mouse bone marrow cultures supplemented with granulocyte/macrophage colony-stimulating factor. J Exp Med *176*, 1693-1702.

Ingersoll, M.A., Platt, A.M., Potteaux, S., and Randolph, G.J. (2011). Monocyte trafficking in acute and chronic inflammation. Trends Immunol *32*, 470-477.

Ioan-Facsinay, A., de Kimpe, S.J., Hellwig, S.M., van Lent, P.L., Hofhuis, F.M., van Ojik, H.H., Sedlik, C., da Silveira, S.A., Gerber, J., de Jong, Y.F., *et al.* (2002). FcgammaRI (CD64) contributes substantially to severity of arthritis, hypersensitivity responses, and protection from bacterial infection. Immunity *16*, 391-402.

Ishibashi, S., Goldstein, J.L., Brown, M.S., Herz, J., and Burns, D.K. (1994). Massive xanthomatosis and atherosclerosis in cholesterol-fed low density lipoprotein receptor-negative mice. J Clin Invest *93*, 1885-1893.

Jakubzick, C., Tacke, F., Ginhoux, F., Wagers, A.J., van Rooijen, N., Mack, M., Merad, M., and Randolph, G.J. (2008). Blood monocyte subsets differentially give rise to CD103+ and CD103- pulmonary dendritic cell populations. J Immunol *180*, 3019-3027.

Joffre, O.P., Segura, E., Savina, A., and Amigorena, S. (2012). Cross-presentation by dendritic cells. Nat Rev Immunol *12*, 557-569.

Jongstra-Bilen, J., Haidari, M., Zhu, S.N., Chen, M., Guha, D., and Cybulsky, M.I. (2006). Low-grade chronic inflammation in regions of the normal mouse arterial intima predisposed to atherosclerosis. Journal of Experimental Medicine *203*, 2073-2083.

Kawahara, I., Kitagawa, N., Tsutsumi, K., Nagata, I., Hayashi, T., and Koji, T. (2007). The expression of vascular dendritic cells in human atherosclerotic carotid plaques. Human Pathology *38*, 1378-1385.

Kelly, M.E., Clay, M.A., Mistry, M.J., Hsieh-Li, H.M., and Harmony, J.A. (1994). Apolipoprotein E inhibition of proliferation of mitogen-activated T lymphocytes: production of interleukin 2 with reduced biological activity. Cell Immunol *159*, 124-139.

Kielian, T., Nagai, E., Ikubo, A., Rasmussen, C.A., and Suzuki, T. (1999). Granulocyte/macrophage-colony-stimulating factor released by adenovirally transduced CT26 cells leads to the local expression of macrophage inflammatory protein 1alpha and accumulation of dendritic cells at vaccination sites in vivo. Cancer Immunol Immunother *48*, 123-131.

King, I.L., Dickendesher, T.L., and Segal, B.M. (2009). Circulating Ly-6C+ myeloid precursors migrate to the CNS and play a pathogenic role during autoimmune demyelinating disease. Blood *113*, 3190-3197.

Koltsova, E.K., Garcia, Z., Chodaczek, G., Landau, M., McArdle, S., Scott, S.R., von Vietinghoff, S., Galkina, E., Miller, Y.I., Acton, S.T., and Ley, K. (2012). Dynamic T cell-APC interactions sustain chronic inflammation in atherosclerosis. J Clin Invest *122*, 3114-3126.

Krupa, W.M., Dewan, M., Jeon, M.S., Kurtin, P.J., Younge, B.R., Goronzy, J.J., and Weyand, C.M. (2002). Trapping of misdirected dendritic cells in the granulomatous lesions of giant cell arteritis. Am J Pathol *161*, 1815-1823.

Kuhlencordt, P.J., Chen, J., Han, F., Astern, J., and Huang, P.L. (2001). Genetic deficiency of inducible nitric oxide synthase reduces atherosclerosis and lowers plasma lipid peroxides in apolipoprotein E-knockout mice. Circulation *103*, 3099-3104.

Kuhlencordt, P.J., Padmapriya, P., Rutzel, S., Schodel, J., Hu, K., Schafer, A., Huang, P.L., Ertl, G., and Bauersachs, J. (2009). Ezetimibe potently reduces vascular inflammation and arteriosclerosis in eNOS-deficient ApoE ko mice. Atherosclerosis *202*, 48-57.

Kushwah, R., and Hu, J. (2011). Complexity of dendritic cell subsets and their function in the host immune system. Immunology *133*, 409-419.

Landsman, L., Varol, C., and Jung, S. (2007). Distinct differentiation potential of blood monocyte subsets in the lung. J Immunol *178*, 2000-2007.

Langlet, C., Tamoutounour, S., Henri, S., Luche, H., Ardouin, L., Gregoire, C., Malissen, B., and Guilliams, M. (2012). CD64 expression distinguishes monocyte-derived and conventional dendritic cells and reveals their distinct role during intramuscular immunization. J Immunol *188*, 1751-1760.

Leon, B., and Ardavin, C. (2008). Monocyte-derived dendritic cells in innate and adaptive immunity. Immunol Cell Biol *86*, 320-324.

Leuschner, F., Rauch, P.J., Ueno, T., Gorbatov, R., Marinelli, B., Lee, W.W., Dutta, P., Wei, Y., Robbins, C., Iwamoto, Y., *et al.* (2012). Rapid monocyte kinetics in acute myocardial infarction are sustained by extramedullary monocytopoiesis. J Exp Med *209*, 123-137.

Libby, P., Lichtman, A.H., and Hansson, G.K. (2013). Immune effector mechanisms implicated in atherosclerosis: from mice to humans. Immunity *38*, 1092-1104.

Liu, K., Victora, G.D., Schwickert, T.A., Guermonprez, P., Meredith, M.M., Yao, K., Chu, F.F., Randolph, G.J., Rudensky, A.Y., and Nussenzweig, M. (2009). In vivo analysis of dendritic cell development and homeostasis. Science *324*, 392-397.

Liu, K., Waskow, C., Liu, X., Yao, K., Hoh, J., and Nussenzweig, M. (2007). Origin of dendritic cells in peripheral lymphoid organs of mice. Nat Immunol *8*, 578-583.

Liu, Y.J. (2001). Dendritic cell subsets and lineages, and their functions in innate and adaptive immunity. Cell *106*, 259-262.

Llodra, J., Angeli, V., Liu, J.H., Trogan, E., Fisher, E.A., and Randolph, G.J. (2004). Emigration of monocyte-derived cells from atherosclerotic lesions characterizes regressive, but not progressive, plaques. Proceedings of the National Academy of Sciences of the United States of America *101*, 11779-11784.

Lopes-Virella, M.F., Binzafar, N., Rackley, S., Takei, A., La Via, M., and Virella, G. (1997). The uptake of LDL-IC by human macrophages: predominant involvement of the Fc gamma RI receptor. Atherosclerosis *135*, 161-170.

Lord, R.S., and Bobryshev, Y.V. (2002). Hallmarks of atherosclerotic lesion development with special reference to immune inflammatory mechanisms. Cardiovasc Surg *10*, 405-414.

Lowes, M.A., Chamian, F., Abello, M.V., Fuentes-Duculan, J., Lin, S.L., Nussbaum, R., Novitskaya, I., Carbonaro, H., Cardinale, I., Kikuchi, T., *et al.* (2005). Increase in TNF-alpha and inducible nitric oxide synthase-expressing dendritic cells in psoriasis and reduction with efalizumab (anti-CD11a). Proc Natl Acad Sci U S A *102*, 19057-19062.

Lutz, M.B., Suri, R.M., Niimi, M., Ogilvie, A.L., Kukutsch, N.A., Rossner, S., Schuler, G., and Austyn, J.M. (2000). Immature dendritic cells generated with low doses of GM-CSF in the absence of IL-4 are maturation resistant and prolong allograft survival in vivo. Eur J Immunol *30*, 1813-1822.

Ma-Krupa, W., Jeon, M.S., Spoerl, S., Tedder, T.F., Goronzy, J.J., and Weyand, C.M. (2004). Activation of arterial wall dendritic cells and breakdown of self-tolerance in giant cell arteritis. J Exp Med *199*, 173-183.

MacDonald, K.P., Rowe, V., Bofinger, H.M., Thomas, R., Sasmono, T., Hume, D.A., and Hill, G.R. (2005). The colony-stimulating factor 1 receptor is expressed on dendritic cells during differentiation and regulates their expansion. J Immunol *175*, 1399-1405.

Macritchie, N., Grassia, G., Sabir, S.R., Maddaluno, M., Welsh, P., Sattar, N., Ialenti, A., Kurowska-Stolarska, M., McInnes, I.B., Brewer, J.M., *et al.* (2012). Plasmacytoid dendritic cells play a key role in promoting atherosclerosis in apolipoprotein E-deficient mice. Arterioscler Thromb Vasc Biol *32*, 2569-2579.

Madhur, M.S., Funt, S.A., Li, L., Vinh, A., Chen, W., Lob, H.E., Iwakura, Y., Blinder, Y., Rahman, A., Quyyumi, A.A., and Harrison, D.G. (2011). Role of interleukin 17 in inflammation, atherosclerosis, and vascular function in

apolipoprotein e-deficient mice. Arterioscler Thromb Vasc Biol *31*, 1565-1572.

Mahley, R.W., Weisgraber, K.H., and Innerarity, T. (1976). Atherogenic hyperlipoproteinemia induced by cholesterol feeding the Patas monkey. Biochemistry *15*, 2979-2985.

Majmudar, M.D., Keliher, E.J., Heidt, T., Leuschner, F., Truelove, J., Sena, B.F., Gorbatov, R., Iwamoto, Y., Dutta, P., Wojtkiewicz, G., *et al.* (2013). Monocyte-directed RNAi targeting CCR2 improves infarct healing in atherosclerosis-prone mice. Circulation *127*, 2038-2046.

Martin, P., Del Hoyo, G.M., Anjuere, F., Arias, C.F., Vargas, H.H., Fernandez, L.A., Parrillas, V., and Ardavin, C. (2002). Characterization of a new subpopulation of mouse CD8alpha+ B220+ dendritic cells endowed with type 1 interferon production capacity and tolerogenic potential. Blood *100*, 383-390.

Mayerl, C., Lukasser, M., Sedivy, R., Niederegger, H., Seiler, R., and Wick, G. (2006). Atherosclerosis research from past to present--on the track of two pathologists with opposing views, Carl von Rokitansky and Rudolf Virchow. Virchows Arch *449*, 96-103.

McKenna, H.J., Stocking, K.L., Miller, R.E., Brasel, K., De Smedt, T., Maraskovsky, E., Maliszewski, C.R., Lynch, D.H., Smith, J., Pulendran, B., *et al.* (2000). Mice lacking flt3 ligand have deficient hematopoiesis affecting hematopoietic progenitor cells, dendritic cells, and natural killer cells. Blood *95*, 3489-3497.

Merad, M., Ginhoux, F., and Collin, M. (2008). Origin, homeostasis and function of Langerhans cells and other langerin-expressing dendritic cells. Nat Rev Immunol *8*, 935-947.

Merad, M., Manz, M.G., Karsunky, H., Wagers, A., Peters, W., Charo, I., Weissman, I.L., Cyster, J.G., and Engleman, E.G. (2002). Langerhans cells renew in the skin throughout life under steady-state conditions. Nat Immunol *3*, 1135-1141.

Miller, G., Pillarisetty, V.G., Shah, A.B., Lahrs, S., Xing, Z., and DeMatteo, R.P. (2002). Endogenous granulocyte-macrophage colony-stimulating factor overexpression in vivo results in the long-term recruitment of a distinct dendritic cell population with enhanced immunostimulatory function. J Immunol *169*, 2875-2885.

Miller, J.C., Brown, B.D., Shay, T., Gautier, E.L., Jojic, V., Cohain, A., Pandey, G., Leboeuf, M., Elpek, K.G., Helft, J., *et al.* (2012). Deciphering the transcriptional network of the dendritic cell lineage. Nat Immunol *13*, 888-899.

Millonig, G., Niederegger, H., Rabl, W., Hochleitner, B.W., Hoefer, D., Romani, N., and Wick, G. (2001a). Network of vascular-associated dendritic cells in intima of healthy young individuals. Arteriosclerosis, Thrombosis, and Vascular Biology *21*, 503-508.

Millonig, G., Schwentner, C., Mueller, P., Mayerl, C., and Wick, G. (2001b). The vascular-associated lymphoid tissue: a new site of local immunity. Curr Opin Lipidol *12*, 547-553.

Min, L., Mohammad Isa, S.A., Shuai, W., Piang, C.B., Nih, F.W., Kotaka, M., and Ruedl, C. (2010). Cutting edge: granulocyte-macrophage colony-

stimulating factor is the major CD8+ T cell-derived licensing factor for dendritic cell activation. J Immunol *184*, 4625-4629.

Minota, S., Cameron, B., Welch, W.J., and Winfield, J.B. (1988). Autoantibodies to the constitutive 73-kD member of the hsp70 family of heat shock proteins in systemic lupus erythematosus. J Exp Med *168*, 1475-1480.

Miyoshi, T., Li, Y., Shih, D.M., Wang, X., Laubach, V.E., Matsumoto, A.H., Helm, G.A., Lusis, A.J., and Shi, W. (2006). Deficiency of inducible NO synthase reduces advanced but not early atherosclerosis in apolipoprotein E-deficient mice. Life Sci *79*, 525-531.

Mullick, A.E., Soldau, K., Kiosses, W.B., Bell, T.A., 3rd, Tobias, P.S., and Curtiss, L.K. (2008). Increased endothelial expression of Toll-like receptor 2 at sites of disturbed blood flow exacerbates early atherogenic events. J Exp Med *205*, 373-383.

Murphy, A.J., Akhtari, M., Tolani, S., Pagler, T., Bijl, N., Kuo, C.L., Wang, M., Sanson, M., Abramowicz, S., Welch, C., *et al.* (2011). ApoE regulates hematopoietic stem cell proliferation, monocytosis, and monocyte accumulation in atherosclerotic lesions in mice. J Clin Invest *121*, 4138-4149.

Nahrendorf, M., Swirski, F.K., Aikawa, E., Stangenberg, L., Wurdinger, T., Figueiredo, J.L., Libby, P., Weissleder, R., and Pittet, M.J. (2007). The healing myocardium sequentially mobilizes two monocyte subsets with divergent and complementary functions. J Exp Med *204*, 3037-3047.

Naik, S.H., Metcalf, D., van Nieuwenhuijze, A., Wicks, I., Wu, L., O'Keeffe, M., and Shortman, K. (2006). Intrasplenic steady-state dendritic cell precursors that are distinct from monocytes. Nat Immunol *7*, 663-671.

Naik, S.H., Sathe, P., Park, H.Y., Metcalf, D., Proietto, A.I., Dakic, A., Carotta, S., O'Keeffe, M., Bahlo, M., Papenfuss, A., *et al.* (2007). Development of plasmacytoid and conventional dendritic cell subtypes from single precursor cells derived in vitro and in vivo. Nat Immunol *8*, 1217-1226.

Nair, J.R., Edwards, S.W., and Moots, R.J. (2012). Mavrilimumab, a human monoclonal GM-CSF receptor-alpha antibody for the management of rheumatoid arthritis: a novel approach to therapy. Expert Opin Biol Ther *12*, 1661-1668.

Nakano, H., Yanagita, M., and Gunn, M.D. (2001). CD11c(+)B220(+)Gr-1(+) cells in mouse lymph nodes and spleen display characteristics of plasmacytoid dendritic cells. J Exp Med *194*, 1171-1178.

Nakashima, Y., Plump, A.S., Raines, E.W., Breslow, J.L., and Ross, R. (1994). ApoE-deficient mice develop lesions of all phases of atherosclerosis throughout the arterial tree. Arterioscler Thromb *14*, 133-140.

Ng, H.P., Burris, R.L., and Nagarajan, S. (2011). Attenuated atherosclerotic lesions in apoE-Fcgamma-chain-deficient hyperlipidemic mouse model is associated with inhibition of Th17 cells and promotion of regulatory T cells. J Immunol *187*, 6082-6093.

Ni, K., and O'Neill, H.C. (2001). Development of dendritic cells from GM-CSF-/- mice in vitro : GM-CSF enhances production and survival of cells. Dev Immunol *8*, 133-146.

Nilsson, J., and Hansson, G.K. (2008). Autoimmunity in atherosclerosis: a protective response losing control? J Intern Med *263*, 464-478.

Ohta, H., Wada, H., Niwa, T., Kirii, H., Iwamoto, N., Fujii, H., Saito, K., Sekikawa, K., and Seishima, M. (2005). Disruption of tumor necrosis factor-

alpha gene diminishes the development of atherosclerosis in ApoE-deficient mice. Atherosclerosis *180*, 11-17.

Onai, N., Obata-Onai, A., Schmid, M.A., Ohteki, T., Jarrossay, D., and Manz, M.G. (2007). Identification of clonogenic common Flt3+M-CSFR+ plasmacytoid and conventional dendritic cell progenitors in mouse bone marrow. Nat Immunol *8*, 1207-1216.

Osterholzer, J.J., Chen, G.H., Olszewski, M.A., Curtis, J.L., Huffnagle, G.B., and Toews, G.B. (2009). Accumulation of CD11b+ lung dendritic cells in response to fungal infection results from the CCR2-mediated recruitment and differentiation of Ly-6Chigh monocytes. J Immunol *183*, 8044-8053.

Palframan, R.T., Jung, S., Cheng, G., Weninger, W., Luo, Y., Dorf, M., Littman, D.R., Rollins, B.J., Zweerink, H., Rot, A., and von Andrian, U.H. (2001). Inflammatory chemokine transport and presentation in HEV: a remote control mechanism for monocyte recruitment to lymph nodes in inflamed tissues. J Exp Med *194*, 1361-1373.

Parajuli, P., Mosley, R.L., Pisarev, V., Chavez, J., Ulrich, A., Varney, M., Singh, R.K., and Talmadge, J.E. (2001). Flt3 ligand and granulocyte-macrophage colony-stimulating factor preferentially expand and stimulate different dendritic and T-cell subsets. Exp Hematol *29*, 1185-1193.

Parastatidis, I., Thomson, L., Fries, D.M., Moore, R.E., Tohyama, J., Fu, X., Hazen, S.L., Heijnen, H.F., Dennehy, M.K., Liebler, D.C., *et al.* (2007). Increased protein nitration burden in the atherosclerotic lesions and plasma of apolipoprotein A-I deficient mice. Circ Res *101*, 368-376.

Paulson, K.E., Zhu, S.N., Chen, M., Nurmohamed, S., Jongstra-Bilen, J., and Cybulsky, M.I. (2010). Resident intimal dendritic cells accumulate lipid and

contribute to the initiation of atherosclerosis. Circulation Research *106*, 383-390.

Pendse, A.A., Arbones-Mainar, J.M., Johnson, L.A., Altenburg, M.K., and Maeda, N. (2009). Apolipoprotein E knock-out and knock-in mice: atherosclerosis, metabolic syndrome, and beyond. J Lipid Res *50 Suppl*, S178-182.

Plantinga, M., Guilliams, M., Vanheerswynghels, M., Deswarte, K., Branco-Madeira, F., Toussaint, W., Vanhoutte, L., Neyt, K., Killeen, N., Malissen, B., *et al.* (2013). Conventional and monocyte-derived CD11b(+) dendritic cells initiate and maintain T helper 2 cell-mediated immunity to house dust mite allergen. Immunity *38*, 322-335.

Plenz, G., Koenig, C., Severs, N.J., and Robenek, H. (1997). Smooth muscle cells express granulocyte-macrophage colony-stimulating factor in the undiseased and atherosclerotic human coronary artery. Arterioscler Thromb Vasc Biol *17*, 2489-2499.

Plump, A.S., and Breslow, J.L. (1995). Apolipoprotein E and the apolipoprotein E-deficient mouse. Annu Rev Nutr *15*, 495-518.

Potteaux, S., Gautier, E.L., Hutchison, S.B., van Rooijen, N., Rader, D.J., Thomas, M.J., Sorci-Thomas, M.G., and Randolph, G.J. (2011). Suppressed monocyte recruitment drives macrophage removal from atherosclerotic plaques of Apoe-/- mice during disease regression. J Clin Invest *121*, 2025-2036.

Pryshchep, O., Ma-Krupa, W., Younge, B.R., Goronzy, J.J., and Weyand, C.M. (2008). Vessel-specific toll-like receptor profiles in human medium and large arteries. Circulation *118*, 1276-1284.

Rajavashisth, T.B., Andalibi, A., Territo, M.C., Berliner, J.A., Navab, M., Fogelman, A.M., and Lusis, A.J. (1990). Induction of endothelial cell expression of granulocyte and macrophage colony-stimulating factors by modified low-density lipoproteins. Nature *344*, 254-257.

Rall, S.C., Jr., Newhouse, Y.M., Clarke, H.R., Weisgraber, K.H., McCarthy, B.J., Mahley, R.W., and Bersot, T.P. (1989). Type III hyperlipoproteinemia associated with apolipoprotein E phenotype E3/3. Structure and genetics of an apolipoprotein E3 variant. J Clin Invest *83*, 1095-1101.

Randolph, G.J., Beaulieu, S., Lebecque, S., Steinman, R.M., and Muller, W.A. (1998). Differentiation of monocytes into dendritic cells in a model of transendothelial trafficking. Science *282*, 480-483.

Reddick, R.L., Zhang, S.H., and Maeda, N. (1994). Atherosclerosis in mice lacking apo E. Evaluation of lesional development and progression. Arterioscler Thromb *14*, 141-147.

Rivollier, A., He, J., Kole, A., Valatas, V., and Kelsall, B.L. (2012). Inflammation switches the differentiation program of Ly6Chi monocytes from antiinflammatory macrophages to inflammatory dendritic cells in the colon. J Exp Med *209*, 139-155.

Robb, L., Drinkwater, C.C., Metcalf, D., Li, R., Kontgen, F., Nicola, N.A., and Begley, C.G. (1995). Hematopoietic and lung abnormalities in mice with a null mutation of the common beta subunit of the receptors for granulocyte-macrophage colony-stimulating factor and interleukins 3 and 5. Proc Natl Acad Sci U S A *92*, 9565-9569.

Robbins, C.S., Chudnovskiy, A., Rauch, P.J., Figueiredo, J.L., Iwamoto, Y., Gorbatov, R., Etzrodt, M., Weber, G.F., Ueno, T., van Rooijen, N., *et al.*

(2012). Extramedullary hematopoiesis generates Ly-6C(high) monocytes that infiltrate atherosclerotic lesions. Circulation *125*, 364-374.

Rosas, M., Gordon, S., and Taylor, P.R. (2007). Characterisation of the expression and function of the GM-CSF receptor alpha-chain in mice. Eur J Immunol *37*, 2518-2528.

Rosenfeld, M.E., Polinsky, P., Virmani, R., Kauser, K., Rubanyi, G., and Schwartz, S.M. (2000). Advanced atherosclerotic lesions in the innominate artery of the ApoE knockout mouse. Arterioscler Thromb Vasc Biol *20*, 2587-2592.

Ross, R. (1999). Atherosclerosis - An Inflammatory Diesease. New England Journal of Medicine *340*.

Ross, R., and Harker, L. (1976). Hyperlipidemia and atherosclerosis. Science *193*, 1094-1100.

Schlitzer, A., McGovern, N., Teo, P., Zelante, T., Atarashi, K., Low, D., Ho, A.W., See, P., Shin, A., Wasan, P.S., *et al.* (2013). IRF4 transcription factor-dependent CD11b+ dendritic cells in human and mouse control mucosal IL-17 cytokine responses. Immunity *38*, 970-983.

Schulz, O., Jaensson, E., Persson, E.K., Liu, X., Worbs, T., Agace, W.W., and Pabst, O. (2009). Intestinal CD103+, but not CX3CR1+, antigen sampling cells migrate in lymph and serve classical dendritic cell functions. J Exp Med *206*, 3101-3114.

Serbina, N.V., and Pamer, E.G. (2006). Monocyte emigration from bone marrow during bacterial infection requires signals mediated by chemokine receptor CCR2. Nat Immunol *7*, 311-317.

Serbina, N.V., Salazar-Mather, T.P., Biron, C.A., Kuziel, W.A., and Pamer, E.G. (2003). TNF/iNOS-producing dendritic cells mediate innate immune defense against bacterial infection. Immunity *19*, 59-70.

Shaposhnik, Z., Wang, X.P., Weinstein, M., Bennett, B.J., and Lusis, A.J. (2007). Granulocyte macrophage colony-stimulating factor regulates dendritic cell content of atherosclerotic lesions. Arteriosclerosis Thrombosis and Vascular Biology *27*, 621-627.

Sheng, J.R., Li, L., Ganesh, B.B., Vasu, C., Prabhakar, B.S., and Meriggioli, M.N. (2006). Suppression of experimental autoimmune myasthenia gravis by granulocyte-macrophage colony-stimulating factor is associated with an expansion of FoxP3+ regulatory T cells. J Immunol *177*, 5296-5306.

Sheridan, J.W., and Metcalf, D. (1972). Studies on the bone marrow colony stimulating factor (CSF): relation of tissue CSF to serum CSF. J Cell Physiol *80*, 129-140.

Shi, C., and Pamer, E.G. (2011). Monocyte recruitment during infection and inflammation. Nat Rev Immunol *11*, 762-774.

Shi, Y., Liu, C.H., Roberts, A.I., Das, J., Xu, G., Ren, G., Zhang, Y., Zhang, L., Yuan, Z.R., Tan, H.S., *et al.* (2006). Granulocyte-macrophage colony-stimulating factor (GM-CSF) and T-cell responses: what we do and don't know. Cell Res *16*, 126-133.

Shimada, K. (2009). Immune system and atherosclerotic disease: heterogeneity of leukocyte subsets participating in the pathogenesis of atherosclerosis. Circ J *73*, 994-1001.

Shore, V.G., and Shore, B. (1973). Heterogeneity of human plasma very low density lipoproteins. Separation of species differing in protein components. Biochemistry *12*, 502-507.

Shortman, K., and Heath, W.R. (2010). The CD8+ dendritic cell subset. Immunol Rev *234*, 18-31.

Shortman, K., and Liu, Y.J. (2002). Mouse and human dendritic cell subtypes. Nat Rev Immunol *2*, 151-161.

Shortman, K., and Naik, S.H. (2007). Steady-state and inflammatory dendritic-cell development. Nat Rev Immunol *7*, 19-30.

Sjoland, H., Eitzman, D.T., Gordon, D., Westrick, R., Nabel, E.G., and Ginsburg, D. (2000). Atherosclerosis progression in LDL receptor-deficient and apolipoprotein E-deficient mice is independent of genetic alterations in plasminogen activator inhibitor-1. Arterioscler Thromb Vasc Biol *20*, 846-852.

Smith, E., Prasad, K.M., Butcher, M., Dobrian, A., Kolls, J.K., Ley, K., and Galkina, E. (2010). Blockade of interleukin-17A results in reduced atherosclerosis in apolipoprotein E-deficient mice. Circulation *121*, 1746-1755.

Smythe, C.D., Skinner, V.O., Bruckdorfer, K.R., Haskard, D.O., and Landis, R.C. (2003). The state of macrophage differentiation determines the TNF alpha response to nitrated lipoprotein uptake. Atherosclerosis *170*, 213-221.

Soehnlein, O. (2012). Multiple roles for neutrophils in atherosclerosis. Circ Res *110*, 875-888.

Stancu, C.S., Toma, L., and Sima, A.V. (2012). Dual role of lipoproteins in endothelial cell dysfunction in atherosclerosis. Cell Tissue Res *349*, 433-446.

Stary, H.C., Chandler, A.B., Dinsmore, R.E., Fuster, V., Glagov, S., Insull, W., Jr., Rosenfeld, M.E., Schwartz, C.J., Wagner, W.D., and Wissler, R.W. (1995). A definition of advanced types of atherosclerotic lesions and a histological classification of atherosclerosis. A report from the Committee on Vascular Lesions of the Council on Arteriosclerosis, American Heart Association. Circulation *92*, 1355-1374.

Stary, H.C., Chandler, A.B., Glagov, S., Guyton, J.R., Insull, W., Jr., Rosenfeld, M.E., Schaffer, S.A., Schwartz, C.J., Wagner, W.D., and Wissler, R.W. (1994). A definition of initial, fatty streak, and intermediate lesions of atherosclerosis. A report from the Committee on Vascular Lesions of the Council on Arteriosclerosis, American Heart Association. Circulation *89*, 2462-2478.

Steinberg, D., and Witztum, J.L. (1990). Lipoproteins and atherogenesis. Current concepts. JAMA *264*, 3047-3052.

Steinman, R.M. (1991). The dendritic cell system and its role in immunogenicity. Annu Rev Immunol *9*, 271-296.

Steinman, R.M., and Cohn, Z.A. (1973). Identification of a novel cell type in peripheral lymphoid organs of mice. I. Morphology, quantitation, tissue distribution. J Exp Med *137*, 1142-1162.

Stoneman, V., Braganza, D., Figg, N., Mercer, J., Lang, R., Goddard, M., and Bennett, M. (2007). Monocyte/macrophage suppression in CD11b diphtheria toxin receptor transgenic mice differentially affects atherogenesis and established plaques. Circ Res *100*, 884-893.

Stratford, N., Britten, K., and Gallagher, P. (1986). Inflammatory infiltrates in human coronary atherosclerosis. Atherosclerosis *59*, 271-276.

Sunderkotter, C., Nikolic, T., Dillon, M.J., Van Rooijen, N., Stehling, M., Drevets, D.A., and Leenen, P.J. (2004). Subpopulations of mouse blood monocytes differ in maturation stage and inflammatory response. J Immunol *172*, 4410-4417.

Swirski, F.K., Libby, P., Aikawa, E., Alcaide, P., Luscinskas, F.W., Weissleder, R., and Pittet, M.J. (2007). Ly-6Chi monocytes dominate hypercholesterolemia-associated monocytosis and give rise to macrophages in atheromata. J Clin Invest *117*, 195-205.

Swirski, F.K., Nahrendorf, M., Etzrodt, M., Wildgruber, M., Cortez-Retamozo, V., Panizzi, P., Figueiredo, J.L., Kohler, R.H., Chudnovskiy, A., Waterman, P., *et al.* (2009). Identification of splenic reservoir monocytes and their deployment to inflammatory sites. Science *325*, 612-616.

Swirski, F.K., Pittet, M.J., Kircher, M.F., Aikawa, E., Jaffer, F.A., Libby, P., and Weissleder, R. (2006). Monocyte accumulation in mouse atherogenesis is progressive and proportional to extent of disease. Proc Natl Acad Sci U S A *103*, 10340-10345.

Tacke, F., Alvarez, D., Kaplan, T.J., Jakubzick, C., Spanbroek, R., Llodra, J., Garin, A., Liu, J.H., Mack, M., van Rooijen, N., *et al.* (2007). Monocyte subsets differentially employ CCR2, CCR5, and CX3CR1 to accumulate within atherosclerotic plaques. Journal of Clinical Investigation *117*, 185-194.

Takizawa, H., Boettcher, S., and Manz, M.G. (2012). Demand-adapted regulation of early hematopoiesis in infection and inflammation. Blood *119*, 2991-3002.

Tamoutounour, S., Henri, S., Lelouard, H., de Bovis, B., de Haar, C., van der Woude, C.J., Woltman, A.M., Reyal, Y., Bonnet, D., Sichien, D., *et al.* (2012).

CD64 distinguishes macrophages from dendritic cells in the gut and reveals the Th1-inducing role of mesenteric lymph node macrophages during colitis. Eur J Immunol *42*, 3150-3166.

Tan, P.S., Gavin, A.L., Barnes, N., Sears, D.W., Vremec, D., Shortman, K., Amigorena, S., Mottram, P.L., and Hogarth, P.M. (2003). Unique monoclonal antibodies define expression of Fc gamma RI on macrophages and mast cell lines and demonstrate heterogeneity among subcutaneous and other dendritic cells. J Immunol *170*, 2549-2556.

Tenger, C., and Zhou, X. (2003). Apolipoprotein E modulates immune activation by acting on the antigen-presenting cell. Immunology *109*, 392-397.

Tezuka, H., Abe, Y., Iwata, M., Takeuchi, H., Ishikawa, H., Matsushita, M., Shiohara, T., Akira, S., and Ohteki, T. (2007). Regulation of IgA production by naturally occurring TNF/iNOS-producing dendritic cells. Nature *448*, 929-933.

Trogan, E., Feig, J.E., Dogan, S., Rothblat, G.H., Angeli, V., Tacke, F., Randolph, G.J., and Fisher, E.A. (2006). Gene expression changes in foam cells and the role of chemokine receptor CCR7 during atherosclerosis regression in ApoE-deficient mice. Proc Natl Acad Sci U S A *103*, 3781-3786.

Tsou, C.L., Peters, W., Si, Y., Slaymaker, S., Aslanian, A.M., Weisberg, S.P., Mack, M., and Charo, I.F. (2007). Critical roles for CCR2 and MCP-3 in monocyte mobilization from bone marrow and recruitment to inflammatory sites. J Clin Invest *117*, 902-909.

Tsoulfa, G., Rook, G.A., Van-Embden, J.D., Young, D.B., Mehlert, A., Isenberg, D.A., Hay, F.C., and Lydyard, P.M. (1989). Raised serum IgG and

IgA antibodies to mycobacterial antigens in rheumatoid arthritis. Ann Rheum Dis *48*, 118-123.

Upmacis, R.K., Crabtree, M.J., Deeb, R.S., Shen, H., Lane, P.B., Benguigui, L.E., Maeda, N., Hajjar, D.P., and Gross, S.S. (2007). Profound biopterin oxidation and protein tyrosine nitration in tissues of ApoE-null mice on an atherogenic diet: contribution of inducible nitric oxide synthase. Am J Physiol Heart Circ Physiol *293*, H2878-2887.

van der Poel, C.E., Spaapen, R.M., van de Winkel, J.G., and Leusen, J.H. (2011). Functional characteristics of the high affinity IgG receptor, FcgammaRI. J Immunol *186*, 2699-2704.

Van Vre, E.A., Bosmans, J.M., Van Brussel, I., Maris, M., De Meyer, G.R., Van Schil, P.E., Vrints, C.J., and Bult, H. (2011). Immunohistochemical characterisation of dendritic cells in human atherosclerotic lesions: possible pitfalls. Pathology *43*, 239-247.

VanderLaan, P.A., Reardon, C.A., and Getz, G.S. (2004). Site specificity of atherosclerosis: site-selective responses to atherosclerotic modulators. Arterioscler Thromb Vasc Biol *24*, 12-22.

Varol, C., Landsman, L., Fogg, D.K., Greenshtein, L., Gildor, B., Margalit, R., Kalchenko, V., Geissmann, F., and Jung, S. (2007). Monocytes give rise to mucosal, but not splenic, conventional dendritic cells. J Exp Med *204*, 171-180.

Varol, C., Vallon-Eberhard, A., Elinav, E., Aychek, T., Shapira, Y., Luche, H., Fehling, H.J., Hardt, W.D., Shakhar, G., and Jung, S. (2009). Intestinal lamina propria dendritic cell subsets have different origin and functions. Immunity *31*, 502-512.

Vasu, C., Dogan, R.N., Holterman, M.J., and Prabhakar, B.S. (2003). Selective induction of dendritic cells using granulocyte macrophage-colony stimulating factor, but not fms-like tyrosine kinase receptor 3-ligand, activates thyroglobulin-specific CD4+/CD25+ T cells and suppresses experimental autoimmune thyroiditis. J Immunol *170*, 5511-5522.

Veniant, M.M., Zlot, C.H., Walzem, R.L., Pierotti, V., Driscoll, R., Dichek, D., Herz, J., and Young, S.G. (1998). Lipoprotein clearance mechanisms in LDL receptor-deficient "Apo-B48-only" and "Apo-B100-only" mice. J Clin Invest *102*, 1559-1568.

Veres, T.Z., Voedisch, S., Spies, E., Valtonen, J., Prenzler, F., and Braun, A. (2013). Aeroallergen challenge promotes dendritic cell proliferation in the airways. J Immunol *190*, 897-903.

Vermaelen, K.Y., Carro-Muino, I., Lambrecht, B.N., and Pauwels, R.A. (2001). Specific migratory dendritic cells rapidly transport antigen from the airways to the thoracic lymph nodes. J Exp Med *193*, 51-60.

Vremec, D., Lieschke, G.J., Dunn, A.R., Robb, L., Metcalf, D., and Shortman, K. (1997). The influence of granulocyte/macrophage colony-stimulating factor on dendritic cell levels in mouse lymphoid organs. Eur J Immunol *27*, 40-44.

Vremec, D., Pooley, J., Hochrein, H., Wu, L., and Shortman, K. (2000). CD4 and CD8 expression by dendritic cell subtypes in mouse thymus and spleen. J Immunol *164*, 2978-2986.

Waltner-Romen, M., Falkensammer, G., Rabl, W., and Wick, G. (1998). A previously unrecognized site of local accumulation of mononuclear cells. The vascular-associated lymphoid tissue. J Histochem Cytochem *46*, 1347-1350.

Wang, Y., Szretter, K.J., Vermi, W., Gilfillan, S., Rossini, C., Cella, M., Barrow, A.D., Diamond, M.S., and Colonna, M. (2012). IL-34 is a tissue-restricted ligand of CSF1R required for the development of Langerhans cells and microglia. Nat Immunol *13*, 753-760.

Weber, C., Meiler, S., Doring, Y., Koch, M., Drechsler, M., Megens, R.T., Rowinska, Z., Bidzhekov, K., Fecher, C., Ribechini, E., *et al.* (2011). CCL17-expressing dendritic cells drive atherosclerosis by restraining regulatory T cell homeostasis in mice. J Clin Invest *121*, 2898-2910.

Weber, C., Zernecke, A., and Libby, P. (2008). The multifaceted contributions of leukocyte subsets to atherosclerosis: lessons from mouse models. Nat Rev Immunol *8*, 802-815.

Wei, J., Zheng, M., Liang, P., Wei, Y., Yin, X., Tang, Y., and Xue, Y. (2013). Apolipoprotein E and its mimetic peptide suppress Th1 and Th17 responses in experimental autoimmune encephalomyelitis. Neurobiol Dis *56*, 59-65.

Wendland, M., Czeloth, N., Mach, N., Malissen, B., Kremmer, E., Pabst, O., and Forster, R. (2007). CCR9 is a homing receptor for plasmacytoid dendritic cells to the small intestine. Proc Natl Acad Sci U S A *104*, 6347-6352.

Whitman, S.C. (2004). A practical approach to using mice in atherosclerosis research. Clin Biochem Rev *25*, 81-93.

Wick, G., Romen, M., Amberger, A., Metzler, B., Mayr, M., Falkensammer, G., and Xu, Q. (1997). Atherosclerosis, autoimmunity, and vascular-associated lymphoid tissue. FASEB J *11*, 1199-1207.

Willman, C.L., Stewart, C.C., Miller, V., Yi, T.L., and Tomasi, T.B. (1989). Regulation of MHC class II gene expression in macrophages by hematopoietic

colony-stimulating factors (CSF). Induction by granulocyte/macrophage CSF and inhibition by CSF-1. J Exp Med *170*, 1559-1567.

Woollard, K.J. (2013). Immunological aspects of atherosclerosis. Clin Sci (Lond) *125*, 221-235.

Workman, C.J., Wang, Y., El Kasmi, K.C., Pardoll, D.M., Murray, P.J., Drake, C.G., and Vignali, D.A. (2009). LAG-3 regulates plasmacytoid dendritic cell homeostasis. J Immunol *182*, 1885-1891.

Wu, H., Gower, R.M., Wang, H., Perrard, X.Y., Ma, R., Bullard, D.C., Burns, A.R., Paul, A., Smith, C.W., Simon, S.I., and Ballantyne, C.M. (2009). Functional role of CD11c+ monocytes in atherogenesis associated with hypercholesterolemia. Circulation *119*, 2708-2717.

Xu, Q., Dietrich, H., Steiner, H.J., Gown, A.M., Schoel, B., Mikuz, G., Kaufmann, S.H., and Wick, G. (1992). Induction of arteriosclerosis in normocholesterolemic rabbits by immunization with heat shock protein 65. Arterioscler Thromb *12*, 789-799.

Xu, Q., Kleindienst, R., Waitz, W., Dietrich, H., and Wick, G. (1993). Increased expression of heat shock protein 65 coincides with a population of infiltrating T lymphocytes in atherosclerotic lesions of rabbits specifically responding to heat shock protein 65. J Clin Invest *91*, 2693-2702.

Xu, Q., Schett, G., Seitz, C.S., Hu, Y., Gupta, R.S., and Wick, G. (1994). Surface staining and cytotoxic activity of heat-shock protein 60 antibody in stressed aortic endothelial cells. Circ Res *75*, 1078-1085.

Xu, Q.B., Oberhuber, G., Gruschwitz, M., and Wick, G. (1990). Immunology of atherosclerosis: cellular composition and major histocompatibility complex class II antigen expression in aortic intima, fatty streaks, and atherosclerotic

plaques in young and aged human specimens. Clin Immunol Immunopathol *56*, 344-359.

Xu, Y., Zhan, Y., Lew, A.M., Naik, S.H., and Kershaw, M.H. (2007). Differential development of murine dendritic cells by GM-CSF versus Flt3 ligand has implications for inflammation and trafficking. J Immunol *179*, 7577-7584.

Yilmaz, A., Rowley, A., Schulte, D.J., Doherty, T.M., Schroder, N.W., Fishbein, M.C., Kalelkar, M., Cicha, I., Schubert, K., Daniel, W.G., *et al.* (2007). Activated myeloid dendritic cells accumulate and co-localize with CD3+ T cells in coronary artery lesions in patients with Kawasaki disease. Exp Mol Pathol *83*, 93-103.

Yilmaz, A., Weber, J., Cicha, I., Stumpf, C., Klein, M., Raithel, D., Daniel, W.G., and Garlichs, C.D. (2006). Decrease in Circulating Myeloid Dendritic Cell Precursors in Coronary Artery Disease. Journal of the American College of Cardiology *48*, 70-80.

Yin, N., Xu, J., Ginhoux, F., Randolph, G.J., Merad, M., Ding, Y., and Bromberg, J.S. (2012). Functional specialization of islet dendritic cell subsets. J Immunol *188*, 4921-4930.

Ylitalo, R., Oksala, O., Yla-Herttuala, S., and Ylitalo, P. (1994). Effects of clodronate (dichloromethylene bisphosphonate) on the development of experimental atherosclerosis in rabbits. J Lab Clin Med *123*, 769-776.

Yuan, Z., Kishimoto, C., Sano, H., Shioji, K., Xu, Y., and Yokode, M. (2003). Immunoglobulin treatment suppresses atherosclerosis in apolipoprotein E-deficient mice via the Fc portion. Am J Physiol Heart Circ Physiol *285*, H899-906.

Zhan, Y., Carrington, E.M., van Nieuwenhuijze, A., Bedoui, S., Seah, S., Xu, Y., Wang, N., Mintern, J.D., Villadangos, J.A., Wicks, I.P., and Lew, A.M. (2011). GM-CSF increases cross-presentation and CD103 expression by mouse CD8(+) spleen dendritic cells. Eur J Immunol *41*, 2585-2595.

Zhan, Y., Vega-Ramos, J., Carrington, E.M., Villadangos, J.A., Lew, A.M., and Xu, Y. (2012). The inflammatory cytokine, GM-CSF, alters the developmental outcome of murine dendritic cells. Eur J Immunol *42*, 2889-2900.

Zhu, S.N., Chen, M., Jongstra-Bilen, J., and Cybulsky, M.I. (2009). GM-CSF regulates intimal cell proliferation in nascent atherosclerotic lesions. J Exp Med *206*, 2141-2149.

Zigmond, E., Varol, C., Farache, J., Elmaliah, E., Satpathy, A.T., Friedlander, G., Mack, M., Shpigel, N., Boneca, I.G., Murphy, K.M., *et al.* (2012). Ly6C hi monocytes in the inflamed colon give rise to proinflammatory effector cells and migratory antigen-presenting cells. Immunity *37*, 1076-1090.

Zou, M., Martin, C., and Ullrich, V. (1997). Tyrosine nitration as a mechanism of selective inactivation of prostacyclin synthase by peroxynitrite. Biol Chem *378*, 707-713.

Appendix 1 – Media and Buffers

PBS (1x)

8g NaCl, 0.2g KCl, 1.44g Na_2HPO_4, 0.24g KH_2PO_4 in 1 litre H_2O, pH 7.4

EasySep™ Buffer

2% FBS, 1mM EDTA in PBS, pH7.4

FACS Buffer

1% normal mouse serum, 1% normal rat serum, 0.5% BSA, 2mM EDTA in PBS, pH 7.4

BD Pharm Lyse™

Pharm Lyse™ concentrate (10x) diluted in distilled water to working concentration (1x), adjusted pH to 7.1 – 7.4

Ammonium Chloride Solution

0.9% ammonium chloride in distilled water

RPMI-1640 Complete Medium

RPMI (4500 mg/ml glucose) 450ml, FBS (10%) 50ml, Antibiotic-Antimycotic (1x) 5ml

DAPI

4',6-Diamidino-2-phenylindole dihydrochloride reconstituted in distilled water and used at 1:20,000 dilution.

IMDM Complete Medium

IMDM 450ml, FBS (5%) 25ml, 200mM L-glutamine 5ml, G418 (1mg/ml)

2% w/v Paraformaldehyde with 30% w/v Sucrose

2g paraformaldehyde, 30g sucrose in 100ml PBS (1x)

Appendix 2 – Antibodies for flow cytometry

Antibody	Company	Clone
CD11c PE-Cy7	eBioscience	N418
CD11b PerCP-Cy5.5	BD Pharmingen	M1/70
IA/IE FITC	eBioscience	M5/114.15.2
CD24 eFluor 450	eBioscience	M1/69
CD64 APC	BioLegend	X54.5/7.1
CD64 PE	BioLegend	X54.5/7.1
IA Alexa Fluor 700	eBioscience	M5/114.15.2
CD45 APC-Cy7	BD Pharmingen	30-F11
Gr-1 PE	BD Pharmingen	RB6-8C5
Gr-1 APC	BD Pharmingen	RB6-8C5
CD103 PE	eBioscience	2E7
Ly6G FITC	eBioscience	RB6-8C5
Sirp α FITC	BD Pharmingen	P84
F4/80 FITC	AbD Serotec	C1:A3-1
c-kit PE-Cy7	eBioscience	2B8
Biotinylated Flt3	eBioscience	A2F10
CD45.2 FITC	eBioscience	104
Streptavidin-PerCP-Cy5.5	eBioscience	NA
CD115 biotin	eBioscience	AFS98
Streptavidin-PB	Invitrogen	NA
CD115 PE	eBioscience	AFS98
CD11c PB	BioLegencd	N418
Biotinylated CD45.1	BD Pharmingen	A20
CD45.1 PerCP-Cy5.5	eBioscience	A20
TER119 APC	eBioscience	TER-119
CD19 APC	eBioscience	eBio1D3
CD3 APC	eBioscience	145-2C11
B220 APC	eBioscience	RA3-6B2

NK1.1 APC	eBioscience	PK136
Sca-1 APC	eBioscience	D7
CD11b APC-Cy7	eBioscience	M1/70
GMRα APC	R&D Systems	698423
CD131 PE	BD Pharmingen	JORO 50
Rat IgG_{2a} APC	eBioscience	NA
Rat IgG_1 PE	eBioscience	NA
Rat IgG_1 eFluor 450	eBioscience	NA
TNF-α eFluor 450	eBioscience	MP6-XT22
GM-CSF PE	eBioscience	MP1-22E9
iNOS (Rabbit anti-mouse)	BD Pharmingen	NA
Anti-Rabbit APC	Invitrogen	NA
Rabbit IgG Isotype	Southern Biotech	NA

Appendix 3 – Antibodies for immunofluorescence

Antibody	Company	Clone
iNOS (Rabbit)	Calbiochem	NA
GM-CSF (Rabbit)	Santa Cruz	FL-144
Nitrotyrosine (Rabbit)	Millipore	NA
I-A/I-E	eBioscience	M5/114.15.2
Armenian Hamster IgG	BD Pharmingen	H94/8
CD11b	eBioscience	M1/70
Rabbit IgG	Jackson Immuno	NA
CD11c	eBioscience	HL-3
CD3ε	eBioscience	145-2C11
Anti-Armenian Hamster HRP	Jackson Immuno	NA
Anti-Rat HRP	Jackson Immuno	NA
Anti-Rat AF647, Cy2	Jackson Immuno	NA
Anti-Armeniam Hamster IgG Dylight 647	Jackson Immuno	NA
Anti-Rabbit Cy3	Jackson Immuno	NA

Appendix 4 – Primers for qPCR

Target gene	Primer sequence (5' → 3')
Flt3 L Forward	GGAGCCCAAATTCCTCCCTGTTGC
Flt3 L Reverse	GGAGCCTCTTCCTAGCCCAGCG
GM-CSF Forward	GCCTGAAGATATTCGAGCAGGGTCTAC
GM-CSF Reverse	GCATTCAAAGGGGATATCAGTCAGAAAGGTT
M-CSF Forward	TCATGAGCAGGAGTATTGCCAA
M-CSF Reverse	GGCAATCTGGCATGAAGTCTC
IL-34 Forward	GGGTCATGGAACTGCTGTACT
IL-34 Reverse	ATCAAGGACCCCGGACTG
GM-CSF Receptor β2	GGACGACTGACTGGGTGATG
GM-CSF Receptor β2	AACACGGCCAAAGTGGAGAG
GM-CSF Receptor α	CCTGCTCTTCTCCACGCTAC
GM-CSF Receptor α	GTCGAAGGTCAGGTTGAGGG
GM-CSF Receptor β	TAGGAAGAGCCTGCAACTCAC
GM-CSF Receptor β	ACTGCATCCTTTGTGGCTCTG
IL-3 Receptor α	AGATGATGATGGCGACCACG
IL-3 Receptor α	GCACATCACGCCAGAACATC
IL-5 Receptor α	GCCATTGACCAAGTGAATCCTC
IL-5 Receptor α	GAGCTCACAGCTGCTCTCAC
IL-3 Forward	TCTGCGAATGACTCTGCGCTGC
IL-3 Reverse	GAGACGGAGCCAGATGCGGG
GAPDH Forward	GACGGCCGCATCTTCTTGTG
GAPDH Reverse	CTTCCCATTCTCGGCCTTGACTGT